

QATAR UNIVERSITY

COLLEGE OF ENGINEERING

THERMO-RHEOLOGICAL CHARACTERIZATION OF NATURAL DEEP

EUTECTIC SOLVENTS (NADES) USED IN CO₂ CAPTURE

BY

YOUSEF ADEL ELHAMARNAH

A Thesis Submitted to

the Faculty of the College of Engineering

in Partial Fulfillment of the Requirements for the Degree of

Masters of Science in Environmental Engineering

June 2019

©2019. Yousef Elhamarnah. All Rights Reserved.

COMMITTEE PAGE

The members of the Committee approve the Thesis of
Yousef defended on 21/04/2019.

Prof. Hazim Qiblawey
Thesis/Dissertation Supervisor

Dr. Mustafa Nasser
Thesis/Dissertation Co-Supervisor

Dr. Alaa AlHawari
Committee Member

Prof. Farouk Mjalli
Committee Member

Approved:

Abdel Magid Hamouda, Dean, College of Engineering

ABSTRACT

Elhamarnah, Yousef, A., Masters: June: 2019, Masters of science in Environmental Engineering

Title: Rheological Characterization of Natural Deep Eutectic Solvents in CO₂ Capture

Supervisor of Thesis: Hazim A. Qiblawey **Co-supervisor of Thesis:** Mustafa S.

Nasser

The rheological behavior of a fluid is an important property that has a distinct impact on its flow behavior, which influences viscosity dependent phenomena and applications such as pumping, mass transfer rates, and hydrodynamics. This thesis herein intended to provide a detailed rheological description of mainly Lactic acid (LA) and Malic acid (MA) based Natural deep eutectic solvents (NADES). The effect of three different hydrogen bond acceptors (HBA) of B-Alanine, Betaine, Choline Chloride nature upon its addition with a fixed hydrogen bond donor (HBD) component at a fixed molar ratio of 1:1. The changes in the rheological properties as a function of physical, thermal and mechanical parameters that provide an indication of the material's tolerance under different field operational circumstances for their potential use as environmental green sorbents for CO₂ capture were intensively investigated. The shear flow and viscoelastic behaviors of all six samples were analyzed and studied for the insurance of effective CO₂ capture. The use of a rheogram was used to describe the effect of forward and backward temperature ramping on the apparent viscosity trend of the LA-based NADES systems. The density was also measured and compared to the apparent viscosity behavior under the effect of temperature. Moreover, the viscoelastic properties were also thoroughly described to best describe and investigate the disturbance in networks on the microstructure level in the NADES structure upon frequency sweep. The rheological characterization of shear flow measurements was

evaluated using the Bingham model, which best implied on the apparent viscosity formulated over shear rate and the dynamic yield stress of the NADES systems.

Keywords: natural deep eutectic solvents; rheology; viscoelastic; choline chloride; betaine; lactic acid; Malic acid, B-Alanine, Betaine

DEDICATION

I dedicate my humble effort herein to my loving and sweet mother Faten Abukaresh, grandmother Yousra Elhamarnah and father Adel Elhamarnah, whose love, affection and prayers made me capable to reach this level of success and honor throughout this journey.

ACKNOWLEDGMENTS

The satiation and euphoria that accompany the successful completion of the thesis would be incomplete without the mention of the people who made it possible. I would like to take the opportunity to thank and express my deep sense of gratitude to my advising professor Hazim Qiblawey. I am greatly indebted to him for providing valuable guidance at all stages of this journey, his advice, constructive suggestions, positive and supportive attitude and encouragement, without which it would have not been possible to complete this thesis report. I also extend my thanks for my Co-supervisor, Dr. Mustafa Nasser who in spite of busy schedule has co-operated with me continuously and indeed, his valuable contribution and guidance have been certainly indispensable for the stay at the Gas Processing Center (GPC). I am also thankful to all the hard-working staff at GPC especially Eng. Musaab, Dan for providing me with all the needy facilities and equipment. Finally, I owe my wholehearted thanks and appreciation to my friends Mohammed Hosni and Nafis Mahmoud at the GPC for their continuous support and assistance through my stay.

TABLE OF CONTENTS

DEDICATION	v
ACKNOWLEDGMENTS	vi
LIST OF TABLES	x
LIST OF FIGURES	xii
ABBREVIATIONS AND ACRONYMS	xvii
1 CHAPTER 1: INTRODUCTION	1
1.1 Introduction on green chemistry and solvents	1
1.2 NADESs as a CO ₂ capture agent	1
1.3 Definition and classifications of DESs	2
1.4 Natural Deep Eutectic Solvents (NADES)	4
1.5 Therapeutic Deep Eutectic Solvents (THEDES)	8
1.6 Rheology	12
1.7 Viscosity	12
1.8 Fluid Flow Regimes	13
1.9 Thixotropy.....	15
1.10 Viscoelasticity.....	16
1.11 Research contribution	17
1.12 Research Objectives.....	18
1.13 Research Outcomes (List of Refereed Publications)	18

2	CHAPTER 2: LITERATURE REVIEW	20
2.1	Ambient Temperature of NADES	20
2.2	Temperature dependency of NADES	24
2.3	Hydration Effect of NADES	32
2.4	Viscoelastic behavior of NADES	59
2.5	Rheological Modeling.....	64
2.5.1	Arrhenius Equation	64
2.5.2	Vogel-Fulcher-Tammann Equation	66
2.5.3	Bingham Equation	68
2.5.4	Herschel-Bulkley Equation.....	72
3	CHAPTER 3: MATERIALS & METHODS.....	74
3.1	Materials used in this work.....	74
3.2	Methodologies.....	75
3.2.1	NADES Synthesis.....	75
3.2.2	Viscosity measurements.....	84
3.2.3	Rheometer	84
3.2.3.1	Anton Paar 302 Rheometer.....	84
3.2.3.2	Basic Components of the MCR Rheometer.....	85
3.2.3.3	Rheological measurements procedure	86
3.2.3.4	Rotational Measurements.....	88
3.2.3.5	Oscillation measurements	89
3.2.4	Density	90
3.2.5	Thermogravimetric Analysis (TGA).....	91

4	CHAPTER 4: RESULTS AND DISCUSSIONS	93
4.1	Part A: Lactic acid based NADES	93
4.1.1	Steady-state flow.....	93
4.1.1.1	Shear stress vs shear rate.....	93
4.1.1.2	Effect of Temperature sweep.....	95
4.1.2	Oscillatory tests.....	99
4.1.2.1	Angular frequency sweep	99
4.1.2.2	Dynamic Temperature ramp sweep	101
4.1.3	Thermal Stability	107
4.1.4	Model regression.....	108
4.1.4.1	Bingham Model	108
4.2	Part B: Malic acid based NADES	110
4.2.1	Steady-state flow.....	110
4.2.2	Thermo-rheological steady-flow behavior.....	112
4.2.3	Oscillatory tests.....	115
4.2.3.1	Angular frequency sweep	115
4.2.3.2	Dynamic temperature ramp sweep.....	117
4.2.4	Thermal Stability	119
4.2.5	Model regression.....	120
4.2.5.1	Bingham Model	120
5	CHAPTER 5: CONCLUSIONS	123
6	FUTURE PERSPECTIVES.....	125
7	REFERENCES	126

LIST OF TABLES

Table 1.1: Physical properties of various Choline Chloride NADESs employed in literature	6
Table 1.2: Physical properties of various THEDESs reported in literature	9
Table 2.1: Overview on the rheological characterization and experimental setups for shear flow behaviors for varies tailor-made Natural Deep Eutectic Solvents	37
Table 2.2: Overview on the rheological characterization and experimental setups for Oscillatory behaviors for various tailor-made Natural Deep Eutectic Solvents (NADES) at ambient conditions.	62
Table 2.3. Arrhenius model parameters for different Natural Deep Eutectic Solvents (NADES).....	66
Table 2.4: Vogel-Fulcher-Tammann model parameters for different Natural Deep Eutectic Solvents (NADES).....	67
Table 2.5: Bingham model parameters for different Natural Deep Eutectic Solvents (NADES).....	70
Table 2.6. Herschel-Bulkley model parameters for different Natural Deep Eutectic Solvents (NADES).....	73
Table 3.1: Specifications and synthesis details of the DES system prepared.....	78
Table 3.2: A group of selected articles on the preparation methods of deep eutectic solvents	80
Table 3.3: Shear flow parameters fixed in the option tools for the RheoPlus software	88
Table 3.4: Pre-Shear flow parameters fixed in the option tools for the RheoPlus software.....	90

Table 3.5: Oscillatory shear flow parameters fixed in the option tools for the RheoPlus software.....	90
Table 4.1: The results obtained from mathematical modelling of the rheogram data of ChCl: La, Be: La, B-Al: La at temperatures from 25-85 °C.....	109
Table 4.2: Summary of the different NADES TGA analysis results obtained from the thermographs.....	120
Table 4.3: The results obtained from mathematical modelling of the rheogram data of ChCl: MA, Be: Ma, B-Al: MA at temperatures from 25-85 °C	122

LIST OF FIGURES

Figure 1.1: The principle of DESs upon mixing HBA with HBD at a certain temperature [32].....	3
Figure 1.2: Schematic binary phase diagram of a eutectic system with dual components [34]	4
Figure 1.3: The velocity, Shear rate and shear stress flow profiles between two parallel plates for non-Newtonian fluids [52].....	13
Figure 1.4: Rheological characterization of different material under the effect of shear rate [52].....	14
Figure 1.5: Apparent viscosity of a fluid that depends on the shear rate at which it is measured [52].....	15
Figure 1.6: Flow curve of Thixotropic and Rheopectic fluids [52].....	16
Figure 2.1: log-log scale representation of the apparent viscosity (Pa.s) vs shear rate (s^{-1}) for Choline Chloride Citric Acid (1:1)[48], Choline Chloride Lactic Acid (1:1) [24], Choline Chloride xylose (1:1)[57] , Choline Chloride Glucose (1:1) [63], Choline Chloride glycerol (1:2) [65], Choline Chloride Urea (1:2)[65], Choline Chloride Ethyl Glycol (1:2) [65] at ambient temperature condition	24
Figure 2.2: log-log representation of the apparent viscosity vs shear rate of different NADES: choline chloride + glucose (1:1)[63], choline chloride + xylose (1:1)[57], choline chloride + phenylacetic Acid (1:2)[25], choline chloride + phenylacetic acid (1:3)[25], choline chloride + phenylacetic acid (1:4)[25], choline chloride + lactic acid (1:1)[24] at high temperature conditions.	28
Figure 2.3: log-log representation of the apparent viscosity vs shear rate of different NADES systems at incremented temperatures for: choline chloride + phenylacetic acid (1:2) [25].....	29

Figure 2.4: log-log representation of the apparent viscosity vs shear rate of different NADES systems at incremented temperatures for: choline chloride + phenylacetic acid (1:3) [25].....	30
Figure 2.5: log-log representation of the apparent viscosity vs shear rate of different NADES systems at incremented temperatures for: choline chloride + phenylacetic acid (1:4) [25].....	30
Figure 2.6: log-log representation of the apparent viscosity vs shear rate of different NADES systems at incremented temperatures for: choline chloride + lactic acid (1:1) [24].....	31
Figure 2.7: log-log representation of the apparent viscosity vs shear rate of different NADES systems at incremented temperatures for: choline chloride + glucose (1:1) [63]	31
Figure 2.8: log-log representation of the apparent viscosity vs shear rate of different NADES systems at incremented temperatures for: choline chloride + xylose (1:1) [57]	32
Figure 2.9: log-log representation of the apparent viscosity vs shear rate of different NADES systems with different hydration ratios : choline chloride + glucose (1:1)[63], choline chloride + glucose (1:1) + 5% H ₂ O[63], choline chloride + xylose (1:1) [57]+ choline chloride + xylose (1:1) + 5% H ₂ O[57], choline chloride + glycerol (1:2) [65], choline chloride + glycerol (1:2) + 10% H ₂ O[65], choline chloride + urea (1:2)[65] , choline chloride + urea (1:2) + 10% H ₂ O [65], choline chloride + ethylene glycol (1:2)[65], choline chloride + ethylene glycol (1:2) + 10% H ₂ O [65] at ambient condition	35

Figure 3.1: From left to right, the original components of NADES at room temperature for ChCl + LA and ChCl + MA: Choline Chloride, Malic Acid, Lactic Acid, and Choline Chloride + Lactic acid (1:1).	76
Figure 3.2 :Set A, Synthesized [LA] , [MA] : [CA] , [FR], [ChCl] based 1:1 NADES systems.....	76
Figure 3.3: Set B & C, Synthesized LA , MA : Be , B-Al based 1:1 NADES systems	77
Figure 3.4: Anton Paar 302 MCR rheometer.....	85
Figure 3.5: CP, PP measuring geometries with different diameter sizes 25,50 mm respectively	87
Figure 3.6: Density Meter by Anton Paar	91
Figure 3.7: Thermogravimetric Analysis instrument.....	92
Figure 4.1: The variation of shear stress as a function of applied shear rate for	94
Figure 4.2: The variation of shear stress as a function of applied shear rate for Be, B-Al, and ChCl: La NADES systems at elevated temperatures from 25-85 °C	95
Figure 4.3: Effect of heating (forward ramp) (dashed line) and cooling (backward ramp) (solid line) on the apparent viscosity at low shear rate of 1 s^{-1} at a temp ramp rate of 3°C , time ramp of 1.6 min using 26 data points for Be. B-Al, ChCl: La NADES systems	96
Figure 4.4: Effect of heating on the apparent viscosity and density (at high shear rate of 1000 s^{-1}) for B-Al, Be, and Chcl: LA NADES systems.....	98
Figure 4.5:3D color surface showing the effect of temperature and time dimensions of the apparent viscosity on Be:LA NADES system	98

Figure 4.6: Complex viscosity & apparent viscosity variation for Be, B-Al, ChCl: La NADES systems at low angular frequency (1 rad. s ⁻¹) and low shear rate (1 s ⁻¹) respectively under heating from ambient temperature conditions to 85°C.....	100
Figure 4.7: Complex viscosity & apparent viscosity variation for Be, B-Al, ChCl: La NADES systems at high angular frequency (100 rad. s ⁻¹) and low shear rate (1000 s ⁻¹) under heating from ambient temperature conditions to 85°C	101
Figure 4.8: The elastic modulus (G') and viscous modulus (G'') at high angular frequency of 100 rad. s ⁻¹ for Be, B-Al, and ChCl: La under the effect of heating from ambient conditions to 85°C.....	102
Figure 4.9: The elastic modulus (G') at low angular frequency of 1 rad. s ⁻¹ for Be, B-Al, and ChCl: La under the effect of heating from ambient conditions to 85°C	103
Figure 4.10: The viscous modulus (G'') at low angular frequency of 1 rad. s ⁻¹ for Be, B-Al, and ChCl: La under the effect of heating from ambient conditions to 85°C	103
Figure 4.11: The elastic modulus (G') at an angular frequency range from 0.1- 100 rad. s ⁻¹ for Be, B-Al, and ChCl: La at room temperature conditions.....	105
Figure 4.12: The viscous modulus (G'') at an angular frequency range from 0.1- 100 rad. s ⁻¹ for Be, B-Al, and ChCl: La at room temperature conditions.....	105
Figure 4.13: The elastic modulus (G') at an angular frequency range from 0.1- 100 rad. s ⁻¹ for Be, B-Al, and ChCl: La at high temperature	106
Figure 4.14: The viscous modulus (G'') at an angular frequency range from 0.1- 100 rad. s ⁻¹ for Be, B-Al, and ChCl: La at high temperature.....	106
Figure 4.15: TGA thermographs of lactic acid based NADES systems	107
Figure 4.16: The variation of applied shear stress as a function of shear rate for Be, B-Al, and ChCl: Ma NADES systems at room temperature conditions.....	111

Figure 4.17: The variation of applied shear stress as a function of shear rate for Be: MA NADES systems at elevated temperatures from 25-85°C.....	112
Figure 4.18: Effect of heating (Ramp up) and cooling (Ramp down) on the apparent viscosity at low shear rate of 1 s^{-1} for B-Al:MA NADES systems.....	113
Figure 4.19: Effect of heating on the apparent viscosity (at high shear rate of 1000 s^{-1}) for B-Al, Be, and ChCl: MA NADES systems.....	114
Figure 4.20: 3D color surface showing the effect of temperature and time dimensions of the apparent viscosity on B-Al: MA NADES system.....	115
Figure 4.21: Effect of elevated temperatures on the storage modulus of ChCl:MA NADES system at room temperature conditions	116
Figure 4.22: Complex viscosity variation for Be:MA, B-Al:MA and ChCl:MA NADES systems at high angular frequency of 100 rad.s^{-1} under heating from ambient temperature conditions to 105°C	117
Figure 4.23: The storage modulus (G') and loss modulus (G'') at high angular frequency of 100 rad.s^{-1} for Be, B-Al, and ChCl:MA under the effect of heating from ambient conditions to 85°C	118
Figure 4.24: TGA thermographs of MA-based NADES systems.....	119

ABBREVIATIONS AND ACRONYMS

ILs	Ionic Liquids	VFT	Vogel–Fulcher–Tamman
DESs	Deep Eutectic solvents	QCM	quartz crystal microbalance
NADES	Natural Deep Eutectic solvents	LVR	linear viscoelastic region
THEDES	therapeutic deep eutectic solvents		
BE	Betaine		
ChCl	Choline Chloride		
B-Al	B-Alanine		
MA	Malic Acid		
CA	Citric Acid		
FR	D-Fructose		
LA	Lactic Acid		
HBA	Hydrogen Bond Acceptor		
HBD	Hydrogen Bond Donor		
VOCs	Volatile Organic Carbon		
LTTMs	Low Transition-Temperature Mixtures		
API	Active Pharmaceutical ingredient		
DFT	density function theory		
TGA	Thermogravimetric Analysis		
HEMA	2-hydroxyethyl methacrylate		

CHAPTER 1. INTRODUCTION

1.1 Introduction on green chemistry and solvents

Organic solvents such as aqueous and non-aqueous solvents were used until the last decades. The solvent choice plays a vital role when scaling up a chemical process. The considered solvent chosen for a process represents about 85% of the mass utilization for a mass utilization in a manufacturing process [1]. The use of classical organic solvents has shown several environmental and safety operational issues during processing such as the emission of volatile organic carbons (VOCs). Therefore, introducing alternative green solvents is essential. The term green chemistry aims the replacement of harmful solvents that may cause side effects to the environment and human health or to ideally achieve solvent free processes. Therefore, establishing a sustainable solvent is a core requirement for improving the CO₂ capture process in post combustion, as most of the energy utilized by the process is depended on the solvent properties [2].

1.2 NADESs as a CO₂ capture agent

In recent years, a new class derived from organic and natural raw material of solvents was introduced to the field of green chemistry known as NADES [3–5]. The potential of considering NADESs comes in their technological adoptability, which has made them promising candidates for various applications and field operations such as chemical engineering, separation operations, materials science and energy-related processes [6–11]. These group of solvents are in current effort among researchers to replace the intrinsic shortcomings of Ionic liquids (ILs) as media for CO₂ capture [12]. Several studies on the use of NADESs for the sequestration of CO₂ have shown their positive impact for improving the enhancement of CO₂ capture and also the capture process cost have been reported in recent literature [13–28]. The development of the

NADES for CO₂ capture requires combinations of HBA: HBD that results in optimum properties that favor the capturing process (e.g. low viscosity, low yield stress, high thermal stability) [29]. For instance, the effect of alternating the HBA using five different quaternary ammonium species for their study on CO₂ capture, using a fixed HBD at a fixed molar ratio [17]. Other studies examined (in contrast to our research group) the effect of increasing the molar ratio of HBA to HBD and vice versa using a single NADES to examine the solubility of CO₂ [14,21–23,25]

As most of the fluids in industrial applications show a non-Newtonian behavior under several operational conditions, predicting their actual behavior under different conditions is a challenge. Rheology plays an important role in the design, evaluation and optimization of typical/transdermal absorbents. It also complements the complex issue of CO₂ capture in petrochemical industries. Although several rheological characterizations conducted by rheologists have demonstrated excellent performance for their use in a wide range of applications especially for their potential in CO₂ capture [22,24,25], due to the lack of NADES shear flow measurements at these conditions, their flow behavior assessment was a difficult task for many researchers [30].

1.3 Definition and classifications of DESs

Deep eutectic solvents (DESs) are mixtures made up of at least two components and may be multiple components in some other cases. The individual component has a melting point higher than the mixture [31]. In general cases, DESs are formed by the complexation of a quaternary ammonium halide salt in a solid form (i.e. hydrogen bond acceptors (HBA)) molecular, with a hydrogen bond donor (HBD) molecule in the form of solid and liquid in some cases, leading to the formation of a what so called a eutectic system (Figure 1.1)

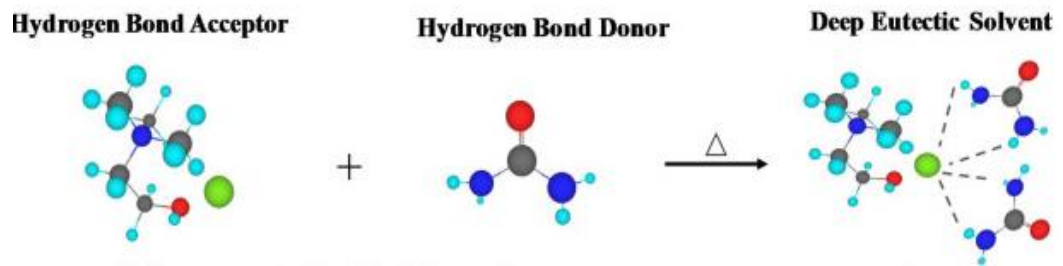


Figure 1.1: The principle of DESs upon mixing HBA with HBD at a certain temperature [32]

Figure 1.2, depicts the general behavior of a binary eutectic system. For a eutectic system to form, the two main components of the system require complete miscibility in the liquid system, while immiscible in their solid state. The liquidus line in the binary system shows the temperatures where the components 'A' & 'B' start to melt. Below this line, the mixtures exhibit a solid form. The enclosed regions show either the liquid mixture of 'A' & 'B' with a solid of 'A', the liquid mixture of 'A' & 'B' with a solid of 'B'. The critical point in this diagram represents the region where the solidus and liquidus regions meet (i.e. eutectic point), which corresponds to the eutectic composition[33].

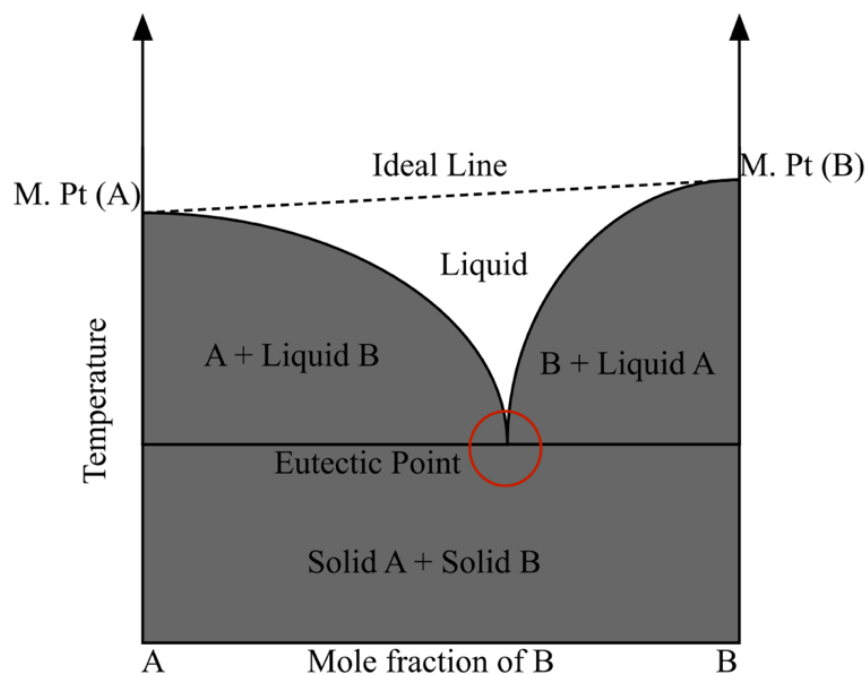


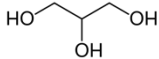
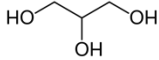
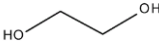
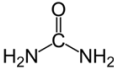
Figure 1.2: Schematic binary phase diagram of a eutectic system with dual components [34].

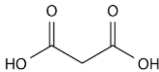
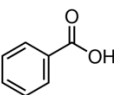
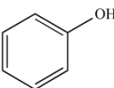
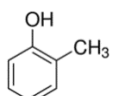
1.4 Natural Deep Eutectic Solvents (NADES)

A specific class of DESs have recently received the attention of several researchers from different disciplines. NADESs were first described by Choi et al. [35,36] Interestingly, this remarkable combination of bio-renewable material known as NADESs, considers Choline Chloride (ChCl), amino acids, natural carboxylic acids, different sugars as the main components of the eutectic mixture. These novel solvents are commonly known for their abundance in nature and relatively cheap starting material, as they only require basic heating (below 100°C) of their raw material, in comparison with commercial DESs and ILs [37]. Moreover, their biocompatibility and biodegradability ease is one of the major drawbacks of several absorbents used in gas separation processes such as handling, disposing, and recycling [38]. Till this moment,

researchers categorize NADES under the general formula of DESs. Therefore, in this piece of work, their potential uses in different engineering fields are collected in order to present their future importance as green solvents for different extraction and separation processes. Table 1-1 shows the most recent studies for the physiochemical characterization of NADESs that are available in open literature.

Table 1.1: Physical properties of various Choline Chloride NADESs employed in literature

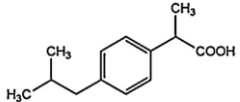
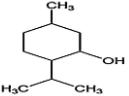
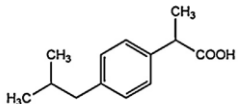
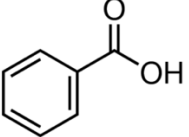
NADES Halide Salt HBD	Molecular structure	Mole Ratio (HBA:HBD)	Melting Point (°C)	Density (g cm ⁻³)	Viscosity (25°C) (mPa.s)	Reference
Glycerol		1:2	-40	1.18	259	[39]
Glycerol		1:3	-32.65	1.2	450	[40]
Ethylene Glycol		1:2	-66	1.12	37	[39,41]
urea		1:2	12	1.25	750	[39,42,43]

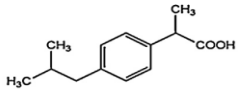
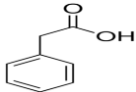
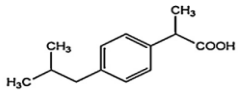
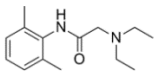
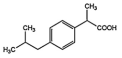
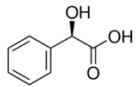
NADES Halide Salt HBD	Molecular structure	Mole Ratio (HBA:HBD)	Melting Point (°C)	Density (g cm ⁻³)	Viscosity (25°C) (mPa.s)	Reference
Malonic Acid		1:1	10	1.25	1124	[39,44]
Benzoic Acid		1:1	95	-	-	[44]
Phenol		1:3	-	1.095	58.8	[45]
<i>O</i> -cresol		1:3	-	1.071	77.6	[45]

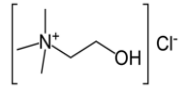
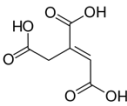
1.5 Therapeutic Deep Eutectic Solvents (THEDES)

The concept of THEDES are similar to NADES, the mixture is also prepared by the combination of two components. The complexation usually occurs between a receiver and recipient components known as the active pharmaceutical ingredient (API). This class of DESs was first discovered by Stott et al. [33] in 1998, who had synthesized a DES mixture made up of menthol and ibuprofen, for the purpose of predicting the effect of skin permeation and development. These solvents are bioactive eutectic systems that are mainly a result of API. Although their main field of interest nowadays are highlighted on their use as potential solvents for pharmaceutical formations, and developers for drug permeability and solubility, yet some studies believe that THEDESs may be used in other extraction or separation processes. Due to their ease of preparation, product purity, and low reported viscosity [46]. However, the lack of research has hindered the development of on this class of DES from the characterization reports and molecular interaction associations between the systems. A list of reported physical properties on THEDESs is given in table 1.2.

Table 1.2: Physical properties of various THEDESs reported in literature

THEDES		THEDES		Mole Ratio	Viscosity	Reference
Component I	Molecular Structure	Component II	Molecular structure	(Component I: Component II)	(mPa.s) (25 °C)	
ibuprofen		(R,S)-(±)-menthol		1:3	80.23	[46]
ibuprofen		Benzoic Acid		1:3	44.15	[46]

					Viscosity	
THEDES Component I	Molecular Structure	THEDES Component II	Molecular structure	Mole Ratio (Component I: Component II)	(mPa.s) (25 °C)	Reference
ibuprofen		phenylacetic acid		1:3	30.27	[46]
ibuprofen		lidocaine		1:1	-	[47]
ibuprofen		R-(-)-mandelic acid		1:3	-	[48]

					Viscosity	
THEDES Component I	Molecular Structure	THEDES Component II	Molecular structure	Mole Ratio (Component I: Component II)	(mPa.s) (25 °C)	Reference
Choline Chloride		Ascorbic Acid		2:1	15,000	[49]

1.6 Rheology

The word rheology is originated from historical Greek which is translated to “*The study of flow and deformation of matter*” [50]. This area focuses on studying and describing the different flow and deformation behaviors of different substances of matter, liquids, different sorts of solids, that have diverse plastic flow behaviors. Rheology offers a great value to studies on the relationship between different parameters such as deformation, time, and different forces. The study of rheology becomes important in sensitive areas such as petrochemical industries. In addition, rheology is used as a semi-quantitative tool in characterization and quality control of recent material under current research development. The rheology measurements for NADES are important in order to characterize the flow behaviors under the effect of different field operating conditions such as temperature, pressure, and shear rate for the different combinations of the solvents.

1.7 Viscosity

The viscosity of a fluid is defined as the quantification of the resistance to deformation under shear stress, which is mainly due to the internal friction within the fluid [51] where parallel fluid layers move at varied velocities as shown the Figure 1.3. The mathematical representation can be shown as following:

$$\tau = \eta \frac{du}{dy} \quad (1)$$

Where τ represents shear stress, η is the coefficient of dynamic viscosity and (du/dy) is the shear rate

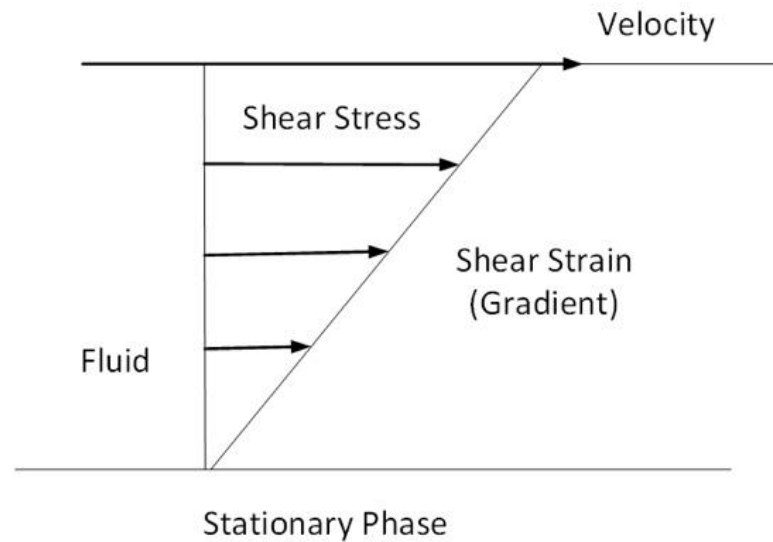


Figure 1.3: The velocity, Shear rate and shear stress flow profiles between two parallel plates for non-Newtonian fluids [52]

The flow resistance in fluids can occur due to several factors such as the frictional forces between particles and fluids, intermolecular and intramolecular forces that occur among the ions and electrically charged particles in the fluid. The parameters that govern the viscosity of a fluid are temperature, time, pressure, shear rate, and the nature of the fluid (i.e. physical and chemical composition of the fluid)

1.8 Fluid Flow Regimes

Fluids are mainly classified into two distinguished categories, Newtonian fluids and non-Newtonian fluids. The Newtonian fluids are commonly known for their constant viscosity over the change in shear or external force. Well defined Newtonian liquids are also known for their low molecular weight, such as water, glycerol, and acetone. On the other hand, non-Newtonian fluids have complete dependency on the imposed shear rate, the reflected behavior of shear can either be thickening or thinning, which can be represented by the Figure 1.4. In most studies, IL are commonly known

for their non-Newtonian behavior but some studies have shown their ability to become Newtonian fluids [51,53]. Furthermore, research conducted on NADES have shown that they mainly behave as Newtonian fluids, however, independent studies imply that they are similar to ILs, as they act as non-Newtonian fluids.

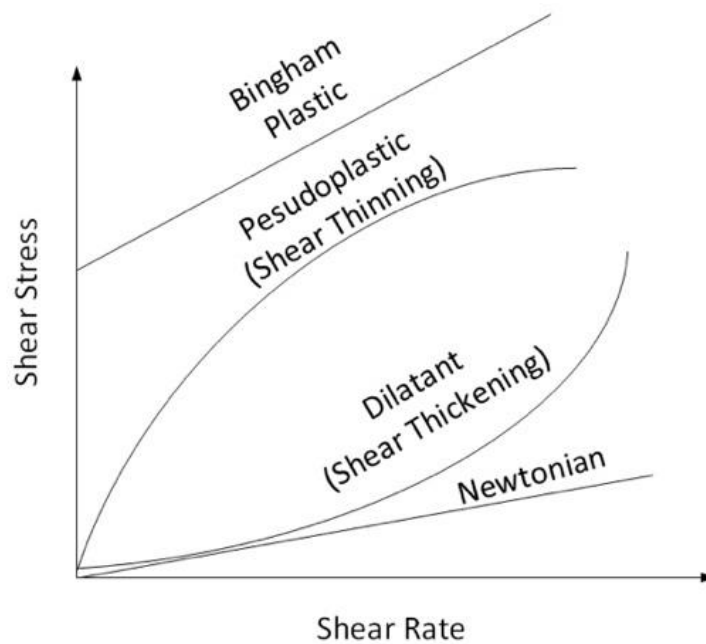


Figure 1.4: Rheological characterization of different material under the effect of shear rate [52]

To investigate the flow behavior under varied shear rates, a rheogram is used to evaluate the flowability of a NADES/ILs through its vastly dependency on the apparent viscosity[53]. This parameter is best to define the non-Newtonian behavior of NADES/ILs i.e. shear thinning, shear thickening. As the shear rate increases, materials tend to illustrate a non-uniform viscosity profile at isothermal conditions [54]. As a result, a successful viscosity profile characterization can describe the flow properties

and deformation (Figure 1.5) which may indicate their expected field applications and uses.

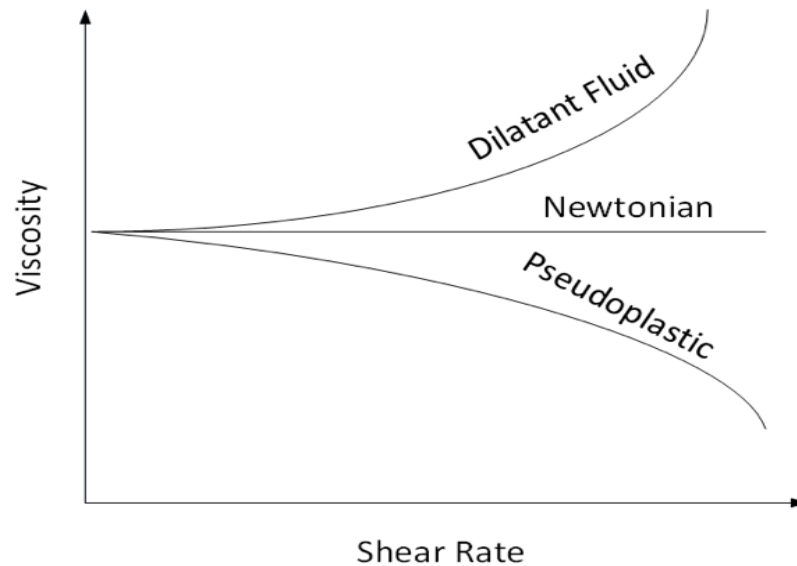


Figure 1.5: Apparent viscosity of a fluid that depends on the shear rate at which it is measured [52]

1.9 Thixotropy

Since the main analogy of NADES with shear rate is found to be classified under non-Newtonian liquids category, the two types of time-dependent (i.e. thixotropic and rheopexy) properties are mainly exhibited. The viscosity of thixotropic systems generally decreases with time but also restructures to its original morphology after a material-specific period of rest. Therefore, a thixotropic material is defined as the material that becomes thinner when an external force is applied. However, when the forces are removed, the internal structure re-establishes and rebuilds to its original

structure after a period of time. On the other hand, the viscosity of rheopectic systems commonly increases with time [55]. The diagram shown in Figure 1.6 shows the flow path exhibited by thixotropic and rheopectic fluids respectively. It is clear that the fluids do not follow the same path while the fluid tries to recover to its initial viscosity after a certain shear rate is applied. The main reason behind this is that the fluid restores its previous structure as a function of time when the stress applied is diminished.

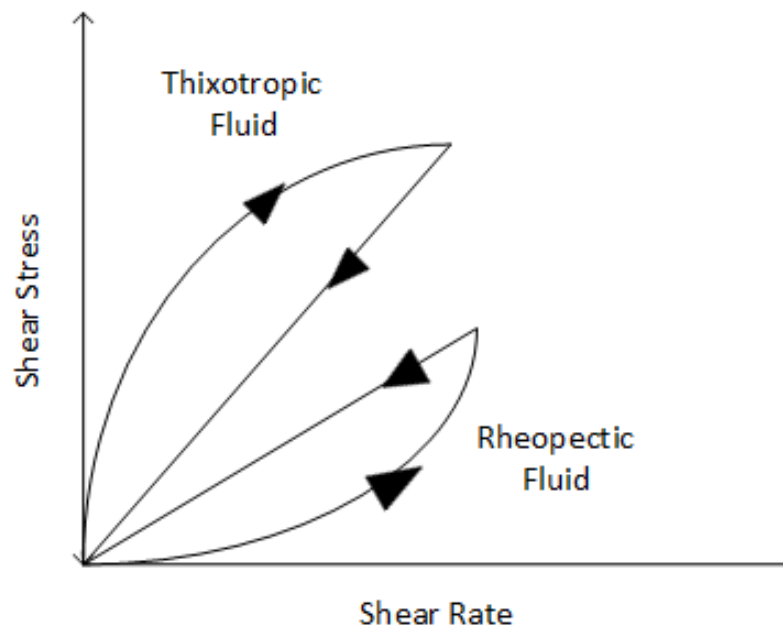


Figure 1.6: Flow curve of Thixotropic and Rheopectic fluids [52]

1.10 Viscoelasticity

Elasticity is the result of a fluid at zero stress reduction to partially recover and to behave as a liquid or an elastic solid [56]. The elastic properties of materials are described by the storage modulus (G' , ratio of elastic stress over strain) and loss modulus (G'' , the ratio of viscous stress over strain) are corresponding to the amount of

energy stored and dissipated during deformation respectively. The effects of these two moduli are combined into the complex modulus (G^*) as shown in the following equation

$$G^* = G' + iG'' \quad (2)$$

The viscoelastic material possesses complex dynamic viscosity (η^*)

$$\eta^* = \frac{G^*}{\omega} \quad (3)$$

Where ω is the angular frequency. Based on the literature reviewed, viscoelastic properties have shown a relatively lower attention of studies in recent literature. Viscoelastic oscillatory measurements were used to avoid any destruction of the networks formed for the structured solvents such as ILs and NADES and to measure the elastic viscoelastic properties of the solvents.

1.11 Research contribution

The findings of this study aim to fill the missing gaps in the field of NADES synthesis and characterization used for CO₂ capture. Current research showed relatively lower attention to studies related to rheological characterization. Although some researchers chose to describe NADES using thermo-physical rheological characterization, yet the focus in most publications are concerned with basic flow data, while paying less attention to importance of the rheological viscoelastic and other properties of NADES.

1.12 Research Objectives

The overall goal of this thesis is to investigate the potential use of NADES systems for a better utilization in CO₂ capture. Accordingly, achieving this overall goal requires fulfillment of three sub-objectives:

1. To understand rheological differences between the selected NADES combinations and compare their shear flow behaviors with alternative NADES present in literature.
2. To investigate the impact of different combinations of NADES based on the thermos-rheological behavior for potential application in CO₂ capture.
3. To analyze the major issue of high viscosity in NADES systems under the effect of different conditions by identifying the transport yield stress requirement for pumping different NADES on a field size CO₂ capture conditioning operation.

1.13 Research Outcomes (List of Refereed Publications)

1. Altamash, Tausif, Mustafa S. Nasser, **Yousef Elhamarnah**, Musaab Magzoub, Ruh Ullah, Baraa Anaya, Santiago Aparicio, and Mert Atilhan. "Gas Solubility and Rheological Behavior of Natural Deep Eutectic Solvents (NADES) via Combined Experimental and Molecular Simulation Techniques." *ChemistrySelect* 2, no. 24 (2017): 7278–95. doi:10.1002/slct.201701223.
2. Altamash, Tausif, Mustafa S. Nasser, **Yousef Elhamarnah**, Musaab Magzoub, Ruh Ullah, Hazim Qiblawey, Santiago Aparicio, and Mert Atilhan. "Gas Solubility and Rheological Behavior Study of Betaine and Alanine Based Natural Deep Eutectic Solvents (NADES)." *Journal of Molecular Liquids* 256 (2018): 286–95. doi:10.1016/j.molliq.2018.02.049.
3. **Elhamarnah, Yousef A.**, Mustafa Nasser, Hazim Qiblawey, Abdelbaki Benamor, Mert Atilhan, and Santiago Aparicio. "A Comprehensive Review on the Rheological

Behavior of Imidazolium Based Ionic Liquids and Natural Deep Eutectic Solvents.”

Journal of Molecular Liquids 277 (2019): 932–58.

doi:10.1016/j.molliq.2019.01.002.

4. **Elhamarnah, Yousef A.**, Mustafa Nasser, Hazim Qiblawey, Abdelbaki Benamor.
"Thermo-Rheological characterization of Lactic Acid Based Natural Deep Eutectic Solvents used in CO₂ Capture." Journal of Molecular Liquids (*Under review*)
5. **Elhamarnah, Yousef A.**, Mustafa Nasser, Hazim Qiblawey, Abdelbaki Benamor.
"Thermo-Rheological characterization of Malic Acid Based Natural Deep Eutectic Solvents for CO₂ Capture." (*Submitted*)
6. **Elhamarnah, Yousef A.**, Dana Al-Risheq, Mustafa Nasser, Hazim Qiblawey, Muftah Elnaas, Abdelbaki Benamor."Recent Progress on Separation Studies Using Deep Eutectic Solvents: Physical Properties and Applications." (*In Progress*)

CHAPTER 2. LITERATURE REVIEW

The available literature that has been generated in the last decade on DESs and in particular with NADESs thermophysical properties include physicochemical properties such as densities, viscosities, gas solubilities etc... [22,24,57–60] Most of the recent reported works focus on the implementation of these materials as novel gas capture agents in order to substitute conventional amine-based solvents with the target of zero upgrading of the existing infrastructure cost. One of the major challenges of these materials is to regulate their pumping costs and deal with their viscous behavior of these solvents. In order either DES or NADES to be considered as alternatives in chemical processes in larger scales by the regulatory authorities, thermophysical properties that include gas solubility performance as well as detailed rheological behavior must be investigated for various potential systems and a systematic analysis of these materials shall be studied in wide scale. Therefore, this review work is crucially important for benchmarking the key rheological properties of NADESs and includes a thorough analysis of already published information and that are available in open literature. In this section, the fundamentals and basic backgrounds on theoretical rheology is discussed in order to understand the analysis and content of the conducted experiments.

2.1 Ambient Temperature of NADES

The advantage in the flow behavior of NADES at room temperature over traditional solvents is that they can be used and operated in different chemical industries [61]. The lack of NADES shear flow measurements at room temperatures made it a difficult task for many researchers to analyze the flow behaviors of different NADES. The focus of this study is to highlight a series of NADES based on a choline chloride as HBA that is coupled with alternating HBD. Reported data showed that the rheological behavior of different mixtures of NADES at room temperature are showing

a universal trend depending on the detailed microstructure of the HBD and HBA. Solvents such as citric acid + glucose and choline chloride + citric acid at 1:1 mole ratios (Figure 2.1) showed a shear-thinning behavior under a controlled shear rate of $0.1 - 1000 \text{ s}^{-1}$ at 23°C . The apparent viscosity initially fluctuated at ranges from 0.1 s^{-1} to 1 s^{-1} from 450 to 230 Pa.s, but as it approached 1 s^{-1} , a Newtonian plateau at a viscosity of approximately $6 \pm 2 \text{ Pa.s}$ was observed and the viscosity became independent of the shear rate. Furthermore, Altamash et al. [24] studied four different low viscosity NADES for the use in gas sorption processes of CO_2 and N_2 which are choline chloride + lactic acid, choline chloride + citric acid, choline chloride + malic acid, choline chloride + lactic acid, and choline chloride + fructose. Nevertheless, the shear flows have shown a common shear thinning behavior among all the solvents at 25°C under a shear rate domain of $0.01\text{-}1000 \text{ s}^{-1}$ at atmospheric pressure. The absolute values of apparent viscosity showed that alternating the HBD has a significant effect on the application of the NADES. The viscosity of choline chloride + citric acid was significantly the highest among the rest, followed by choline chloride + malic acid which had viscosity values of 1003.1, 40.079 Pa.s respectively. Conversely, chlorine chloride + lactic acid and chlorine chloride + fructose showed a relatively lower viscosity (0.412 and 0.625 Pa.s) in comparison with the other two systems. Although this work showed the initial viscosity values for the mentioned systems, yet the apparent viscosity profile for only the choline chloride + lactic acid was represented in a rheogram (Figure 2.1). Das et al. [62] discussed the use of choline chloride + ethylene glycol, choline chloride + urea, choline chloride + glycerol NADES with evenly prepared mole ratios of 1:2 for the extraction of k-carrageenan from *Kappaphycus alvarezii*. In spite the rheogram presented for the NADES mentioned, the focus was not intensively qualitative. Although Das et al. [62] were among the few to study the flow

behaviors of more than one type of NADES, however, they did not approach the rheological explanation of the NADES behaviors at room temperature. Furthermore, the study of this set of NADES was one of the most successfully prepared solvents in terms of low viscosity. Initial viscosities at 10 s^{-1} for anhydrous choline chloride + ethylene glycol, choline chloride + urea, choline chloride + glycerol (Figure 2.1) was measured as 0.16, 0.42, and 0.35 Pa.s respectively., the change in apparent viscosity after increasing the shear rate to 50 s^{-1} was decreased to 0.046, 0.127, and 0.12 Pa.s respectively. As a result, the apparent viscosities measured in this study were successfully the lowest values obtained in literature. Despite the general conclusion about NADES is that they behave like non-Newtonian liquids (more towards solid-like behavior) at room temperature under varied shear rate, yet Aroso et al.[57] also elaborated on a series of HBD with choline chloride; xylose, glucose (Figure 2.1) and sucrose have shown that they are very viscous liquids with a Newtonian behavior. Rheological characterization of this set of NADES showed a constant trend in the viscosity profile, which was completely independent to applied shear rate. The study offered a sample rheogram for choline chloride + xylose (1:1) showing a constant change in the viscosity profile of 116 Pa.s. In another published work, Aroso et al. [63] presented the shear flow of Choline Chloride + glucose (1:1), alike to the conditions of the previously studied NADES combinations. In both papers, the general discussion was to set an agreement on the general behavior of NADES is that they are Newtonian liquids, independent of shear rate, and with very high viscosity at room temperature conditions. In contrast, Paula et al. [48] has discussed their disappointment of trying to apply rheological characterization for a selection of NADES such as citric acid + sucrose (1:1), citric acid + glucose (1:1), and choline chloride + citric acid (1:1, 2:1), as most of them exhibited a solid-like behavior at room temperature. Likewise, Aroso

et al. [57] also discussed his disability of performing rheological characterization on choline chloride + citric acid (1:1) and choline chloride + tartaric acid (2:1,1:1,1:2) due to the less mobility and high viscosity of the sample stating that the viscosity has exceeded the equipment limits ($<10,000$ Pa.s). Yan et al. [64] reported that the chemical nature of the component such as the halide salt type, mole ratio, and the HBD are the main reasons of high viscosity at room temperature, which brings us to the conclusion that NADES are solid-like material at room temperature conditions.

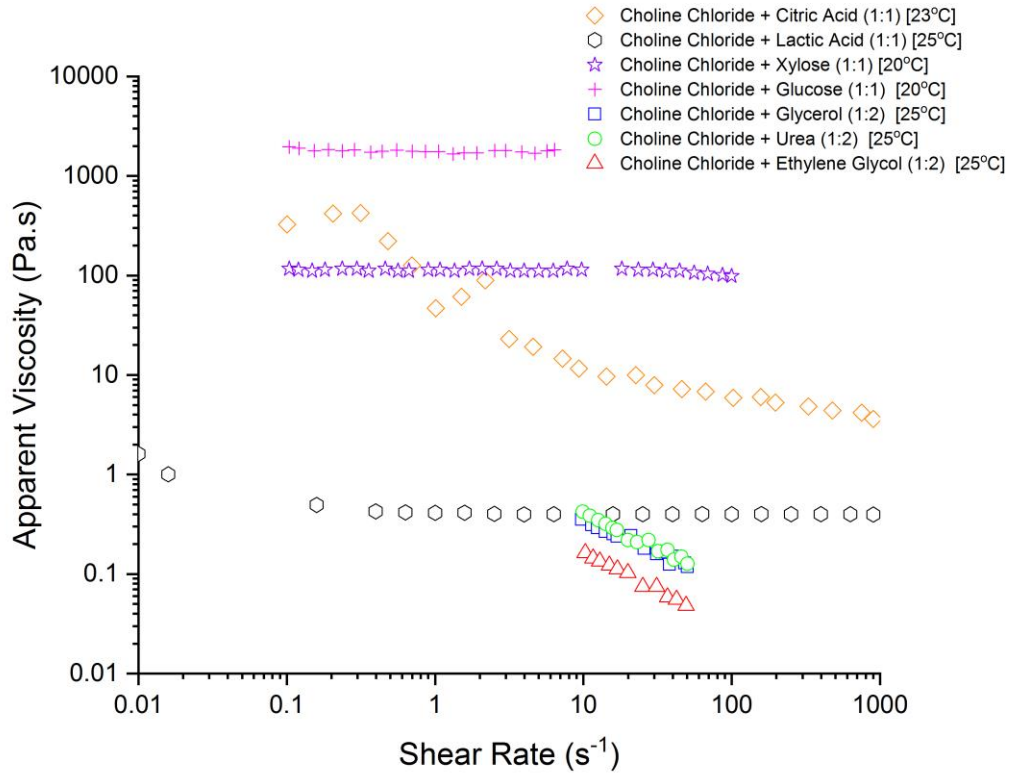


Figure 2.1: log-log scale representation of the apparent viscosity (Pa.s) vs shear rate (s^{-1}) for Choline Chloride Citric Acid (1:1)[48], Choline Chloride Lactic Acid (1:1) [24], Choline Chloride xylose (1:1)[57] , Choline Chloride Glucose (1:1) [63], Choline Chloride glycerol (1:2) [65], Choline Chloride Urea (1:2)[65], Choline Chloride Ethyl Glycol (1:2) [65] at ambient temperature condition

2.2 Temperature dependency of NADES

The general analogy in NADES systems with increasing temperature is that the viscosity trend decreases with increase in the shear rate. Yan et al. [64] elaborated on the transport phenomena explanation for NADES systems, through his study on the usage of NADES as a heat transfer fluid. The main reason behind the significant decrease in viscosity with temperature increase is a result of the structural breakdown

caused by the structure thermal expansion and shearing effect, they also observed that at such conditions, the mixture starts to converge and physically behave as the pure HBD. In other studies, at high temperature conditions, the molecules flow smoothly and become less viscous because of the decrease in their internal resistance [66–68]. In a series of studies, Aroso et al. [57,63] measured the apparent viscosity at a fixed shear rate from 0.1-100 s⁻¹ under a series in the range of temperatures of 60 - 100 °C for choline chloride + glucose and choline + xylose (1:1) (Figure 2.2) (Figure 2.3.e,f). As the temperature increased, the initial viscosity (at 0.1 s⁻¹) ranged from 10.34- 0.68 Pa.s for the glucose system and from 2.29-0.42 Pa.s for the xylose system. At high shear rate (100 s⁻¹), the difference in magnitude for the viscosity reduced significantly, this is due to the structural breakdown for all the systems. At low temperature conditions, the viscosity of most NADES ranged from 0.05 Pa.s all the way up to 2000 Pa.s under different shear effects varying from 0.01 s⁻¹ to 1000 s⁻¹ by only changing the hydrogen bond donor and a slight addition of water contents for some components, while some other relevant properties remained constant. However, the difference was minimized when it came to high temperature conditions, the differences ranged from as little as 0.01 Pa.s to 2000 Pa.s over the same shear rate mentioned earlier. Hence, if the application required being low temperature, attention should be given to the donor. On the other hand, if the application is at high temperature, such dependence is not significant. As the shear rate began to achieve 100 s⁻¹, the change in viscosity was minimal reaching steady-state conditions. It can be concluded from this study that at high shear rate, the flow behavior for both tested NADES systems is independent of temperature and shear rate. Furthermore, Altamash et al. [24,25] reported extensive work on thermo-physical NADES characterization for a group of NADES systems at different temperatures for their promising use as cheap, and environmentally green

absorbents in CO₂ capture. As per their study on the four-different choline chloride 1:1 based NADES, they also extended the work to study the mole ratio effect under the effect of different temperatures for a solitary NADES system. In their work, choline chloride + phenylacetic acid system was measured at varied temperatures (35,55,75, and 90 °C). The apparent viscosity at continuous shear rate increase from 0.01 to 100 s⁻¹ was decreasing at all the applied temperatures. Their findings were similarly consistent with the general trend of NADES systems investigated in the literature. Moreover, the effect of mole ratio for the phenylacetic acid exhibited a dual behavior notice, for mole ratios of (1:2) and (1:3) under an intermediate shear rate of 10 s⁻¹, the flow behavior showed usual shear-thinning due to the breakdown of its structure. Although most of the studied look at the shear flow behavior of NADES, Altamash et al. [25] were the only to conduct a study on the different molar ratio behavior for a single system, which shows the lack in rheological properties for such an effect. The explained trends previously explained can be shown in Figure 2.3.e,f. Based on this conclusion, Ghaedi et al.[66] , who had conducted a group of studies based on six similar based HBA of phosphonium using three molar ratios of 1:4,1:10, and 1:16 under a temperature range from 25°C to 70°C also shows a matching agreement with the findings of Altamash et al.. They have showed that the increase of temperature decreases the viscosity with increasing quantity of HBD in a NADES system. On the other hand, the 1:4 system showed an unusual semi-solid material behavior at 35°C. Furthermore, when the viscosity as a function of temperature was measured for the 1:4 mole ratio, a viscosity value of over 6000 Pa.s was initially exhibited. However, with increasing the temperature, when the melting point (55°C) was achieved, a gel-like material began to form and the viscosity dramatically dropped to 1.2 Pa.s. In addition, Altamash et al [25] came to another interesting conclusion, in which they elaborated on

the molar ratio effectiveness on NADES viscosity as a function of temperature. As it was said that the molar ratio becomes an independent factor on viscosity at higher temperature ranges, while it significantly affects the behavior at low temperature conditions. This inference will have a significant application in many areas that require low viscosity at high temperatures to minimize pumping costs and practical usage in solvent applications that will increase the mass transport rates [66]. The systems choline chloride + lactic acid, choline chloride + citric acid, choline chloride + malic acid, choline chloride + malic acid, and choline chloride + fructose shown in Figure 2.2 to Figure 2.6 also validated their explanation to the behavior of the NADES. This latter result is in keeping with the previous studies showing that the viscosity decreases with temperature even at different NADES systems.

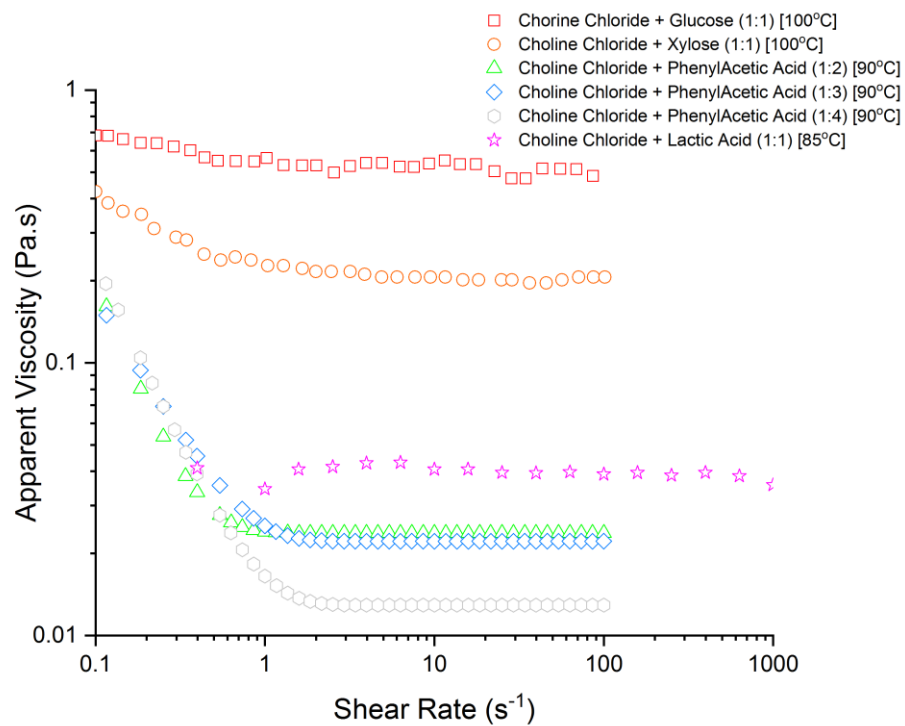


Figure 2.2: log-log representation of the apparent viscosity vs shear rate of different NADES: choline chloride + glucose (1:1)[63], choline chloride + xylose (1:1)[57], choline chloride + phenylacetic Acid (1:2)[25], choline chloride + phenylacetic acid (1:3)[25], choline chloride + phenylacetic acid (1:4)[25], choline chloride + lactic acid (1:1)[24] at high temperature conditions.

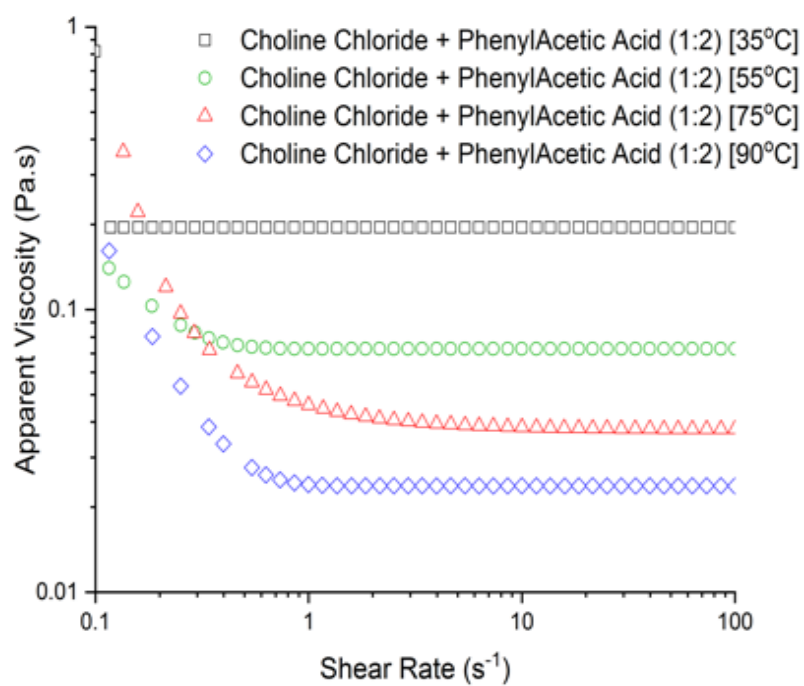


Figure 2.3: log-log representation of the apparent viscosity vs shear rate of different NADES systems at incremented temperatures for: choline chloride + phenylacetic acid (1:2) [25]

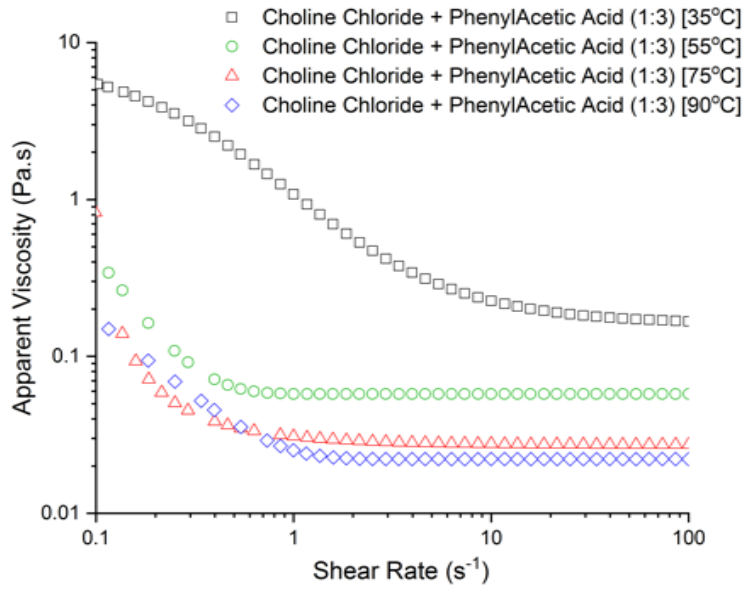


Figure 2.4: log-log representation of the apparent viscosity vs shear rate of different NADES systems at incremented temperatures for: choline chloride + phenylacetic acid (1:3) [25]

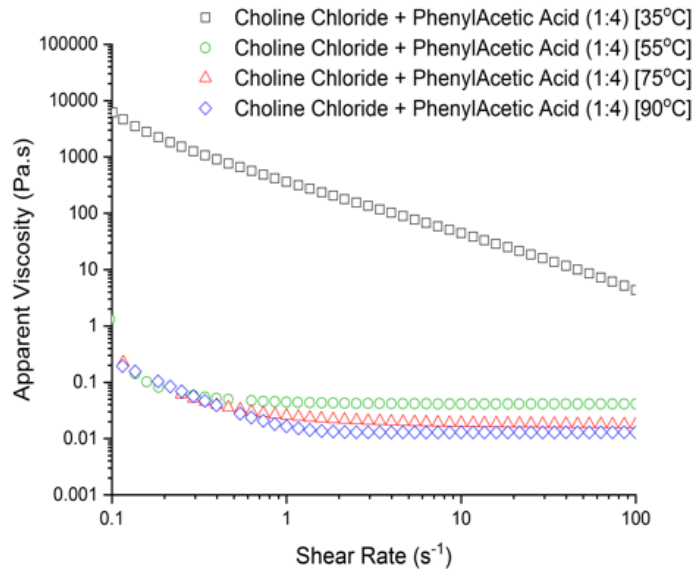


Figure 2.5: log-log representation of the apparent viscosity vs shear rate of different NADES systems at incremented temperatures for: choline chloride + phenylacetic acid (1:4) [25]

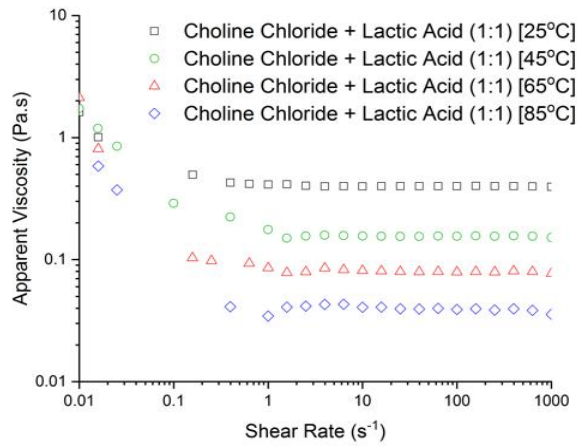


Figure 2.6: log-log representation of the apparent viscosity vs shear rate of different NADES systems at incremented temperatures for: choline chloride + lactic acid (1:1) [24]

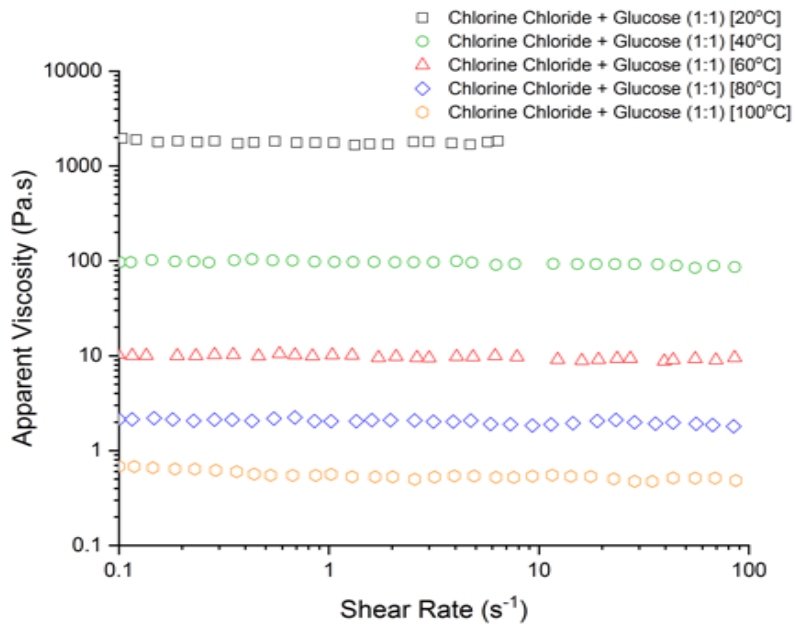


Figure 2.7: log-log representation of the apparent viscosity vs shear rate of different NADES systems at incremented temperatures for: choline chloride + glucose (1:1) [63]

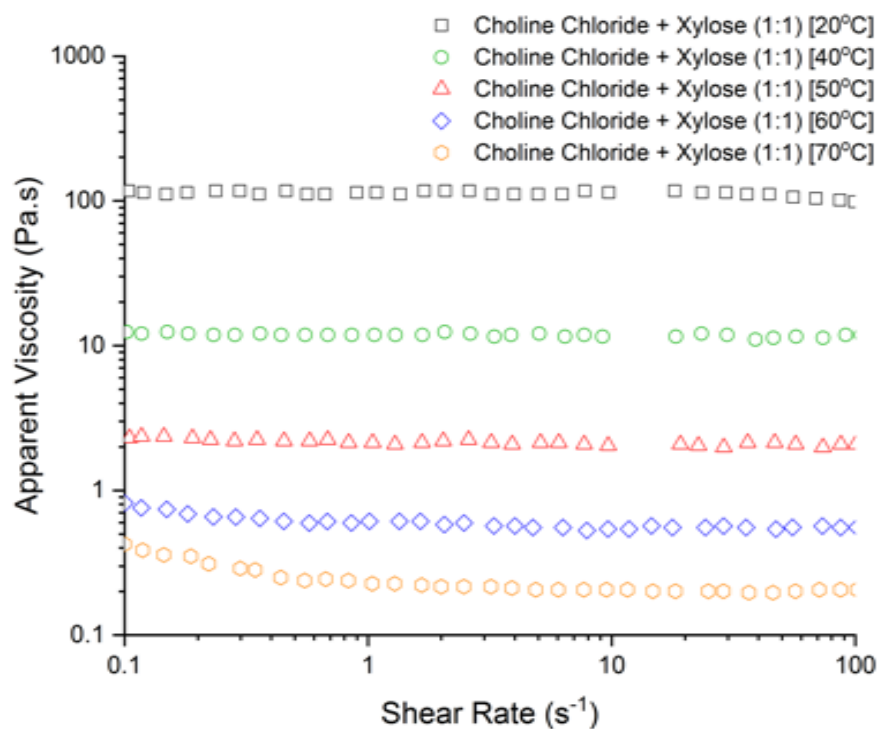


Figure 2.8: log-log representation of the apparent viscosity vs shear rate of different NADES systems at incremented temperatures for: choline chloride + xylose (1:1) [57]

2.3 Hydration Effect of NADES

Water plays a major role as a solvent for many living organisms and cells. Simple inclusion of water to flowing systems such as mineral oil makes it a versatile solution in several applications. The addition of water as a co-solvent to a NADES system can be considered as an impurity when handled in commercial applications that consequently lead to a significant change in the nature of a NADES. For instance, through moderate addition of water to a NADES, the phase separation ability and its absorption capability can be controlled [69–71]. In addition, hydration of NADES also has a significant effect in the creation and the shape control of nanoparticle

synthesis.[72] Water addition has also been shown to negatively affect the solubility of CO₂ on NADES with the increase of water percentage [69]. The interaction of water with binary tailor-made NADES system gives an additional reason to study the mechanisms involved in terms of molecular structure and the physiochemical properties, as these interactions clearly show its importance in different applications [73]. In the same study by Aroso et al [63][57], a specific rheological investigation was reported for the choline chloride + xylose (1:1) and choline chloride + glucose (1:1) (Figure 2.9) systems at different water contents of 0,1,3, and 5 wt. % at various different temperatures. At null water content, the relatively vast shear viscosity for glucose showed a constant Newtonian behavior over the shear rate of 0.1 to 100 s⁻¹. The shear viscosity was initially reported as 2000 Pa.s over the shear domain at ambient conditions. As the water content was increased to the system, the shear viscosity began to significantly decrease with shear especially at room temperature, where the viscosity was found to decreased to 400 Pa.s with only 1% added, 90 Pa.s at 3 wt% , and 25 Pa.s at 5% of water, respectively. In comparison with higher temperatures, at 100°C, the effect of hydration was negligible, as the change between the four water percentages only altered the viscosity from 1 Pa.s to 0.3 Pa.s. Dai et al. [74] has shown that the strong hydrogen bonding between the HBA and HBD are weakened down when water molecules are added. This is explained by the fact that the presence of any small amount of water molecules tend to form hydrogen bonds that decreases the viscosity that acts as plasticizer. Likewise, the choline chloride + xylose (1:1) system showed the same behavior over different water content under elevated shear rates. At room temperature, the shear viscosity showed a moderately lower order of magnitude than the glucose at 0% water, where the viscosity was found approximately to be 110 Pa.s. At 1,3, and 5 wt% water content, the viscosity decreased to 80, 22, 10 Pa.s, respectively. On the other

hand, at higher temperatures under the same shear rate, the temperature had insignificant effects on the shear viscosity, as the shear viscosity was only lowered from 0.3 Pa.s to 0.2 Pa.s at 100°C for this system. Das et al.[62] considered three different NADES systems as discussed (i.e. choline chloride + urea/ethylene glycol/glycerol (1:2) previously. The study involved the investigation of adding 10% wt of H₂O (Figure 2.9) of each system respectively. The main purpose of applying rheology in this study was to highlight the nature of k-carrageenan in the gel formation using different solvents. The apparent viscosity for all the systems was measured at room temperature conditions under moderate shear rates of 10-50 s⁻¹; where all the NADES showed non-Newtonian behavior in all cases. Its viscosity values showed a gradual decline as the shear rate interval was increased. Shear flow behaviors mainly showed that the anhydrate NADES had a lower degree of flowability, which makes them a stiff-like solvents over the measured domain. On the other hand, hydrated NADES showed a relatively higher degree of flowability and less stiff behavior. It can be concluded that these solvents can be used in applications that are water-content dependent such as pumping. Consequently, hydrated NADES were favored over the non-hydrated NADES, as the hydrated were more superior in quality and more effective in the extraction.

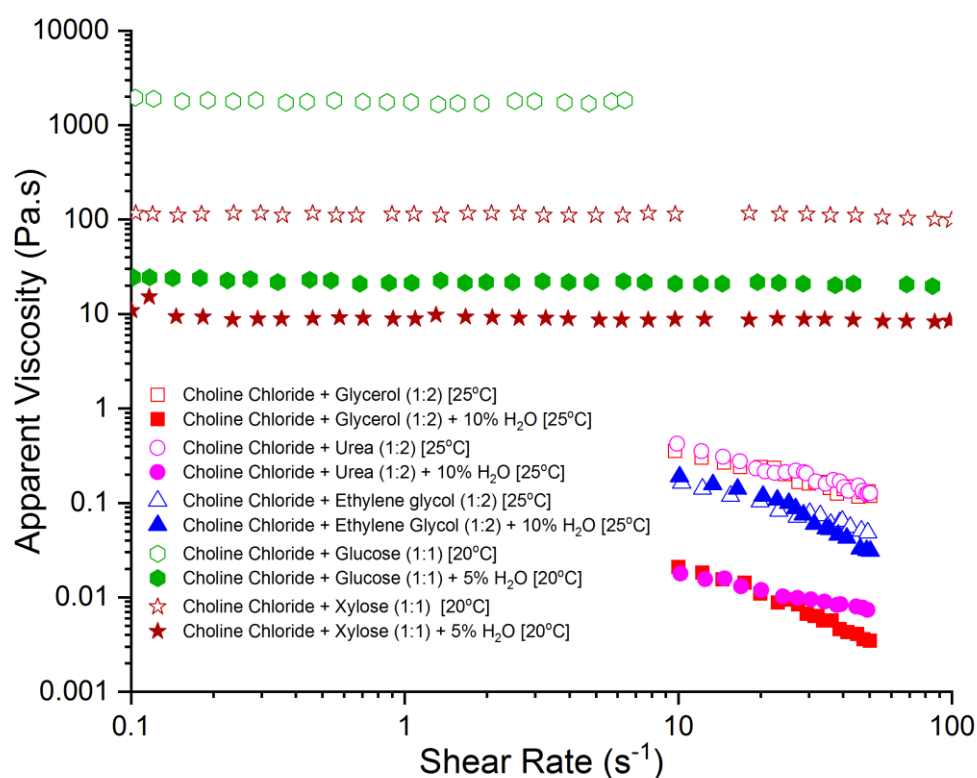


Figure 2.9: log-log representation of the apparent viscosity vs shear rate of different NADES systems with different hydration ratios : choline chloride + glucose (1:1)[63], choline chloride + glucose (1:1) + 5% H₂O[63], choline chloride + xylose (1:1) [57]+ choline chloride + xylose (1:1) + 5% H₂O[57], choline chloride + glycerol (1:2) [65], choline chloride + glycerol (1:2) + 10% H₂O[65], choline chloride + urea (1:2)[65] , choline chloride + urea (1:2) + 10% H₂O [65], choline chloride + ethylene glycol (1:2)[65], choline chloride + ethylene glycol (1:2) + 10% H₂O [65] at ambient condition

Next the behavior of different combinations for NADES/ILs is considered i.e. changing the cation and anion in IL while varying the Hydrogen Bond Donor (HBD) and holding the Hydrogen Bond Acceptor (HBA) constant for NADES. A combination

of all the recent efforts conducted on all the solvents were extracted, grouped, and categorized in order to visualize the main factors that can potentially influence the change in apparent viscosity over high shear rate. Due to the relevance of Natural Deep Eutectic Solvents rheology on process design and performance, many studies on the apparent viscosity are published in literature. Table 2.1 gives an intensive overview of all the key research papers, mainly highlighting the initial viscosity and steady-state viscosity for all the solvents with different scenarios. It shows the type of NADES with the type of additive studied, shear rate range, temperature range, and the fixed shear rate for the apparent viscosity against measurements if found.

Table 2.1: Overview on the rheological characterization and experimental setups for shear flow behaviors for varies tailor-made Natural Deep Eutectic Solvents

Full name	Additive		Viscosity Vs Shear rate			Viscosity vs Temperature			Ref
	Shear rate range		Temp	Initial	Steady-	Temp	Initial	Steady-	
			.	Viscosity	state	p.	Viscosity	state	
				y	Viscosity	ity	Viscosity		
(s ⁻¹)		(°C)	(Pa.s)	(Pa.s)	(°C)	(Pa.s)	(Pa.s)		
Choline Chloride + Ethylene Glycol (1:2)	-	-	-	-	-	27-87	0.4	0.15	[75]
Choline Chloride + Ethylene Glycol (1:2)	-	-	-	-	-	27-87	0.44	0.1	
Choline Chloride + Glycerol (1:2)	-	-	-	-	-	27-87	2.5	0.3	
Choline Chloride + Urea (1:2)	-	-	-	-	-	27-87	5	0.6	
Choline Chloride + Malonic Acid (1:1)	-	-	-	-	-	27-87	12.9	2	

Full name	Additive		Viscosity Vs Shear rate			Viscosity vs Temperature				
	Concentration	Solvent	Shear	Temp	Initial	Shear	Temp.	Initial	Steady-	Ref
			rate	.	Viscosit	rate		Viscos	state	
			range		y	range		ity	Viscosity	
(s ⁻¹)	(°C)	(Pa.s)	(Pa.s)	(°C)	(Pa.s)	(Pa.s)				
Choline Chloride + Malonic Acid (1:1)	-	-	-	-	-	27-87	0.5	0.55		
Choline Chloride + Ethylene Glycol (1:2)	-	-	-	-	-	17-87	0.4	0.15		
Choline Chloride + Ethylene Glycol (1:2)	5wt%	-	-	-	-	17-87	0.3	0.14		
	H ₂ O									
Choline Chloride + Ethylene Glycol (1:2)	20wt%	-	-	-	-	17-87	0.18	0.1		
	H ₂ O									
Choline Chloride + Ethylene Glycol (1:2)	25wt%	-	-	-	-	17-87	0.15	0.09		
	H ₂ O									

Full name	Additive		Viscosity Vs Shear rate			Viscosity vs Temperature		
	e		Temp	Initial Viscosity	Shear rate range	Temp.	Initial Viscosity	Shear rate range
	Shear rate range	(s ⁻¹)						
Choline Chloride + Ethylene Glycol (1:2)	-	-	-	-	-	17-87	0.51	0.13
refCholine Chloride + Ethylene Glycol (1:2)	5wt%	-	-	-	-	17-87	0.37	0.12
	H ₂ O							
Choline Chloride + Ethylene Glycol (1:2)	10wt%	-	-	-	-	17-87	0.33	0.11
	H ₂ O							
Choline Chloride + Malonic Acid (1:1)	-	-	-	-	-	17-87	0.16	0.08
Choline Chloride + Malonic Acid (1:1)	-	-	-	-	-	17-87	0.12	0.075

Full name	Additive		Viscosity Vs Shear rate			Viscosity vs Temperature		
	Shear rate range	(s ⁻¹)	Temp	Initial	Shear	Temp.	Initial	Shear
			.	Viscosity	rate		Viscosity	rate
				y	range		ity	range
		(°C)	(Pa.s)	(Pa.s)	(°C)	(Pa.s)	(Pa.s)	
Choline Chloride + Malonic Acid (1:1)	-	-	-	-	-	17-87	0.07	0.065
Choline Chloride + Urea (1:2)	-	-	-	-	-	17-87	7.6	1.1
Choline Chloride + Urea (1:2)	-	-	-	-	-	17-87	1.5	1
Choline Chloride + Urea (1:2)	-	-	-	-	-	17-87	1.2	1
Benzyltributylammonium Chloride + Phenol (1:3)	-	1-1000	25	0.4	0.4	20-70	0.65	0.1
Benzyltributylammonium Chloride + Ethylene Glycol (1:3)	-	1-1000	25	0.2	0.2	20-70	0.32	0.1

[76]

Full name	Additive		Viscosity Vs Shear rate			Viscosity vs Temperature		
	Shear rate range (s ⁻¹)	Temp (°C)	Initial Viscosity (Pa.s)	Shear rate range (Pa.s)	Temp (°C)	Initial Viscosity (Pa.s)	Shear rate range (Pa.s)	
			Temp (°C)	Initial Viscosity (Pa.s)	Shear rate range (Pa.s)	Temp (°C)	Initial Viscosity (Pa.s)	Shear rate range (Pa.s)
			Temp (°C)	Initial Viscosity (Pa.s)	Shear rate range (Pa.s)	Temp (°C)	Initial Viscosity (Pa.s)	Shear rate range (Pa.s)
Benzyltributylammonium Chloride + Lactic Acid (1:3)	-	1-1000	25	10	10	20-70	2.26	0.2
Benzyltributylammonium Chloride + Glycerol (1:3)	-	1-1000	25	3	3	20-70	1.8	0.22
Citric Acid + Glucose (1:1)	-	0.1-1000	23	280	30	-	-	- [48]
Choline Chloride + Citric Acid (1:1)	-	0.01-1000	23	350	3.5	-	-	-
Choline Chloride + Urea (1:2)	-	-	-	-	-	20-100	1.5	0.05 [77]

Full name	Additive		Viscosity Vs Shear rate			Viscosity vs Temperature		
	Shear rate range (s ⁻¹)	Temp (°C)	Initial Viscosity (Pa.s)	Shear rate range (Pa.s)	Temp.	Initial Viscosity	Shear rate range	
			Temp.	Initial Viscosity	Temp.	Initial Viscosity	Shear rate range	
								Temp.
Choline Chloride + Urea (1:2)	-	-	-	-	20-100	0.75	0.05	
Choline Chloride + Urea (1:2)	-	-	-	-	20-100	0.39	0.05	
Choline Chloride + Urea (1:2)	-	-	-	-	20-100	0.32	0.05	
Choline Chloride + Urea (1:2)	-	-	-	-	20-100	0.21	0.05	
Choline Chloride + Urea (1:2)	-	-	-	-	20-100	1.67	0.1	

Full name	Additive		Viscosity Vs Shear rate			Viscosity vs Temperature		
	e		Temp	Initial	Shear	Tem	Initial	Shear
	Shear rate range		.	Viscosity	rate range	p.	Viscosity	rate range
	(s ⁻¹)		(°C)	(Pa.s)	(Pa.s)	(°C)	(Pa.s)	(Pa.s)
Choline Chloride + Urea (1:2)	-	-	-	-	-	20-100	0.91	0.1
Choline Chloride + Urea (1:2)	-	-	-	-	-	20-100	0.49	0.1
Choline Chloride + Urea (1:2)	-	-	-	-	-	20-100	0.35	0.1
Choline Chloride + Urea (1:2)	-	-	-	-	-	20-100	0.2	0.1
Choline Chloride + Urea (1:2)	-	-	-	-	-	20-100	5	0.12

Full name	Additive		Viscosity Vs Shear rate			Viscosity vs Temperature		
	e		Temp	Initial	Shear	Tem	Initial	Shear
	Shear rate range		.	Viscosity	rate range	p.	Viscosity	rate range
	(s ⁻¹)		(°C)	(Pa.s)	(Pa.s)	(°C)	(Pa.s)	(Pa.s)
Choline Chloride + Urea (1:2)	-	-	-	-	-	20-100	1.3	0.12
Choline Chloride + Urea (1:2)	-	-	-	-	-	20-100	0.3	0.12
Choline Chloride + Urea (1:2)	-	-	-	-	-	20-100	0.2	0.12
Choline Chloride + Urea (1:2)	-	-	-	-	-	20-100	0.15	0.12
Choline Chloride + Xylose (1:1)	-	0.1-100	10	450	430	-	-	- [57]
Choline Chloride + Xylose (1:1)	-	0.1-100	20	110	90	-	-	-
Choline Chloride + Xylose (1:1)	-	0.1-100	30	35	30	-	-	-

Full name		Additive	Viscosity Vs Shear rate			Viscosity vs Temperature		
		e	Temp	Initial	Shear	Tem	Initial	Shear
		Shear	.	Viscosit	rate	p.	Viscos	rate
		rate		y	range		ity	range
range	(s ⁻¹)	(°C)	(Pa.s)	(Pa.s)	(°C)	(Pa.s)	(Pa.s)	
Choline Chloride + Xylose (1:1)	-	0.1-100	40	12	10	-	-	-
Choline Chloride + Xylose (1:1)	-	0.1-100	50	5	4	-	-	-
Choline Chloride + Xylose (1:1)	-	0.1-100	60	2	2	-	-	-
Choline Chloride + Xylose (1:1)	-	0.1-100	70	1.1	1	-	-	-
Choline Chloride + Xylose (1:1)	-	0.1-100	80	0.8	0.65	-	-	-
Choline Chloride + Xylose (1:1)	-	0.1-100	90	0.6	0.4	-	-	-
Choline Chloride + Xylose (1:1)	-	0.1-100	100	0.4	0.2	-	-	-
Choline Chloride + Xylose (1:1)	-	0.1-100	10	300	250	-	-	-
Choline Chloride + Xylose (1:1)	-	0.1-100	20	80	80	-	-	-
Choline Chloride + Xylose (1:1)	-	0.1-100	30	26	25	-	-	-
Choline Chloride + Xylose (1:1)	-	0.1-100	40	9	9	-	-	-

Full name		Additive	Viscosity Vs Shear rate			Viscosity vs Temperature		
		e	Temp	Initial	Shear	Temp	Initial	Shear
		Shear rate range	.	Viscosity	rate range	p.	Viscosity	rate range
		(s ⁻¹)	(°C)	(Pa.s)	(Pa.s)	(°C)	(Pa.s)	(Pa.s)
Choline Chloride + Xylose (1:1)	-	0.1-100	50	4	3.5	-	-	-
Choline Chloride + Xylose (1:1)	-	0.1-100	60	2	1.5	-	-	-
Choline Chloride + Xylose (1:1)	-	0.1-100	70	1	0.9	-	-	-
Choline Chloride + Xylose (1:1)	-	0.1-100	80	0.7	0.45	-	-	-
Choline Chloride + Xylose (1:1)	-	0.1-100	90	0.5	0.3	-	-	-
Choline Chloride + Xylose (1:1)	-	0.1-100	100	0.4	0.18	-	-	-
Choline Chloride + Xylose (1:1)	-	0.1-100	10	70	60	-	-	-
Choline Chloride + Xylose (1:1)	-	0.1-100	20	20	19	-	-	-
Choline Chloride + Xylose (1:1)	-	0.1-100	30	8	8	-	-	-
Choline Chloride + Xylose (1:1)	-	0.1-100	40	3.8	3	-	-	-
Choline Chloride + Xylose (1:1)	-	0.1-100	50	1.9	1.5	-	-	-

Full name		Additive	Viscosity Vs Shear rate			Viscosity vs Temperature		
		e	Temp	Initial	Shear	Tem	Initial	Shear
		Shear	.	Viscosit	rate	p.	Viscos	rate
		rate		y	range		ity	range
range	(s ⁻¹)	(°C)	(Pa.s)	(Pa.s)	(°C)	(Pa.s)	(Pa.s)	
Choline Chloride + Xylose (1:1)	-	0.1-100	60	1	0.8	-	-	-
Choline Chloride + Xylose (1:1)	-	0.1-100	70	0.8	0.42	-	-	-
Choline Chloride + Xylose (1:1)	-	0.1-100	80	0.5	0.28	-	-	-
Choline Chloride + Xylose (1:1)	-	0.1-100	90	0.4	0.19	-	-	-
Choline Chloride + Xylose (1:1)	-	0.1-100	100	0.38	0.13	-	-	-
Choline Chloride + Xylose (1:1)	-	0.1-100	10	25	21	-	-	-
Choline Chloride + Xylose (1:1)	-	0.1-100	20	10	10	-	-	-
Choline Chloride + Xylose (1:1)	-	0.1-100	30	4.8	4.1	-	-	-
Choline Chloride + Xylose (1:1)	-	0.1-100	40	2.6	2	-	-	-
Choline Chloride + Xylose (1:1)	-	0.1-100	50	1.5	1.5	-	-	-
Choline Chloride + Xylose (1:1)	-	0.1-100	60	0.8	0.7	-	-	-

Full name		Additive		Viscosity Vs Shear rate			Viscosity vs Temperature				
		Shear rate range (s ⁻¹)	Temp (°C)	Initial Viscosity (Pa.s)	Shear rate range (Pa.s)	Temp. (°C)	Initial Viscosity (Pa.s)	Shear rate range (Pa.s)			
Choline Chloride + Xylose (1:1)	-	0.1-100	70	0.6	0.45	-	-	-			
Choline Chloride + Xylose (1:1)	-	0.1-100	80	0.5	0.25	-	-	-			
Choline Chloride + Xylose (1:1)	-	0.1-100	90	0.4	0.2	-	-	-			
Choline Chloride + Xylose (1:1)	-	0.1-100	100	0.3	0.12	-	-	-			
Choline Chloride + PhenylAcetic Acid (1:2)	-	0.1-100	35	1	0.45	27-97	0.8	0.2 [25]			
Choline Chloride + PhenylAcetic Acid (1:3)	-	0.1-100	35	8	0.4	27-97	6	0.2			
Choline Chloride + PhenylAcetic Acid (1:4)	-	0.1-100	35	8000	8.1	27-97	7000	0.1			

Full name		Additive	Viscosity Vs Shear rate			Viscosity vs Temperature			
			Shear rate range (s ⁻¹)	Temp	Initial Viscosity	Shear rate range (Pa.s)	Temp	Initial Viscosity	Shear rate range (Pa.s)
				°C	(Pa.s)	(Pa.s)	°C	(Pa.s)	(Pa.s)
				.	y		p.	ity	range
Choline Chloride + PhenylAcetic Acid (1:2)	-	0.1-100	55	0.4	0.08	-	-	-	
Choline Chloride + PhenylAcetic Acid (1:3)	-	0.1-100	55	0.38	0.07	-	-	-	
Choline Chloride + PhenylAcetic Acid (1:4)	-	0.1-100	55	1	0.035	-	-	-	
Choline Chloride + PhenylAcetic Acid (1:2)	-	0.1-100	75	0.3	0.042	-	-	-	
Choline Chloride + PhenylAcetic Acid (1:3)	-	0.1-100	75	0.18	0.03	-	-	-	

Full name	Additive		Viscosity Vs Shear rate			Viscosity vs Temperature		
	-	Shear rate range (s ⁻¹)	Temp (°C)	Initial Viscosity (Pa.s)	Shear rate range (Pa.s)	-	-	-
Choline Chloride + PhenylAcetic Acid (1:4)	-	0.1-100	75	0.1	0.02	-	-	-
Choline Chloride + PhenylAcetic Acid (1:2)	-	0.1-100	90	0.15	0.03	-	-	-
Choline Chloride + PhenylAcetic Acid (1:3)	-	0.1-100	90	0.15	0.025	-	-	-
Choline Chloride + PhenylAcetic Acid (1:4)	-	0.1-100	90	0.5	0.015	-	-	-
Choline Chloride + Thiourea (1:2)	-	0-200	60	1.39	0.4	-	-	-

[78]

Full name		Additive		Viscosity Vs Shear rate			Viscosity vs Temperature		
		e		Temp	Initial	Shear	Tem	Initial	Shear
		Shear	rate						
		rate	range	p.	Viscosity	rate	p.	Viscosity	rate
(s ⁻¹)	(Pa.s)	(Pa.s)	(°C)	(Pa.s)	(°C)	(Pa.s)	(Pa.s)		
Chlorine Chloride : Urea (1:2)	-	10-50	25	550	350	-	-	-	[62]
Choline Chloride + Ethylene Glycol (1:2)	-	10-50	25	200	70	-	-	-	
Chlorine Chloride : Glycerol (1:2)	-	10-50	25	550	400	-	-	-	
Chlorine Chloride : Urea (1:2)	-	10-50	25	20	10	-	-	-	
Choline Chloride + Ethylene Glycol (1:2)	-	10-50	25	200	40	-	-	-	
Chlorine Chloride : Glycerol (1:2)	-	10-50	25	20	4	-	-	-	
Chlorine Chloride : Glucose (1:1)	-	0.1-100	10	-	-	-	-	-	[63]
Chlorine Chloride : Glucose (1:1)	-	0.1-100	20	2000	2000	-	-	-	
Chlorine Chloride : Glucose (1:1)	-	0.1-100	30	350	348	-	-	-	

Full name		Additive	Viscosity Vs Shear rate			Viscosity vs Temperature			
			Shear rate range (s ⁻¹)	Temp	Initial	Shear	Tem	Initial	Shear
				.	Viscosity	rate	p.	Viscosity	rate
				(°C)	(Pa.s)	(Pa.s)	(°C)	(Pa.s)	(Pa.s)
Chlorine Chloride : Glucose (1:1)	-	0.1-100	40	100	900	-	-	-	
Chlorine Chloride : Glucose (1:1)	-	0.1-100	50	27	25	-	-	-	
Chlorine Chloride : Glucose (1:1)	-	0.1-100	60	10	10	-	-	-	
Chlorine Chloride : Glucose (1:1)	-	0.1-100	70	5	4	-	-	-	
Chlorine Chloride : Glucose (1:1)	-	0.1-100	80	2	2	-	-	-	
Chlorine Chloride : Glucose (1:1)	-	0.1-100	90	1	1	-	-	-	
Chlorine Chloride : Glucose (1:1)	-	0.1-100	100	0.7	0.6	-	-	-	
Chlorine Chloride : Glucose (1:1)	-	0.1-100	10	2000	1950	-	-	-	
Chlorine Chloride : Glucose (1:1)	-	0.1-100	20	600	600	-	-	-	
Chlorine Chloride : Glucose (1:1)	-	0.1-100	30	110	100	-	-	-	
Chlorine Chloride : Glucose (1:1)	-	0.1-100	40	35	30	-	-	-	

Full name	Additive	Viscosity Vs Shear rate			Viscosity vs Temperature			
		Shear rate range (s ⁻¹)	Temp	Initial	Shear	Tem	Initial	Shear
			.	Viscosit	rate	p.	Viscos	rate
				y	range		ity	range
		(°C)	(Pa.s)	(Pa.s)	(°C)	(Pa.s)	(Pa.s)	
Chlorine Chloride : Glucose (1:1)	-	0.1-100	50	15	15	-	-	-
Chlorine Chloride : Glucose (1:1)	-	0.1-100	60	7	7	-	-	-
Chlorine Chloride : Glucose (1:1)	-	0.1-100	70	3	3.5	-	-	-
Chlorine Chloride : Glucose (1:1)	-	0.1-100	80	1.8	1.8	-	-	-
Chlorine Chloride : Glucose (1:1)	-	0.1-100	90	1	1	-	-	-
Chlorine Chloride : Glucose (1:1)	-	0.1-100	100	0.5	0.5	-	-	-
Chlorine Chloride : Glucose (1:1)	-	0.1-100	10	350	300	-	-	-
Chlorine Chloride : Glucose (1:1)	-	0.1-100	20	90	80	-	-	-
Chlorine Chloride : Glucose (1:1)	-	0.1-100	30	20	18	-	-	-
Chlorine Chloride : Glucose (1:1)	-	0.1-100	40	9	9	-	-	-
Chlorine Chloride : Glucose (1:1)	-	0.1-100	50	5.5	6	-	-	-

Full name	Additive		Viscosity Vs Shear rate			Viscosity vs Temperature		
	e		Temp	Initial Viscosity	Shear rate	Temp.	Initial Viscosity	Shear rate
	Shear rate range	(s ⁻¹)						
Chlorine Chloride : Glucose (1:1)	-	0.1-100	60	2	3	-	-	-
Chlorine Chloride : Glucose (1:1)	-	0.1-100	70	1.5	1.8	-	-	-
Chlorine Chloride : Glucose (1:1)	-	0.1-100	80	0.8	0.8	-	-	-
Chlorine Chloride : Glucose (1:1)	-	0.1-100	90	0.6	0.6	-	-	-
Chlorine Chloride : Glucose (1:1)	-	0.1-100	100	0.4	0.25	-	-	-
Chlorine Chloride : Glucose (1:1)	-	0.1-100	10	68	60	-	-	-
Chlorine Chloride : Glucose (1:1)	-	0.1-100	20	25	20	-	-	-
Chlorine Chloride : Glucose (1:1)	-	0.1-100	30	10	9	-	-	-
Chlorine Chloride : Glucose (1:1)	-	0.1-100	40	4.5	4	-	-	-
Chlorine Chloride : Glucose (1:1)	-	0.1-100	50	2.8	2	-	-	-
Chlorine Chloride : Glucose (1:1)	-	0.1-100	60	1.5	1	-	-	-

Full name	Additive		Viscosity Vs Shear rate			Viscosity vs Temperature			
	Shear rate range	(s ⁻¹)	Temp	Initial	Shear	Temp	Initial	Shear	
			(°C)	Viscosity	rate	p.	Viscosity	rate	
			(Pa.s)	(Pa.s)	(Pa.s)	(°C)	(Pa.s)	(Pa.s)	
Chlorine Chloride : Glucose (1:1)	-	0.1-100	70	1	0.8	-	-	-	
Chlorine Chloride : Glucose (1:1)	-	0.1-100	80	0.7	0.55	-	-	-	
Chlorine Chloride : Glucose (1:1)	-	0.1-100	90	0.5	0.4	-	-	-	
Chlorine Chloride : Glucose (1:1)	-	0.1-100	100	0.4	0.2	-	-	-	
Chlorine Chloride : Glycerol (1:2)	-	-	-	-	-	17-97	0.41	0.09	
Choline Chloride + Ethylene Glycol (1:2)	-	-	-	-	-	17-97	0.1	0.05	
Chlorine Chloride : Citric Acid (1:1)	7.8wt% PVA	0.1- 1000	25	0.35	0.42	-	-	-	[79]

Full name	Additive		Viscosity Vs Shear rate			Viscosity vs Temperature		
	e		Temp	Initial Viscosity	Shear rate range	Temp.	Initial Viscosity	Shear rate range
	Shear rate range	(s ⁻¹)						
Chlorine Chloride : Citric Acid (1:1) 9.8 wt% PVA	-	0.1-1000	25	0.56	0.58	-	-	-
Chlorine Chloride : Lactic Acid (1:1)	-	0.01-100	25	1.6	0.4	-	-	- [62]
Chlorine Chloride : Lactic Acid (1:1)	-	0.01-100	45	1.4	0.18	-	-	-
Chlorine Chloride : Lactic Acid (1:1)	-	0.01-100	65	2	0.08	-	-	-

Full name		Additive		Viscosity Vs Shear rate			Viscosity vs Temperature		
		e		Temp	Initial Viscosity	Shear rate range	Temp.	Initial Viscosity	Shear rate range
		Shear rate range	(s ⁻¹)						
		(s ⁻¹)	(°C)	(Pa.s)	(Pa.s)	(°C)	(Pa.s)	(Pa.s)	
Chlorine Chloride : Lactic Acid (1:1)	-	0.01-100	85	0.58	0.04	-	-	-	
Chlorine Chloride : Lactic Acid (1:1)	-	-	-	-	-	15-95	0.28	0.08	
Chlorine Chloride : Malic Acid (1:1)	-	-	-	-	-	15-95	3.5	0.3	
Chlorine Chloride : Citric Acid (1:1)	-	-	-	-	-	15-95	1000	0.95	
Chlorine Chloride : Fructose (1:1)	-	-	-	-	-	15-95	0.36	0.1	

Full name	Additive		Viscosity Vs Shear rate			Viscosity vs Temperature			
	Shear rate range	(s ⁻¹)	Temp	Initial	Shear	Temp	Initial	Shear	
			.	Viscosity	rate	p.	Viscosity	rate	
				y	range		ity	range	
		(°C)	(Pa.s)	(Pa.s)	(°C)	(Pa.s)	(Pa.s)		
Chlorine Chloride : p-toluensulfonic acid (2:1)	-	-	-	-	-	7--67	1.83	0.1	[80]
Chlorine Chloride : trichloroacetic acid (2:1)	-	-	-	-	-	7--67	1	0.09	
Chlorine Chloride : monochloroacetic acid (2:1)	-	-	-	-	-	7--67	0.2	0.05	
Chlorine Chloride : propionic acid (2:1)	-	-	-	-	-	7--67	0.1	0.05	

2.4 Viscoelastic behavior of NADES

Mukesh et al.[81] prepared choline chloride and orcinol with a polymerized 0.35, 0.5 and 1% v/v of 2-hydroxyethyl methacrylate (HEMA). Results revealed that the nature of this polymerized gel combination was highly stretchable. The quality of the gel from the physical strength and reusability was described through the structural matrix of the solvent. When HEMA and NADES solution (unpolymerized mixture) were measured, the magnitude of $G'' > G'$, meaning that the formed mixture was viscous. On the other hand, the polymerized mixture showed values of $G' \gg G''$, indicating a true gel formation. Furthermore, crossover of the moduli only occurred at high frequencies in the unpolymerized mixture, which showed a liquid-like solution, while no crossover was found before for the polymerized HEMA with increasing frequency. Moreover, the stretching/flexible behavior was studied by considering the recovery of G' of the ion-gel obtained for the 1:0.35 NADES:HEMA. The sample was loaded under varied strain at 1 Hz frequency for 300 s, while strain was applied to the sample, both of the moduli decreased until 500% of the applied strain was established. The strain effect was continued on the ion gel to study the fracture on the sample. It was shown that both of the moduli remained almost constant for the entire duration, meaning that the ion gels were not affected by strain and unfractured. As a result, this showed how this combination of polymerized NADES can be an excellent flexible and durable nature ion gel with a high stretchable nature. Das et al. [65] studied the viscoelasticity of three different deep eutectic solvents prepared by the complexation of choline chloride with urea, ethylene glycol and glycerol as well as their hydrated counterparts were used for the selective extraction of a hydrocolloid (*k*-carrageenan) from sea moss algae (*Kappaphycus. Alvarezii*). The time dependency measurements for all the kC gels showed a gel like behavior ($G' \gg G''$) during the entire period of extraction, where the

difference between the G' and G'' was relatively high for the case the kC gels extracted using choline chloride + glycerol (1:2) and hydrated choline chloride + ethylene glycol 1:2. Moreover, they concluded that the presence of the NADES enhanced less stiffness and better viscoelasticity in comparison with other conventional extraction methods like water as a solvent. Furthermore, the crossover of G' and G'' found as a result of increasing the angular frequency for all the kC gel systems, spots the attention of how weak the gels are, whereas the G'' and predominate over the G' for a wide frequency range, which shows that the presence of different flow components in the tailored gel that are viscous liquids at lower frequencies. However, at higher frequency ranges, the G' started to become predominant in manganite over G'' indicating an elastic nature of these gels. Furthermore, Altamash et al. [22,24] looked at the interaction forces between different pure combinations of HBA (choline chloride, B-alanine, and betaine) with different natural organic HBD (lactic acid, malic acid, citric acid, and fructose) with 1:1 molar ratios using oscillatory viscoelasticity. Throughout their studies, they have shown a consistent agreement between all the combinations in terms of the solvent behavior even at high temperatures, where the values of G'' were always higher than G' over the applied frequency from 0.1 – 100 rad/s. As a result, this shows that all the solvents were viscous liquids at all temperatures. The differences between G'' and G' reveal the presence of the initiative flow components within the gel structure. As the storage modulus diminishes ($G' \rightarrow 0$) an ideal viscous flow behavior (i.e. less stiffness) is witnessed. However, at high frequency and room temperature, the sample that contains malic acid as a HBD showed values of G' (7.2×10^4 Pa for betaine + malic acid and 3.3×10^4 Pa for alanine + malic acid) which is higher than G'' in comparison with lactic acid based magnitudes (2.3×10^2 Pa for B-alanine + lactic acid and 1.1×10^2 Pa for betaine + lactic acid). Moreover, they have concluded that with the increase

in temperature for the NADES, all the systems showed shear thinning behaviors over the applied frequency as a result of the interaction forces between the HBA and HBD forces and the thermal expansion. In conclusion, they elaborated on highly recommending choline chloride + lactic acid, betaine + lactic acid, B-alanine + lactic acid, and choline chloride + fructose for CO₂ applications since preheating or pumping of sorbents is required.

Table 2.2: Overview on the rheological characterization and experimental setups for Oscillatory behaviors for various tailor-made Natural Deep Eutectic Solvents (NADES) at ambient conditions.

DES used	Additive	Angular Frequency range	Strain amplitude (%)	Observations and conclusions	measurements	References
choline chloride+ urea 1:2	0 %			1) using pure NADES as solvents showed viscous liquid behaviour in the angular frequency range of 500-650 s ⁻¹ .		
choline chloride+ ethylene glycol 1:2	Hydrated 10%	0.05- 800 1/s	0.1% and frequency 0.01 Hz	2) After the crossover of the moduli, the store modulus started to become predominant over the loss modulus indicating elastic nature of the gels at higher frequency range	G',G'' vs angular frequency,Complex viscosity vs temperaure	[62]
choline chloride+ glycerol 1:2	Hydrated					

Name	Additive	Angular Frequency range	Strain amplitude (%)	Observations and conclusions	measurements conducted	References
Betaine + Malic acid				1) The greater difference in the values of G'' and G' (e.g. $G'' \gg G'$) indicating presence of more flow components in the gels making the gels behave like viscous liquid and as the $G' \rightarrow 0$ the material behave as ideal viscous	G', G'' vs angular	
Betaine + Lactic acid	-	0.1-100 rad/s	0.10	flow behavior	frequency, complex	[22]
B-alanine + Malic acid				2)The values of G', G'' , and η^* decreased as the temperature increased for all NADES systems as expected for the shear thinning materials and this is mainly due to the changes in the interaction forces between the hydrogen bond donor and hydrogen acceptor of the NADES and due to the thermal expansion	viscosity, G, G'' vs temperature	
B-alanine + Lactic acid						

2.5 Rheological Modeling

The aim of rheological modeling is to find a suitable and applicable fit for the experimental data collected after conducting the rheological measurements using mathematical models of different polynomial degrees. The models will describe the behavior of the fluid using the relationship between shear stress and shear rate. The collected data is then graphically represented for the shear rate-shear stress model, which will determine the best fit for the model. Several rheological models have been used and developed in literature in order to describe the rheological characteristics of NADES solvents and others as well. However, it is important to mention that no typical rheological model will give a clear explanation on the flow characteristics for all the NADES systems over their entire shear rate domain. After a rheological model is found suitable, the rheological data are then extended to model the flow behavior in other geometries (i.e. pipe flow or annular flow). Section 2.5 and onwards describe different rheological models from literature that focus on studying the flow resistance for NADES systems and the significant meaning of the equation being described.

2.5.1 Arrhenius Equation

The temperature dependency of the viscosity represents an exponential-like decay for most ILs and NADES. In order to account for the overall effect of temperature, a governing equation known as the Arrhenius equation is mostly used to describe the flow resistance for both ILs and NADES under different temperatures. This equation can be defined as in equation (1):

$$\ln \eta = \ln \eta_0 + \frac{E_A}{RT} \quad (4)$$

In this equation η is the dynamic viscosity ($10^6 Pa \cdot s$) that is measured at each temperature, η_0 is the viscosity parameter ($10^6 Pa \cdot s$) and also referred to as the pre-exponential factor in other references [82], R is the universal gas constant ($kJ \cdot mol^{-1} \cdot K^{-1}$), T is the absolute temperature (K) and E_A is the activation energy of the flow ($kJ \cdot mol^{-1}$). Throughout their studies on suspension rheology of hematite in ILs and pure ILs, Altin et al.[83] explained that the E_A parameter explains the structural form of the ILs, and they concluded that the strong intermolecular forces between the ions resulted in larger values of E_A for the suspension ILs with lower (20 % wt. of Fe_2O_3) than the ones with higher (% 40 wt Fe_2O_3). Likewise, Pamies et al.[82] also showed that the addition of aligned and non-aligned multiwalled carbon nanotubes (MWCNTs) influence the activation energy of 1-ethyl-3-methylimidazolium tosylate, as these additives have the ability to enhance the capacity of dispersion to flow in comparison with pure ILs and eventually lowering the activation energy. On the other hand, activation energy for NADES systems implies that the degree of flowability is dependent on the constituent particles [76]. In order for the solvent to flow, it must overcome the barrier energy of the E_A . Similar to ILs, the higher E_A generally describes the difficulty for particles to move. Furthermore, Aroso et al. [57] looked at the activation energy effect for choline chloride + xylose. Results have shown that the activation energy also decreases with the increase of water content present in the system, as the substantially hydrogen bond interactions decreases. It is also noteworthy to mention that the Arrhenius expression is a subclass of the general Vogel–Fulcher–Tamman (VFT), having $T_0 = 0$. Table 2.3 lists the Arrhenius model parameters for the selected NADES.

Table 2.3. Arrhenius model parameters for different Natural Deep Eutectic Solvents (NADES)

NADES	η_0 ($10^9 \times \text{Pa.s}$)	E_a (kJ/mol)	References
benzyltributylammonium chloride + phenol (1:3)	0.04	56.8	
benzyltributylammonium chloride + ethylene glycol (1:3)	3.05	44.9	[76]
benzyltributylammonium chloride + lactic acid (1:3)	0.0008	71.9	
benzyltributylammonium chloride + glycerol (1:3)	0.017	63.9	
choline chloride xylose @ 1:1	0.018	71.02	
choline chloride glucose @ 1:1	5.9×10^{-5}	91.52	
choline chloride sucrose @ 1:1	3.9×10^{-5}	104.5	
choline chloride citric acid @ 1:1	5.5×10^{-5}	96.15	
choline chloride tartaric acid @ 1:1	3.1×10^{-6}	102.08	
betaine citric acid @ 1:1	4.3×10^{-5}	97.79	[57]
betaine tartaric acid @ 1:1	6.9×10^{-6}	101.94	

2.5.2 Vogel-Fulcher-Tammann Equation

The general followability and transport property of ILs and NADES can also be modeled using The Vogel–Fulcher–Tammann (VFT) expression, which is a temperature dependence fitting model that best describes the molecular interactions, such as the van

der Waals type weak interactions and strong hydrogen bonding [84]. The parameters (Table 2.4) of this model include; η : dynamic viscosity (Pa.s), η_0, η_∞, A' (Equation 5-7): limiting high-temperature viscosity (Pa.s), B' : parameter related to free activation energy (K), T : temperature (K), T_0/T_∞ : Vogel temperature (K). Cui et al. [80] used a slightly modified notation to describe the Vogel–Fulcher–Tammann, where they replaced the B' parameter with activation energy and the K_B using E_A/K_B .

$$\eta = A' e^{\frac{B'}{T-T_0}} \quad (5)$$

$$\eta = \eta_0 e^{D^* \left(\frac{T_0}{T-T_0} \right)} \quad (6)$$

$$\eta = \eta_\infty e^{\left(\frac{E_a}{K_B(T-T_0)} \right)} \quad (7)$$

Table 2.4: Vogel-Fulcher-Tammann model parameters for different Natural Deep Eutectic Solvents (NADES)

NADES	η_0 or A' (Pa.s)	B' (K)	T_∞ or T_0 (K)	Reference
benzyltributylammonium chloride + phenol (1:3)	7.21×10^{-5}	748	211	
benzyltributylammonium chloride + ethylene glycol (1:3)	1.85×10^{-5}	1295	161	
benzyltributylammonium chloride + lactic acid (1:3)	3.23×10^{-5}	1046	209	[76]
benzyltributylammonium chloride + glycerol (1:3)	7.20×10^{-6}	1619	173	
choline chloride p- toluenesulfonic acid	1.30×10^{-4}	8478	200	
choline chloride trichloroacetic acid	6.29×10^{-5}	1033	181	[80]
choline chloride monochloro- roacetic acid @ 1:1:0	1.25×10^{-4}	788	183	

NADES	η_0 or A' (Pa.s)	B' (K)	T_∞ or T_0 (K)	Reference
choline chloride propionic acid @ 1:1:0	1.06×10^{-4}	855	162	[80]

2.5.3 Bingham Equation

The Bingham equation describes the viscosity function and to estimate the dynamic yield stress values [24], basically implies that the material is solid-like at low rates and stresses [85]. In addition, this model accounts for the behavior of many shear-thinning materials at low shear rates, but the calculated value of shear stress depends on the shear rate ranges used for the extrapolation procedure [59]. The Bingham model just takes into account the region with constant slope and in this case, it covers higher shear rates [86]. Another possibility is that the fluid behaves as a Bingham plastic, like for example toothpaste, in which the viscosity appears to be infinite until a certain value of shear stress is achieved [48]. The Bingham Equation for non-Newtonian fluids is given as following

$$\tau = \tau_B + \eta_B \dot{\gamma} \quad (9)$$

Where τ represents the shear stress, τ_B is the Bingham yield stress and η_B is the Bingham plastic viscosity, $\dot{\gamma}$ is the shear rate. The magnitude of τ_B is a useful parameter that can be used as indicative of the amount of minimum stress required disrupting the networked structure in order to initiate the flow. A yield stress below τ_B for the mixture means that the mixture behaves as a rigid solid [24]. In general, the yield stresses of all NADES decreased with increasing temperature as expected for the shear thinning materials. The differences in the yield stress values are mainly due to the changes in molecular mobility, such as chain rigidity, interaction forces between the hydrogen bond donor and hydrogen acceptor of the NADES and the molecular weight. The change of the yield stress values as a function of temperature is similar to the viscosity data (Table 2.6) [24].

Table 2.5: Bingham model parameters for different Natural Deep Eutectic Solvents (NADES)

NADES	τ_B (mPa)	η_B (mPa.s)	Ref.
choline chloride + phenylacetic acid based @ 1:2 - 55°C	16.8	73.6	
choline chloride + phenylacetic acid based @ 1:2 - 75 °C	6.7	38.3	
choline chloride + phenylacetic acid based @ 1:2 - 90 °C	0.9	25.2	
choline chloride + phenylacetic acid based @ 1:3 - 35 °C	712.4	160.4	
choline chloride + phenylacetic acid based @ 1:3 - 55 °C	35	60.7	
choline chloride + phenylacetic acid based @ 1:3 - 75 °C	14.9	24.5	
choline chloride + phenylacetic acid based @ 1:3 - 90 °C	9.1	24.4	
choline chloride + phenylacetic acid based @ 1:4 - 55 °C	31.2	35.3	
choline chloride + phenylacetic acid based @ 1:4- 75 °C	6.1	18.0	
choline chloride + phenylacetic acid based @ 1:4 - 90 °C	1.4	13.0	

NADES	τ_B (mPa)	η_B (mPa.s)	References
choline chloride + lactic acid @ 25 °C	271.41	396.7	
choline chloride + lactic acid @ 45 °C	228.13	153.1	
choline chloride + lactic acid @ 65 °C	155.8	78.0	
choline chloride + lactic acid @ 85 °C	207.38	36.6	
choline chloride + malic acid @ 25 °C	958109	27492.0	
choline chloride + malic acid @ 45 °C	84657	9100.7	
choline chloride + malic acid @ 65 °C	4484.7	2509.0	
choline chloride + malic acid @ 85 °C	174.73	797.1	
choline chloride + citric acid @ 25 °C	968834	834114.0	[24]
choline chloride + citric acid @ 45 °C	948834	41657.0	
choline chloride + citric acid @ 65 °C	124813	10298.0	
choline chloride + citric acid @ 85 °C	35866	3489.4	
choline chloride + fructose @ 25 °C	3029.6	482.1	
choline chloride + fructose @ 45 °C	862.77	239.2	
choline chloride + fructose @ 65 °C	607.42	100.1	
choline chloride + fructose @ 85 °C	663.41	38.9	

2.5.4 Herschel-Bulkley Equation

The Herschel-Bulkley model is frequently used to calculate the yield stress region by fitting the data from rheograms [85] or the region at low shear rates while the Bingham model just takes into account the region with constant slope and in this case it covers higher shear rates [86]. This model fits most flow curves with a good correlation coefficient, and for this reason, it is the most widely used model [59]. However, one of the drawbacks of the Herschel-Bulkley equation is that it does not distinguish whether the observed change in viscosity is due to the change in time or shear stress since these two variables are changed simultaneously [86]. Furthermore, this model defines a fluid with three parameters. The model is mathematically described as

$$\tau = \tau_0 + \eta_0 \gamma^n \quad (8)$$

where τ represents the shear stress (mPa.), τ_0 is the yield stress (mPa), γ is the shear strain rate s^{-1} and n is the flow behavior index. [86] As shown in Table 2.5, it can be seen that a lower value of n is an indication of a more non-Newtonian behavior or a shear thinning fluid. According to the extracted, the mixtures are more Newtonian as $n \sim 1.0$ as the temperature and the concentration of PhOAc increased [25] where this comes to an agreement with other deep eutectic solvents. The values of n listed in Table 2.5 are approximately similar, and all the n values in the tables are approximately of 1, regardless to the additional decimal places.

Table 2.6. Herschel-Bulkley model parameters for different Natural Deep Eutectic Solvents (NADES)

NADES	τ_0 (mPa)	η_0 (mPa s ⁿ)	N	Reference s
choline chloride + phenylacetic acid based @ 1:2 - 35°C	16.3	205.6	0.945	
choline chloride + phenylacetic acid based @ 1:2 - 55°C	14.2	74.1	0.958	
choline chloride + phenylacetic acid based @ 1:2 - 75 °C	24.5	35.3	0.977	
choline chloride + phenylacetic acid based @ 1:2 - 90°C	9.4	23.8	1	
choline chloride + phenylacetic acid based @ 1:3 - 35 °C	551.0	187.1	0.826	[25]
choline chloride + phenylacetic acid based @ 1:3 - 55°C	370.0	59.9	0.977	
choline chloride + phenylacetic acid based @ 1:3 - 75 °C	9.0	25.6	1	
choline chloride + phenylacetic acid based @ 1:3 - 90°C	2.8	21.7	1	
choline chloride + phenylacetic acid based @ 1:4 – 55 °C	37.9	340.9	0.888	
choline chloride + phenylacetic acid based @ 1:4- 75°C	4.3	19.2	1	
choline chloride + phenylacetic acid based @ 1:4 - 90°C	5.1	13.1	1	[25]

CHAPTER 3. MATERIALS & METHODS

The aim of the experimental part in this section is to synthesize a group of novel NADES systems with varying the HBD component and the HBA respectively. A study on the different possible ways to produce these solvents from literature was collected in a single table to clarify and demonstrate the different techniques and methodologies done in literature. Furthermore, the rheological behavior of the synthesized systems was measured from different rheological perspectives such as the shear flow and oscillatory tests done on the MCR rheometer by Anton paar. In order to get a better and more precise understanding of the rheological characteristics of the NADES systems, the effect of temperature was also studied for both types of measurements.

3.1 Materials used in this work

All the raw components used to prepare and synthesize the reported NADES. The HBA ChCl salt having melting point of 575 K and with purity of 97.0% was purchased from Iolitech, while Alanine (Al) with $\geq 98\%$ purity (CAS Number 56-41-7) with melting point of 258 °C, betaine (Be) with $\geq 98\%$ purity (CAS Number 107-43-7) with melting point of 310 °C were purchased from Sigma Aldrich. DL-Malic Acid MA with 99% purity (CAS Number 6915-15-7), Citric Acid CA with 99.5% purity (CAS Number 77-92-9), DL-Lactic Acid LA with 85% purity (CAS Number 50-21-5) and D-(-)-Fructose Fr with 99% purity (CAS Number 57-48-7) were purchased from Sigma Aldrich. The solid particle HBDs in the form of powder were typically treated under vacuum at 60°C for about 48 hours to insure sample clearance of any moisture content. In addition, containers of 40 mL volume were used to store all the synthesized NADES systems, due to their well sealing capability for liquid samples.

3.2 Methodologies

3.2.1 NADES Synthesis

The synthesis of all the [ChCl], [Al], and [Be] based NADES with a fixed preparation molar ratio of 1:1 was done using two different methods. The first method was simply done by simple mixing of the HBD and HBA in a single compartmented container and stirred using a metallic stirring rod in a glove box where ambient conditions such as temperature and atmospheric pressure are controlled. The mixture is then heated until a homogenous color transformation was established. The NADES systems were all found to be liquid at ambient temperature conditions. All the samples were stored in dry and room temperature environment after being synthesized (Figure 3.1 – 3.3).



Figure 3.1: From left to right, the original components of NADES at room temperature for ChCl + LA and ChCl + MA: Choline Chloride, Malic Acid, Lactic Acid, and Choline Chloride + Lactic acid (1:1).

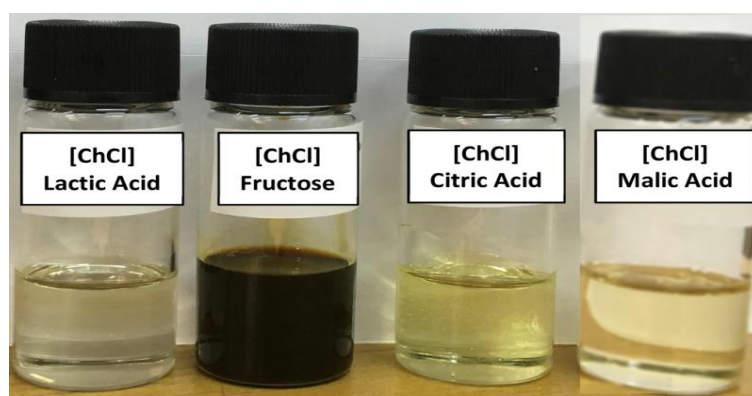


Figure 3.2 :Set A, Synthesized [LA] , [MA] : [CA] , [FR], [ChCl] based 1:1 NADES systems

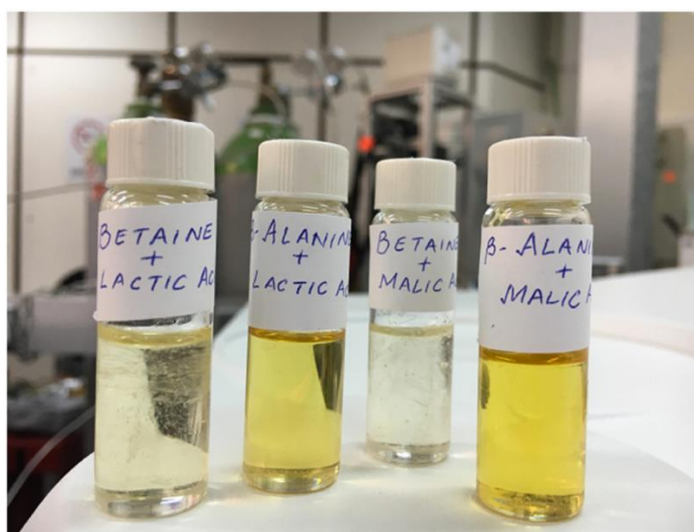


Figure 3.3: Set B & C, Synthesized LA , MA : Be , B-Al based 1:1 NADES systems

Moreover, the second method was done by using machinery mixing (i.e. rotatory evaporator). Glassware was dried at 70°C using a vacuum oven in advance to ensure that they are free of any moisture content. The mole ratio was scaled to approximately 0.025 M (i.e. 6.98 g of ChCl and 2.25 g of lactic acid for instance). The samples were weighted using a KERN 770 Electronic analytical balance and sampled using Ederol filter paper and then added to a 100mL round bottom flask and placed onto the hot steam rotatory mixer. The temperature was set to 60°C at atmospheric pressure and a constant rotational speed of 90 rpm for mixing duration of 60mins long until clear and transparent liquid was formed, where the synthesis took place in a liquid water bath. The ChCl:LA was stored in a 40mL glass bottle. The resulted DES was noticed to be very viscous after it was transferred from the round glass flask. Furthermore, other trials and intermediate techniques were investigated for the synthesis of NADES such as the particle grinding using the mortar and pestle to establish fine powder prior addition in order to insure well mixing of the solvents. Also,

in order to overcome the formation of a molten solvent, a few droplets of water was added to the solvent. The addition of water to some solvents was done in order to lower their highly viscous nature such as solvents with [MA] and [CA] as an HBD. The impact of adding water was found to leave a profound impact, the mixture was completely changed from a very viscous molten to a liquid form of DES. The prepared DES systems are summarized in the Table 3.1 below.

Table 3.1: Specifications and synthesis details of the DES system prepared

S.	Component I	Component II	Mole Ratio	Weight (Gram)	Liquid at T/°C	Remark
N	(HBA)	(HBD)				
1	Choline Chloride	Lactic Acid	1:1	115	25	-
2	Choline Chloride	Malic Acid	1:1	98	25	-
3	Choline Chloride	Citric Acid	1:1	166	53	-
4	Choline Chloride	D-Fructose	1:1	160	25	-
5	Betaine	Malic Acid	1:1	41	50-51	-
6	Betaine	Lactic Acid	1:1	35	25	Thick-Liquid
7	β -Alanine	Lactic Acid	1:1	40	25	-
8	β -Alanine	Malic Acid	1:1		45	-

In Table 3.2, an extensive list of reported techniques and methodologies used for preparing NADES systems. is . The table shows the required chemicals, operating conditions, the main mixing equipment and tools, and any other specific preparation instructions or precautions done while synthesis of the NADES.

Table 3.2: A group of selected articles on the preparation methods of deep eutectic solvents

Temperature (°C)	*Pressure (atm)	Duration (hr)	Processes	Equipment used	Comments	Reference
70-90	1	-	Mixing/Vaccum heating	Magnetic stirrer	Avoid humid areas, stop when completely homogenous	[87]
80	1	2	Shaking/Heating	incubator shaker (Brunswick Scientific Model INNOVA 40R)	Shake @ 300rpm until a homogenous solution, Karl Fisher titration to measure moisture content	[88]
80	1	-	Mixing/Heating	-	Deionized water used in experiments was purified by a Milli-Q system (ChCl,Bet + EG was found stable)	[89]

Temperature (°C)	*Pressure (atm)	Duration (hr)	Processes	Equipment used	Comments	Reference
60	1	-	Drying/Mixing/Heating	thermostatic oil bath with a temperature controller IKA ETS-D5 for heating + Magnetic stirrer	Stop when mixture forms a transparent liquid	[90]
120	1	3	Mixing/Heating	Glove box	surrounding must contain less than 5 ppm moisture	[91]
80	1	2	Shaking/Heating	incubator shaker (Brunswick Scientific Model INNOVA 40R)	Shake @ 400rpm, Stop when homogenous transparent colorless liquid	[92]
80-85	1	-	Mixing/Heating	20 ml vial + closed with a crimp cap, Magnetic stirrer	-	[37]
80	1	-	Mixing/Heating	-	Various combinations with different mole ratios were achieved	[93]

Temperature (°C)	*Pressure (atm)	Duration (hr)	Processes	Equipment used	Comments	Reference
100	1	-	Heating method	heated DURING constant stirring until a homogeneous liquid is formed	-	[94]
25	1	-	Grinding method	mortar with a pestle	Grinding until a homogeneous liquid is formed, nitrogen atmosphere	[94]
50	1	0.25	Heating/cooling/Drying	Schlenk	DL-Menthol was the hydrogen bond acceptor , cooling after 15mins till room temperature : if we will either get paste/liquid/ or unstable	[95]
100	1	-	Mixing / Heating	-	Either mixing at 25oc OR heating at 100oc , Preparation temperature depends on the molar ratio	[96]

Temperature (°C)	*Pressure (atm)	Duration (hr)	Processes	Equipment used	Comments	Reference
-20-200	-	-	Freezing / Drying	-	2:1 molar ratio urea: chl was freezed, then dried to obtain a clear viscous liquid	[97]
50	1	-	Mixing/drying	rotary evaporator	kept under vacuum for 24 h, afterwhich they were stored in a desiccator	[98]

The HBA & HBD are genialized for any type of NADES ammonium salt or acid respectively.

*The pressure was assumed to atmospheric since it was not mentioned in literature.

3.2.2 Viscosity measurements

Measuring the viscosity of a sample depends on its physical state. As a result, there are numerous ways to determine the viscosity of a fluid. Equipment and devices such as the traditional viscometer, quartz crystal microbalance (QCM), and rheometers are used to determine the viscosity of different fluids.

3.2.3 Rheometer

In recent research, the use of a rheometer is the most common. This device is a bench scale apparatus that determines rheological properties through basic concepts of fluid mechanics. Rheometry is an international testing procedure that provides additional information on material that are being tested. The viscosity for instance, is measured using the relationship between the shear rate and shear stress of a fluid.

3.2.3.1 Anton Paar 302 Rheometer

The Anton Paar MCR (Modular Compact Rheometer) 302 is a dynamic and much more complex designed device that offers higher accuracy than other viscosity measuring devices. This Rheometer was used to measure all the rheological properties of the NADES solvents in the current study. The upmost exclusive feature in the Anton Paar 302 is the air-bearing supported synchronous EC motor, which offers more accuracy for sample testing. The motor is fixed with coils and magnets with opposite poles that result in the production of magnetic poles. The delivery of precise torque is a result of the rotating flux created when the coils and magnets attract each other, creating a frictionless movement of the motor. The main components of the MCR Rheometer are shown in Figure 3.4 listed on the diagram from 1-4.

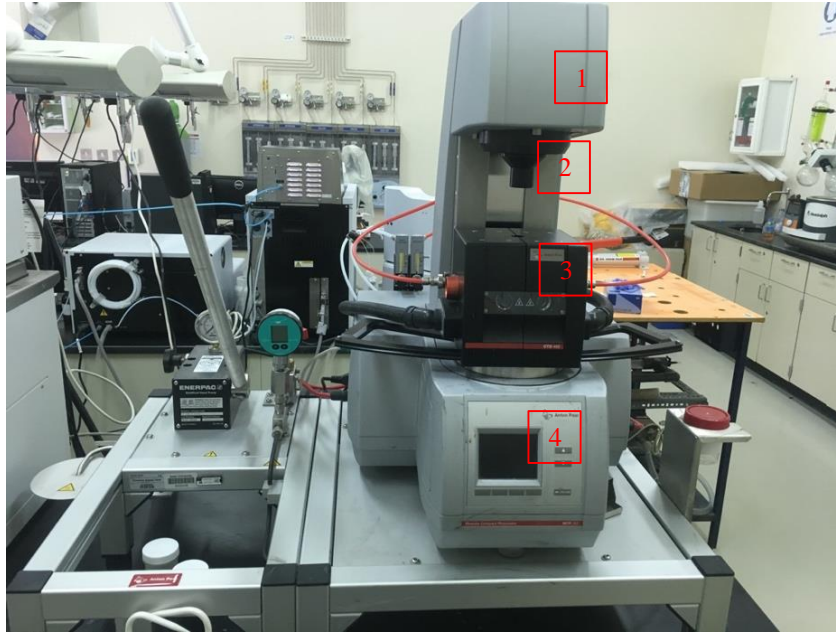


Figure 3.4: Anton Paar 302 MCR rheometer

3.2.3.2 Basic Components of the MCR Rheometer

The rheometer is physically made up of high-grade stainless steel which consists of several mechanical, electrical, and highly sensitive measuring parts that play an important role on the sample accuracy. Inside the head of the rheometer, it internally contains 4 major parts that control the movement of the rotational tools, which are the optical encoder, electronic commutated motor, air bearings and normal force sensors, and the motor coupling. The optical encoder is responsible for measuring the shear rate and the shear strain of the measured samples. This is done by controlling the rotational speed (shear rate) and by measuring the command speed given by the motor displacement (shear strain). The electronically commutated motor is responsible for controlling the torque signals done by the result of rotation and the sample response (Shear stress). The air bearings and capacitive normal force sensors (label 1) have the

ability to measure or control the normal force applied (normal stress) and also position the motor. Furthermore, label 2 on figure 3.4 shows the motor coupling, which estimates the precision of the measuring systems that can be installed such as the cone-plate, parallel plate, concentric cylinder, solid rectangular fixture geometries. Label 3 is the main sampling chamber that is responsible for adapting the temperature set by the user and is where the measurements take place after all the addition of any accessories or settings. Label 4 shows the monitoring screen that reports all the actions occurring in the rheometer such as the temperature, torque signal, and other operational parameters such as the measuring gap between the plates and the normal force.

3.2.3.3 Rheological measurements procedure

Prior sampling the NADES to the rheometer, the solvents are heated and stirred on a hot plate using a magnetic stirrer-heater for 10-15 mins, to avoid any damage or sticky stains of the samples on the sensitive measuring plates. In the meantime, the PC, Rheometer, and air compressor are initially turned on as the sample is warmed up. The rheometer is controlled by a featured software from Anton Paar called the RheoPlus. The software offers many advantages over other rheometry software's such as the ability to freely design any shear flow or oscillatory experiment through the use of a systematic algorithm planned by the user. Moreover, the software also features the ability of editing and analyzing the data generated statistically and measured by the user-friendly interface present.

The algorithm is designed based on the type of experiment conducted and also the type of material being tested. Parameters such as the shear rate interval, temperature and shear strain, must be specified in order to start with the experiment. 50 mm diameter cone and plate measurement geometry were used with a gap of 0.104 mm. The cone and plate (CP) geometry were favored over the parallel plate (PP) configuration for

these set of experiments due to the presence of limited particle size particle presents within the NADES samples (particle size $\leq 5 \mu\text{m}$). In addition, the CP geometry were also favored over the CC configuration (Figure 3.5) due to the limited sample quantity.

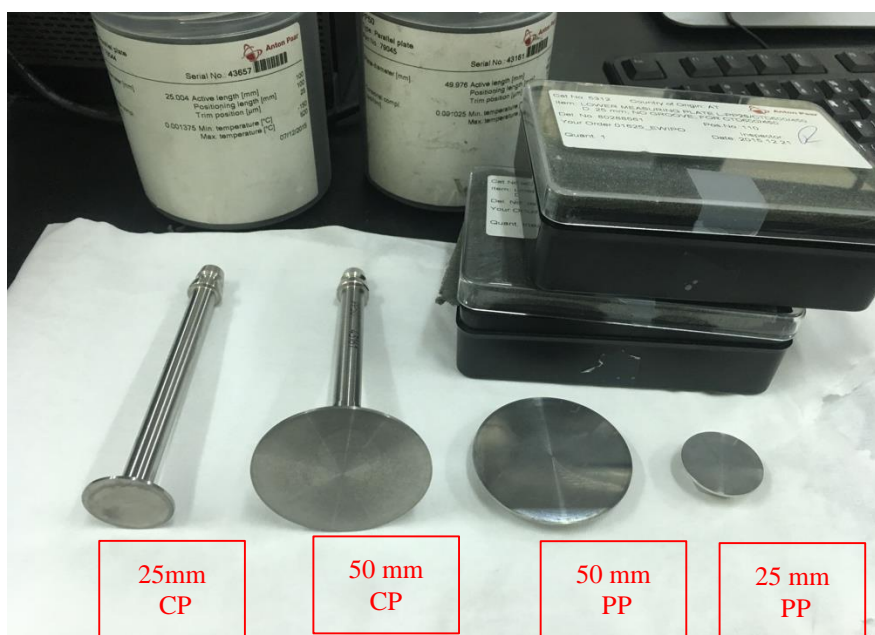


Figure 3.5: CP, PP measuring geometries with different diameter sizes 25,50 mm respectively

The initiating steps such as motor efficiency checkup, measuring gap, temperature setpoint were performed by the software before sampling. Samples such as ChCl:LA and ChCl: FR were placed onto the measuring device with a pipette, while the rest of samples such as ChCl: MA, ChCl:CR, and all the Be and B-Al based NADES were spread onto the measuring device using a spatula due to their relatively higher viscosity. The samples were allowed to rest on the measuring plate before conducting any measurements.

3.2.3.4 Rotational Measurements

The shear flow behaviors and viscosity measurements for all NADES were investigated with shear controlled rotational measurements. Controlled shear stress tests were conducted by varying the shear rate from 0.01-1000 s⁻¹ for all the measurements. The rheological properties set on the device prior starting the experiment for the NADES flow curve measurements were summarized in Table 3.3 below.

Table 3.3: Shear flow parameters fixed in the option tools for the RheoPlus software

Parameter	value
Shear rate (1/s)	0.01-1000
Data points	50
Single point duration (s)	12
Temperature range (°C)	25, 50,75,100,105

The apparent viscosity against shear rate was measured for each NADES individually. The effect of increasing temperature on each solvent was applied on different temperatures ranging from room temperature to a temperature magnitude as high as 105°C. A fresh sample was placed on the measuring plate for each temperature measurement in order to avoid any possible chances of structure or breakdown due to high temperature. In parallel, the shear rate vs shear stress for all the samples was also measured. In addition, the viscosity versus time was also measured for all the samples. The experimental plan for this part was divided into four different time intervals, the

first interval had the sample measure for a duration of 1min, while the second, third and fourth round had the measurement run for 5,10, and 15mins respectively. The same procedure was carried out for the temperature range 25°C-85°C

3.2.3.5 Oscillation measurements

The viscoelastic behavior of the NADES was studied with oscillatory measurements using the same measuring configuration for the shear flow measurements. The oscillation tests use a technique where the sinusoidal strain is used. The dynamic amplitude and frequency sweeps were applied for the stability determination of the molecular structure and other structural characterizations and interaction forces between the selected HBA and HBD. The dynamic amplitude sweep measurements were initially applied to the samples prior the main oscillation tests in order to define the linear viscoelastic region (LVR) for the samples in order to select the proper strain for frequency sweep measurements. A range from 0.01 to 100 % strain % was selected in order not to overwhelm the sample and not to exceed a strain value that may cause the destruction of the interior bonding. Based on the 0.1% constant strain value from the LVR test, the dynamic frequency test was applied to the samples from a value 0.1 – 100 rad/s. G' and G'' parameters were measured using this test in order to classify the type of structure for the NADES samples. Table 3.4 and Table 3.5 show preliminary parameters used to run the experiment for both the pre-shearing and the flow curve measurements.

Table 3.4: Pre-Shear flow parameters fixed in the option tools for the RheoPlus software

Parameter	value
Shear rate (1/s)	0.01 (constant)
Data points (1 point/s)	5

Table 3.5: Oscillatory shear flow parameters fixed in the option tools for the RheoPlus software

Parameter	value
Shear strain (%)	10 (oscillating)
Data points (1 point/s)	25
Initial angular frequency (rad/s)	100
Final angular frequency (rad/s)	0.1

3.2.4 Density

Density was measured at different temperatures using an Anton Paar DMA 4500M densitometer which uses the oscillating U-tube sensor principle shown in Figure 3.6. Densitometer calibration was calibrated by using the reference density values of water, which were obtained from the fundamental equation of state by Wagner and Pruss (uncertainty lower than ± 0.003 % in the full pressure and temperature ranges) and further detailed calibration was conducted recently done using with dimethyl sulfoxide (DMSO) at different temperatures. Temperature was measured in the oscillating U-tube to an average uncertainty of ± 0.05 K. The uncertainty of the pressure measurements in densitometer is 0.005 MPa. The combined relative uncertainty of

density measurements considering samples purity was estimated as 0.3 % ($\pm 0.00005 \text{ g m}^{-3}$).



Figure 3.6: Density Meter by Anton Paar

3.2.5 Thermogravimetric Analysis (TGA)

Thermal stability, decomposition temperature, and onset temperature were analyzed using PerkinElmer Pyris 6 TGA instrument for all prepared NADES (Figure 3.7). To obtain weight loss curve with temperature, NADES were heated from 30 to 700 °C at the rate of 5 °C min⁻¹ under dried atmosphere using N₂ gas. TGA analyzer was tested periodically with calcium oxalate by conducting weight loss experiment to verify the performance.



Figure 3.7: Thermogravimetric Analysis instrument

CHAPTER 4. RESULTS AND DISCUSSIONS

4.1 Part A: Lactic acid based NADES

4.1.1 Steady-state flow

The results of rotary shear tests and different flow behavior of lactic acid-based NADES are presented under the effect of temperature and time. The viscosity magnitudes and rheograms are measured using rotational tests as a function of shear rate within the range 0.01 to 1000 s⁻¹ under similar conditions applied in CO₂ capture plants.

4.1.1.1 Shear stress vs shear rate

In Figure 4.1, the shear stress for all the lactic acid-based solvents show a change with the increase in the shear rate interval. The gradual increase in shear stress however does not intersect with the origin point; therefore, the behavior of all the samples is represented as a non-Newtonian behavior at room temperature conditions [48]. As the shear rate is increased, the effect of the HBA becomes dominant, and the NADES respond to shear rate was significantly affected by the nature of the HBA. The samples B-Al and Be require a higher yield stress than the ChCl based one, which means that the NADES based with B-AL and Be HBA can withstand higher yield stress than that of ChCl. The shear stress begins to gradually reach steady-state as the shear rate approaches 1000 s⁻¹ and the solvents reach their limit viscosities. The shear thinning behavior can also be explained by the degradation of the physical networks by the increasing the shear rate until the viscosity of the NADESs showed a nearly Newtonian behavior [99].

In Figure 4.2, the shear stress of ChCl: La NADES was measured at four different elevated temperatures of 25,45,65, and 85 °C. The usual shear thinning behavior was noticed in the steady shear flow at the measured temperature intervals.

As can be seen, the shear stress under shear rate dependency was decreasing as the temperature increased. The attribution of this behavior was similar to that in our previous study, this phenomena was explained by the structural breakdown caused by the structural thermal expansion [24]. Furthermore, the ChCl: La study also revealed that the effect of temperature is dependent to the yield stress, and that the slope and duration of Hooke's law is mostly a factor of the nature of the HBA: HBD.

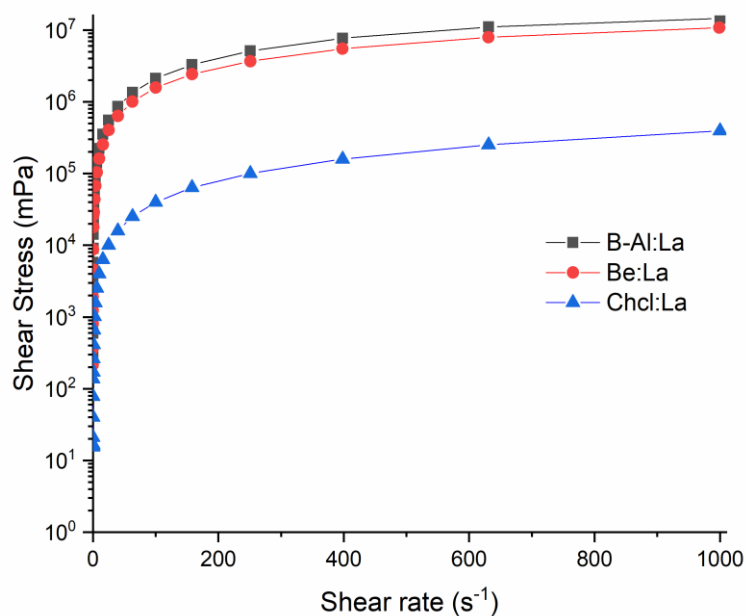


Figure 4.1: The variation of shear stress as a function of applied shear rate for Be, B-Al, and ChCl: La NADES systems at room temperature conditions

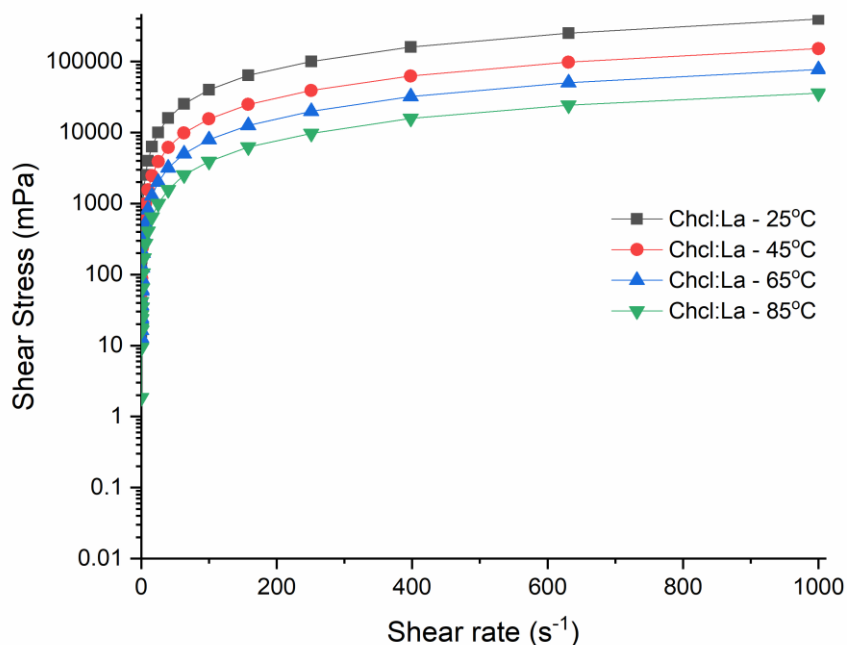


Figure 4.2: The variation of shear stress as a function of applied shear rate for Be, B-Al, and ChCl: La NADES systems at elevated temperatures from 25-85 °C

4.1.1.2 Effect of Temperature sweep

The dynamic temperature ramp studies simulate production cycles, storage and use conditions or evaluate long term stability of the use of NADESs for CO₂ capture in action. Rheological testing can predict the behavior of the solvent's structure to resist disturbances in temperature, under both heating (i.e. forward ramp) and cooling (i.e. backward ramp) without large costly batch studies. According to Figure 4.3, nearly 2 decades decrease in the apparent viscosity of Be: La and B-Al: La during forward ramp, while a relatively slighter decrease in the viscosity for ChCl: La was noticed over the temperature range from 25°C to 65°C. Moreover, the reverse process (backward ramp) from 65°C to 25°C was also investigated, the rheological results showed comparable

profiles for both tests. Accordingly, this ensures that the effect of the lactic acid HBD plays a significant role in determining the shear flow.

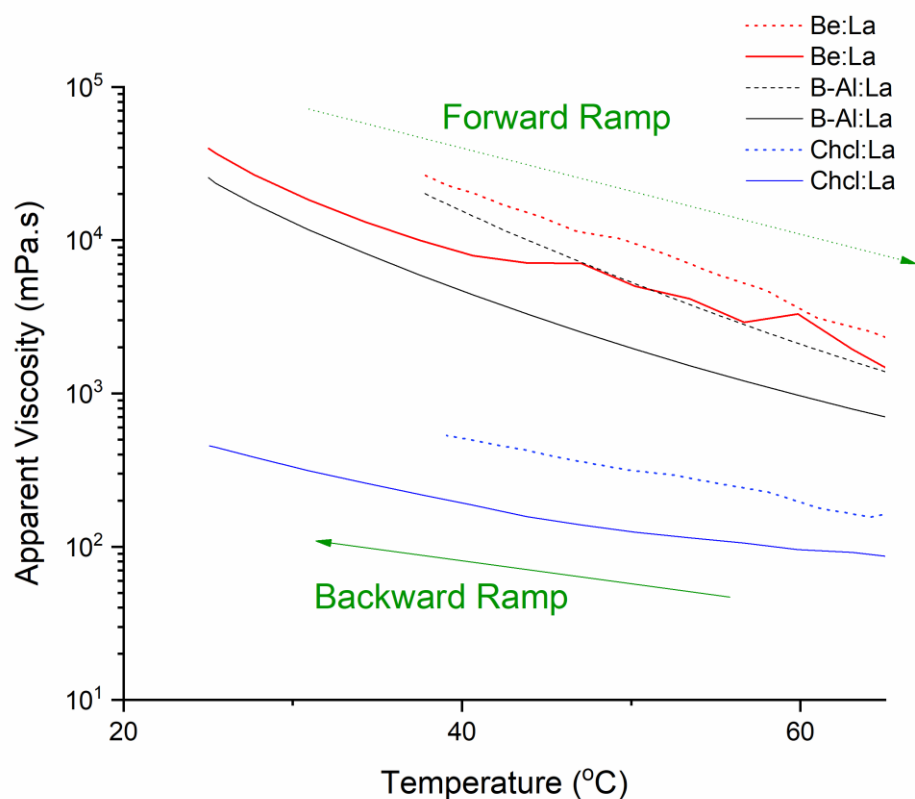


Figure 4.3: Effect of heating (forward ramp) (dashed line) and cooling (backward ramp) (solid line) on the apparent viscosity at low shear rate of 1 s^{-1} at a temp ramp rate of 3°C , time ramp of 1.6 min using 26 data points for Be, B-Al, ChCl: La NADES systems

As with other NADES, the analogy of La-based NADES apparent viscosity decreased with the increase of temperature asymptotically as shown in figure 4.4 [30]. The larger the HBA hydrocarbon chain is, the higher its viscosity becomes. Over the temperature domain, both B-Al: La and Be: La systems exhibited a similar viscosity behavior of initially $2 \times 10^4 \text{ mPa.s}$ at room temperature, and then started to gradually decrease to eventually reach a viscosity lower than its initial value by 2 orders of

magnitude of approximately 300 mPa.s at 85°C for both the systems. On the other hand, the behavior of the ChCl: La was found to represent a much more bulky and compact behavior in comparison to Be: La and B-Al: La systems with temperature, as the temperature effect on the viscosity was found to decrease from 400 mPa.s to 40 mPa.s. In contrast to viscosity, the density of the NADES showed identical flow behavior over the same temperature range, where linear monotonically decreasing density profiles was observed. Among the density profiles shown, B-Al showed the highest density value. According to the density measurements present herein the La-based systems can be ranked as B-Al: La > Be: La > ChCl: La. This behavior clearly shows the strength of the hydrogen bonding between the HBA and HBD in the B-Al: La system and also its significant role in the shear flow viscosity trend.

The rheological behavior of NADES have shown to represent a non-Newtonian behavior due to the rupture of the three-dimensional network with applied shear at elevated temperatures and a time dependent structure. Figure 4.5, represents a three-dimensional representation of the effect of both temperature and time on the apparent viscosity of Be: La. It is clear from the mish illustrated that Be: La shows a time dependency element, where the viscosity decreases with the temperature increase.

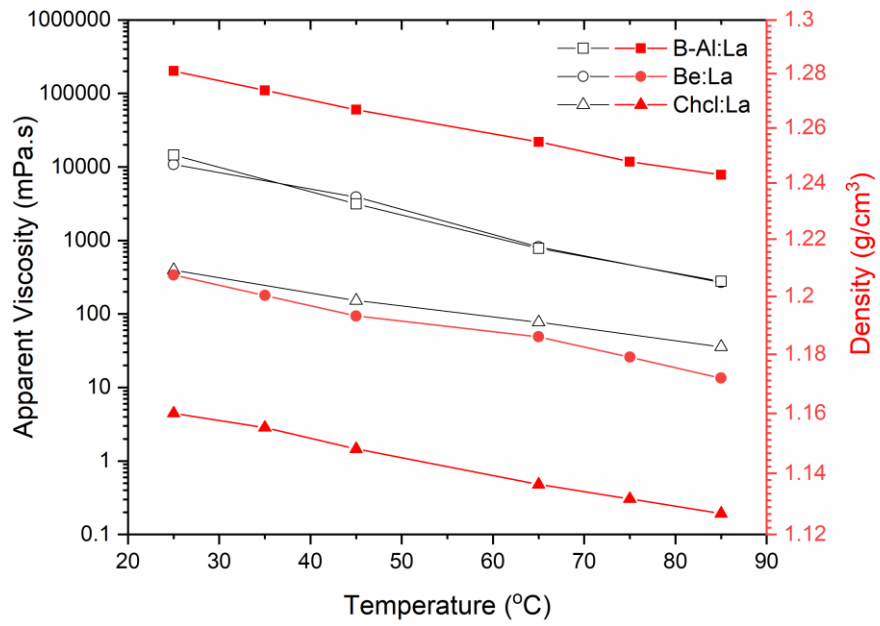


Figure 4.4: Effect of heating on the apparent viscosity and density (at high shear rate of 1000 s^{-1}) for B-Al, Be, and Chcl: LA NADES systems

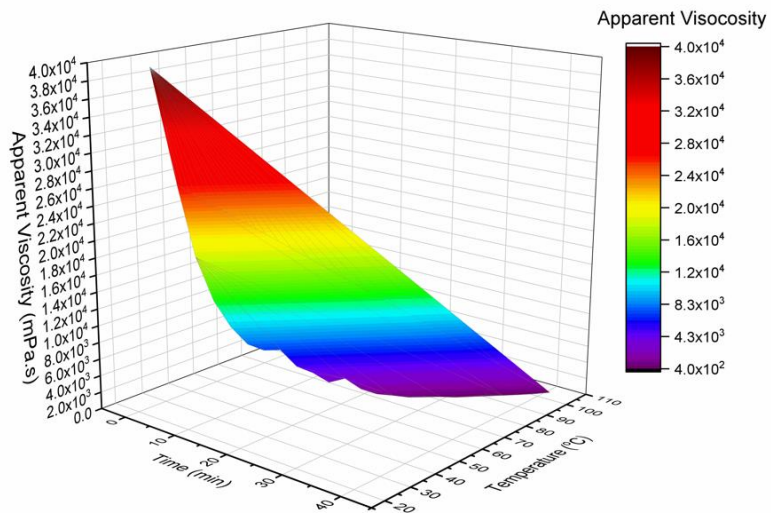


Figure 4.5:3D color surface showing the effect of temperature and time dimensions of the apparent viscosity on Be:LA NADES system

4.1.2 Oscillatory tests

Oscillatory measurement is a significant approach and analysis methodology used to measure the elastic properties of recently developed materials. The measurements enhance the shear flow studies by understanding the interaction forces between the HBA and HBD of NADES on the microscopic level. Unlike shear flow measurements, oscillatory measurements are remarkable for molecular structures with critical and complex molecular interactions as this category of measurements avoids damaging any kind of materials with networks such as NADES [100].

4.1.2.1 Angular frequency sweep

The oscillation test initially started with an amplitude sweep in order to determine the linear viscoelastic region (i.e. LVR test) of the sample. The linear viscoelastic region is a critical point that accurately evaluates the relationship between the molecular structure and the viscoelastic behavior independent of any imposed strain. The measurements were performed over a range of oscillation frequencies that vary from 0.1 to 100 rad/s under constant amplitude oscillation at different temperatures (25-85°C).

Figure 4.6,7 demonstrates the complex viscosity under the effect of elevated temperatures against the apparent viscosity at low applied frequency sweeping/low shear rate and high applied frequency sweeping/high shear rate respectively, maintained at a constant strain of 0.1% that's within the LVR range of the NADES sample. The influence of temperature on the complex viscosity was studied from 25°C to 105°C at a constant angular frequency of 100 rad. s⁻¹. The complex viscosity trends show a clear effect of temperature stability on the La-based NADES. All 3 samples represented an immediate effect with the increase of temperature. The complex viscosity of the Be: La and B-Al: La showed a sharp decrease in viscosity over the

temperature range, while the viscosity of ChCl: La was evenly decreased. When comparing the three system's complex viscosity, it can be noticed that the ChCl: La maintained and resisted its complex viscosity over the temperature interval, showing a gel-like structural behavior, while both Be: La and B-Al: La's complex viscosity drastically dropped indicating that the gel structure broke down. It is noteworthy to mention that this phenomenon witnessed in complex viscosity measurements was identical to the apparent viscosity measured during shear-flow behavior of these systems. ChCl: LA has a more resistive structure and network build up was observed at high temperatures.

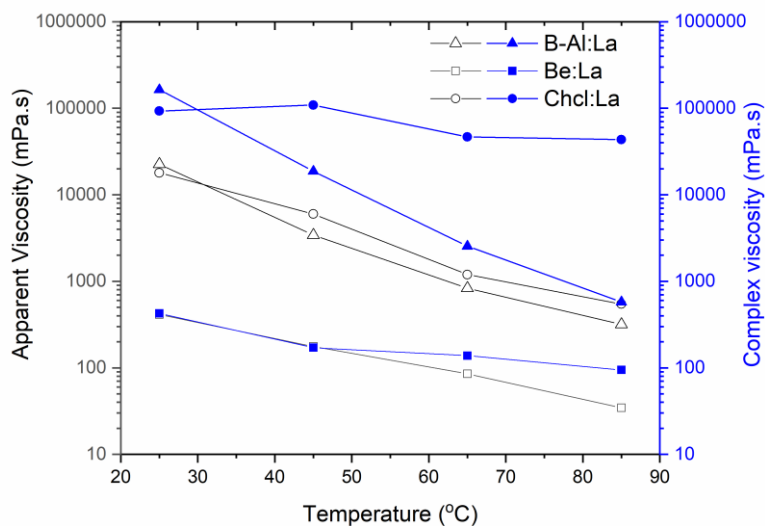


Figure 4.6: Complex viscosity & apparent viscosity variation for Be, B-Al, ChCl: La NADES systems at low angular frequency (1 rad. s^{-1}) and low shear rate (1 s^{-1}) respectively under heating from ambient temperature conditions to 85°C

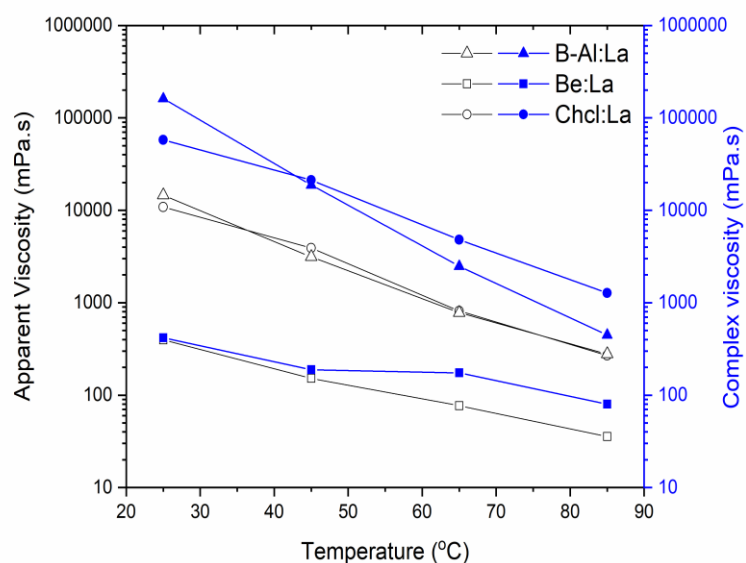


Figure 4.7: Complex viscosity & apparent viscosity variation for Be, B-Al, Chcl: La NADES systems at high angular frequency (100 rad. s^{-1}) and low shear rate (1000 s^{-1}) under heating from ambient temperature conditions to 85°C

4.1.2.2 Dynamic Temperature ramp sweep

Figures 4.8, 4.9 and 4.10 show the elastic modulus (G') and viscous modulus (G'') for Be: La, B-Al: La, and Chcl: La as a function of temperature from 25°C to 85°C at a constant angular frequency of 100 rad. s^{-1} (high angular frequency) Be: La and ChCl:LA have shown a stable and consistent behavior over the temperature domain. A minimal change in the flow regime is observed as the temperature increases for both the G' and G'' , while a steep structural breakdown in the G' was observed for B-Al:La after 35°C , which means that the systems have good physical stability, and their internal structure is not easily disturbed. Moreover, the viscoelastic behavior of the La based NADESs showed $G'' > G'$, indicating that a viscous and low stiff behavior of the NADESs samples dominate over the elastic behavior and also that the samples exhibit predominantly a viscous liquid rather than a solid like material [22]. The differences

between G'' and G' reveal the presence of the initiative flow components within the gel structure and as G' diminishes (i.e. $G' \rightarrow 0$), an ideal viscous flow behavior (i.e. less stiffness) is witnessed. The higher values of G' and G'' in B-Al: La and Be: La suggests that they have a compact structural strength and rigid structure at the gel state, whereas a softer viscoelastic structure for ChCl: La is observed. This remarkable behavior of NADESs over different temperatures best suits the industrial needs as a CO_2 capturing agent.

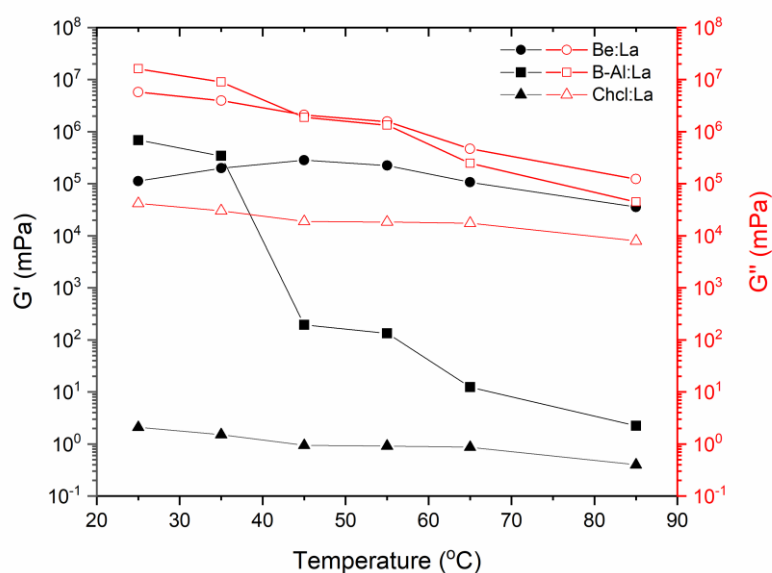


Figure 4.8: The elastic modulus (G') and viscous modulus (G'') at high angular frequency of 100 rad. s^{-1} for Be, B-Al, and ChCl: La under the effect of heating from ambient conditions to 85°C

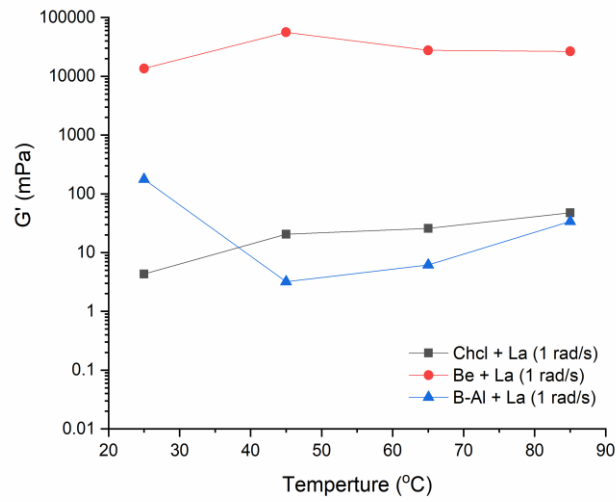


Figure 4.9: The elastic modulus (G') at low angular frequency of 1 rad. s^{-1} for Be, B-Al, and ChCl: La under the effect of heating from ambient conditions to 85°C

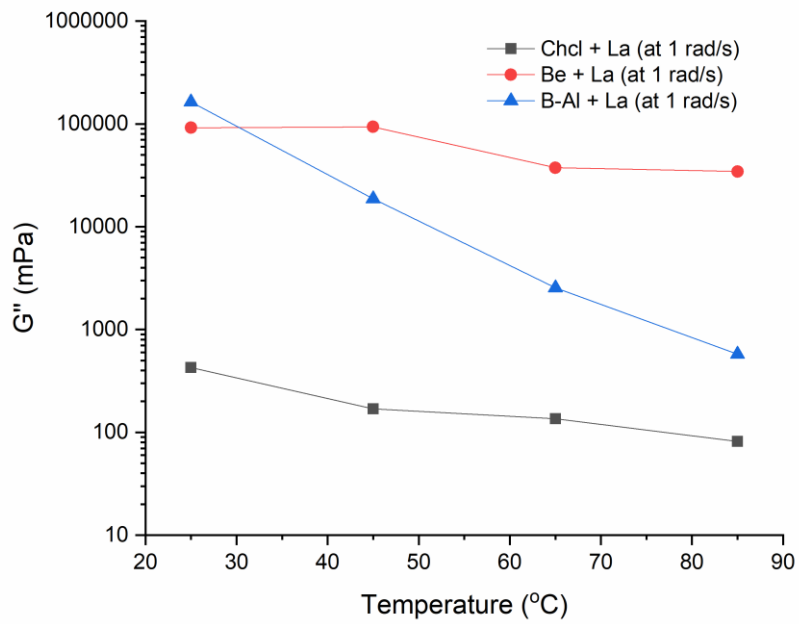


Figure 4.10: The viscous modulus (G'') at low angular frequency of 1 rad. s^{-1} for Be, B-Al, and ChCl: La under the effect of heating from ambient conditions to 85°C

Figure 4.11-14, show the result of frequency sweep in a dynamic test through examining the G' , G'' against angular frequency (ω) of the lactic acid based NADES systems at different temperature points ranging from ambient temperature conditions, to a temperature of 85°C. At room temperature conditions, all the three systems showed a G'' greater than G' , meaning that the general behavior of all lactic acid based NADES is liquid, Moreover, similar structural behavior was noticed for the lactic acid NADES at 85°C.

Figure 4.13-14 show that the linear viscoelastic region of G' was the longest for Be + LA, representing an initial thick semi-solid structure that showed a constant plateau, that is independent of angular frequency. The departure and breakdown from the linear behavior of G' occurs for B-Al + La and ChCl + La was found to deviate at different levels of angular frequency with the increase in temperature. The deviation from its original structural behavior at low angular frequency was higher under higher temperatures, meaning that lower stress is required to disturb the networks of the structures at lower temperature than higher ones, resulting in a structural breakdown a lot easier. Moreover, a structure reestablishment was observed at all temperatures for the NADES systems. The recovery of the structure originated to its initial structure at high angular frequency under room temperature conditions, while a gradual recovery was spotted for the rest of the temperatures. This behavior of LA based NADES suggests that at isothermal conditions, the general analogy of the NADES agree with the findings under varied temperature conditions.

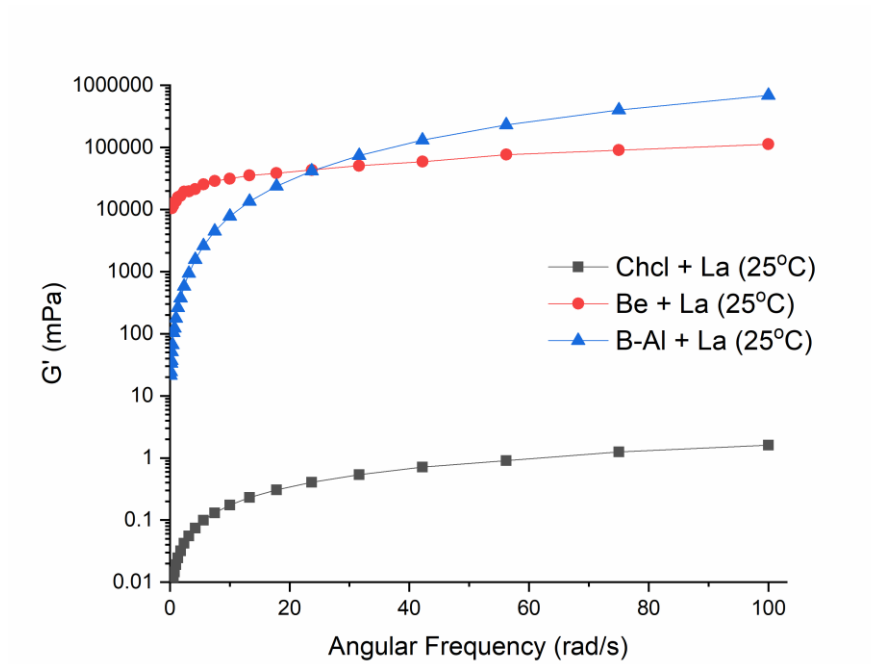


Figure 4.11: The elastic modulus (G') at an angular frequency range from 0.1- 100 rad. s^{-1} for Be, B-Al, and Chcl: La at room temperature conditions

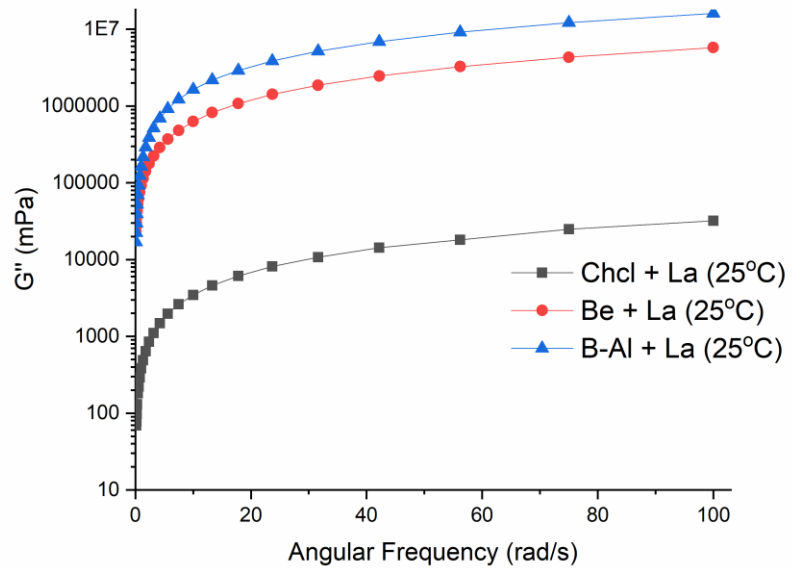


Figure 4.12: The viscous modulus (G'') at an angular frequency range from 0.1- 100 rad. s^{-1} for Be, B-Al, and Chcl: La at room temperature conditions

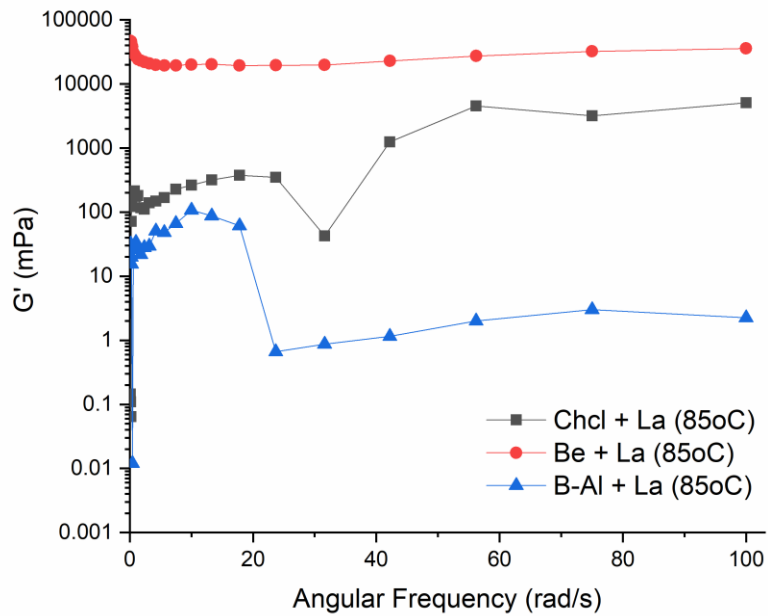


Figure 4.13: The elastic modulus (G') at an angular frequency range from 0.1- 100 rad. s^{-1} for Be, B-Al, and Chcl: La at high temperature

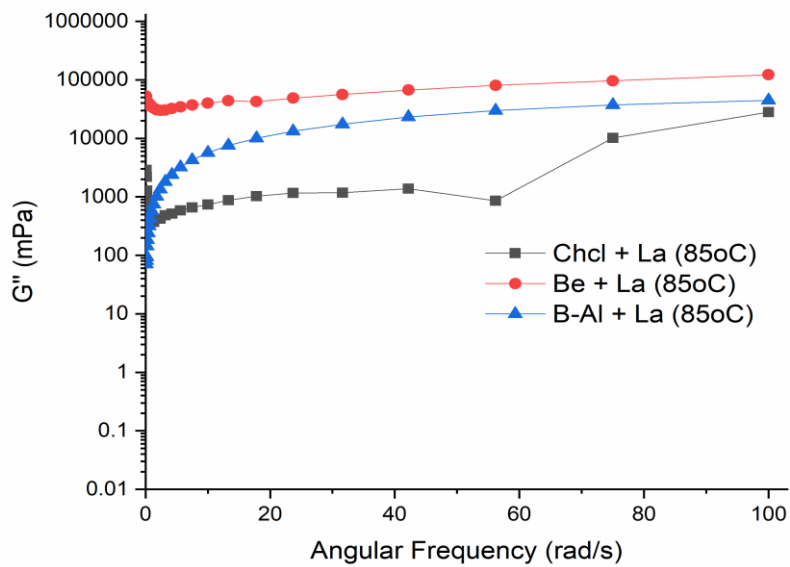


Figure 4.14: The viscous modulus (G'') at an angular frequency range from 0.1- 100 rad. s^{-1} for Be, B-Al, and Chcl: La at high temperature

4.1.3 Thermal Stability

Figure 4.15 shows the thermogravimetric analysis (TGA) performed on the B-Al:LA, Be:La, ChCl:La NADES to quantify their thermal stability. B-Al:La and Be:La NADES samples have showed very similar decomposition trends and they followed a consistent single step degradation with approximated thermal decomposition temperature (T_{dec}) values of around ~ 220 °C. ChCl:La. NADES samples decomposition trend also followed a single step degradation with approximated T_{dec} values of ~ 187 °C. The results clearly show that effect of the HBA and HBD are present, playing a decisive role in demonstrating the thermal stability of the NADESs. Moreover, the overall observations also show their potential applicability as promising pre- and post-combustion CO₂ capture agents.

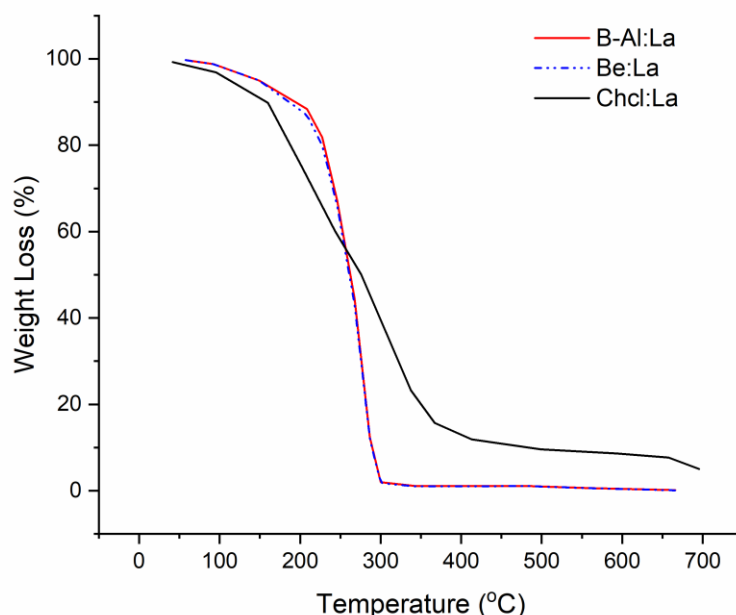


Figure 4.15: TGA thermographs of lactic acid based NADES systems

4.1.4 Model regression

The fluid behavior was interpreted by the flow and viscosity curves, apparent viscosity, limit viscosity, and yield stress were noticed. The Bingham model is one of the most common mathematical models used to fit non-Newtonian fluids. It was applied in order to assess and transform rheogram data values obtained from experimental results into meaningful rheological behavior of the different La based NADES systems.

4.1.4.1 Bingham Model

In general, the yield stresses of all the La-based NADES (Table 4.1) decreased with increasing temperature as expected for any shear thinning fluid. The differences in the yield stress values are mainly due to the changes in molecular mobility, such as chain rigidity, interaction forces between the hydrogen bond donor and hydrogen acceptor of the NADES and the molecular weight. The change of the yield stress values as a function of temperature is similar to the to the viscosity data [24]. The τ_0 of all three La-based NADES showed extremely high magnitudes for B-Al: La and Be: La (i.e. 338,000, 233,000 mPa respectively) indicating their intensive energy requirement for disrupting the network structure in order to initiate the flow regime. On the other hand, the low values of τ_0 in the ChCl: La system indicate a positive advantage for industrial CO₂ application, especially during pumping. The reported values are showed to fluctuate in the case of ChCl: La, however they were under the acceptable error limit. The statistical measure of the viscosity data was fitted and a coefficient of determination (R^2) predicated that the Bingham regression predictions perfectly fit the present data as $R^2 \approx 1$ for all the systems.

Table 4.1: The results obtained from mathematical modelling of the rheogram data of Chcl: La, Be: La, B-Al: La at temperatures from 25-85 °C.

	Temperature (°C)	τ_0 (mPa)	η_0 (mPa.s)	R^2
B-Al: La	25	338000	15600	0.98107
	45	11214	3164.5	0.99953
	65	578.48	783.23	0.99998
	85	222.14	279.13	0.99996
Be: La	25	233000	11300	0.98599
	45	27389	3975.9	0.99854
	65	2656.5	818.19	0.99986
	85	974.5	268.56	0.99993
Chcl: La	25	0.018147	0.40025	1
	45	0.0056303	0.15561	0.99998
	65	0.024442	0.079044	0.99996
	85	0.015328	0.039323	0.99982

4.2 Part B: Malic acid based NADES

4.2.1 Steady-state flow

Figure 4.16 represents the measured yield stress as a function shear rate for Be:MA, B-Al:MA and ChCl:MA NADES systems. The shear stress was measured over a shear rate interval ranging from 0.01 to 1000 s⁻¹ at ambient temperature condition. The shear stress for all the MA-based systems generally showed a change in the shear stress with shear rate. As the shear rate was gradually increased, the yielding of the NADES samples differed based on the nature of HBA salt present. Be:MA showed a very stiff and solid like behavior under low shear rate, as no yielding was achieved. In a similar manner, B-Al:MA presented a highly viscous nature under the effect of shear, where the flow of the sample began to initiate at a shear rate of 320 s⁻¹ with a very high yield stress requirement of <10⁷ mPa. On the hand, ChCl:MA showed a relatively less viscous nature than the MA-based on Be and B-Al; where the lowest yield stress was achieved to initiate the flow over the entire shear rate interval. As a result, this finding strongly agrees with our previous studies, showing that the effect of ChCl as an HBA represents the most promising component for NADES as a sorbent with low pumping cost requirements for CO₂ capture. This behavior can be attributed by the degradation of the physical networks within the ChCl:MA micro's structure with the increase in shear rate [99].

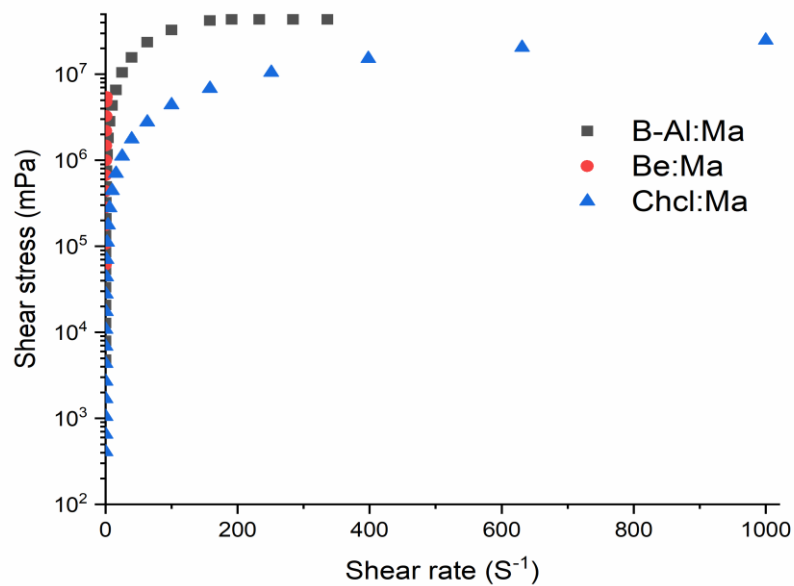


Figure 4.16: The variation of applied shear stress as a function of shear rate for Be,B-Al, and ChCl: Ma NADES systems at room temperature conditions

Figure 4.17 shows a further investigation on the Be:MA flowability and yielding at elevated temperatures. The shear stress against shear rate for Be:MA NADES was measured at five different temperatures of 25,45,65,85 and 105°C. As discussed earlier, the Be:MA showed a very resistive nature at ambient temperature. However, with the increase in temperature, usual shear thinning behavior was observed from 45°C to 105°C with a decrease in the yield requirement. This phenomena was also observed and explained in our previous rheological studies through screening of different NADES combinations for CO₂ by a structural breakdown that was caused as a result of the structural thermal expansion [24]. This behavior also reveals temperature dependency of NADES to initiate a flow over a complete cycle from low to high shear rate regardless of how viscous the NADES combination is.

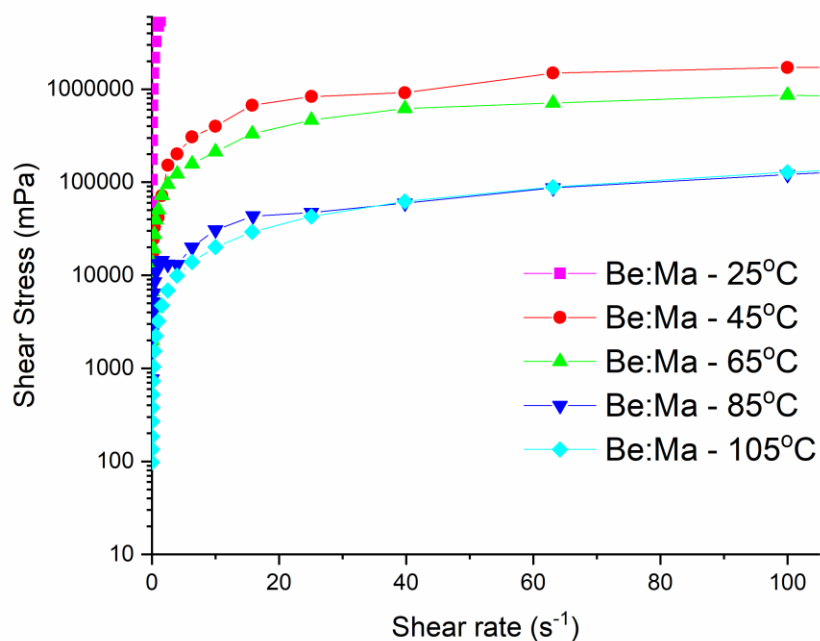


Figure 4.17: The variation of applied shear stress as a function of shear rate for Be:MA NADES systems at elevated temperatures from 25-85°C

4.2.2 Thermo-rheological steady-flow behavior

Figure 4.18 shows the dynamic temperature ramp test conducted for B-Al:MA thermostability which ensures the long-term use of NADES for their use as CO₂ capture sorbents. This temperature variation under a dynamic sweep can characterize the behavior of the NADES intermolecular structure to resist the effect of temperature at a fixed strain under both heating and cooling conditions. During the heating ramp (i.e. forward ramp) and at room temperature conditions, the initial apparent viscosity of the B-Al:MA showed a magnitude of approximately 5×10^5 mPa.s. The viscosity began to rapidly decrease with the increase of temperature to finally reach an apparent viscosity value of 2×10^2 mPa.s at 105°C. The cooling process was then reversed for the same sample (i.e. backward ramp) over the same temperature interval from 105°C to 25°C,

showing an exponential profile with temperature. The trends executed showed for both profiles seem to reflect the effect of the HBA in determining the shear flow. This finding for the apparent viscosity behavior may be also correlated to the hole theory [40,43], which states that the volumetric factor attributing by the nature of the individual components have a more effective role in determining the viscous behavior of the NADES than the intermolecular interactions between the HBA and HBD. Therefore, on the basis of this theory, the viscosity of the NADES mainly correspond to the hole size available of the HBD and HBA [92,101,102].

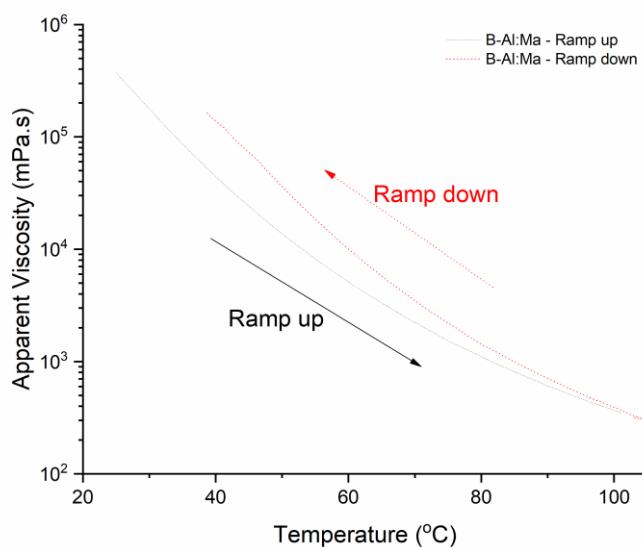


Figure 4.18: Effect of heating (Ramp up) and cooling (Ramp down) on the apparent viscosity at low shear rate of 1 s^{-1} for B-Al:MA NADES systems

Figure 4.19 represents the effect of temperature on the apparent viscosity and the density in parallel on B-Al:MA and ChCl:LA under a fixed shear rate of 1000 s^{-1} . Both the density and apparent viscosity have shown a uniform profile consistency with one

another representing a true linear monotonically decrease, where a sharp decrease in both profiles for the NADES samples showed a common trend revealing the common analogy for most NADES under the effect of heating [30]. In contrast to viscosity, the type of component selected as an HBA has a distinct effect on the density of the NADES system. According to the hole theory [103], the increase in hole radius and free volume availability are directly proportional and significantly contribute to the size of the HBA molecule, hence, smaller molecules decrease the density of the NADES. As a result, this implies that the density of the NADES system depends on the active groups and the chain's length present in the HBAs.

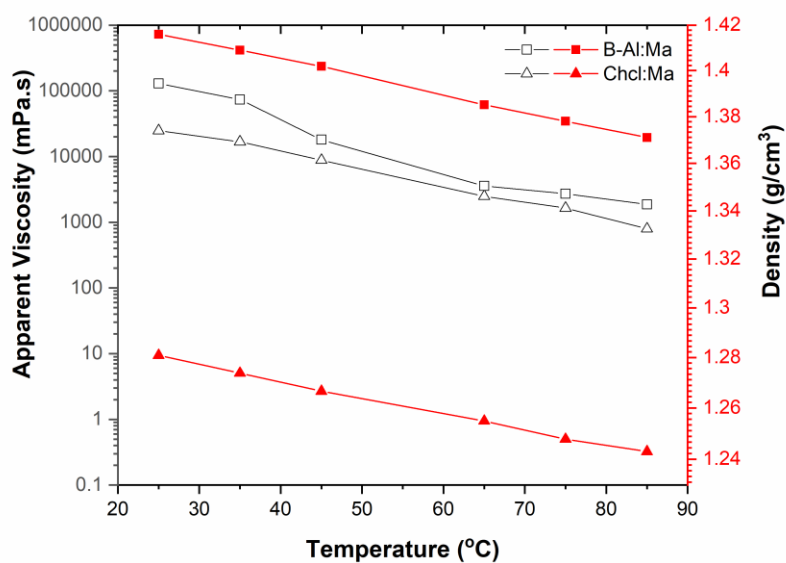


Figure 4.19: Effect of heating on the apparent viscosity (at high shear rate of 1000 s^{-1}) for B-Al, Be, and ChCl: MA NADES systems

Figure 4.20 shows a 3D representation of the shear flow under the effect of both time and temperature parameters on the apparent viscosity of B-Al: MA NADES system.

The 3D surface showed that the system represents a time-dependent thixotropy, non-Newtonian, shear thinning and stability characteristic, where the apparent viscosity clearly showed a decrease with the increase in temperature.

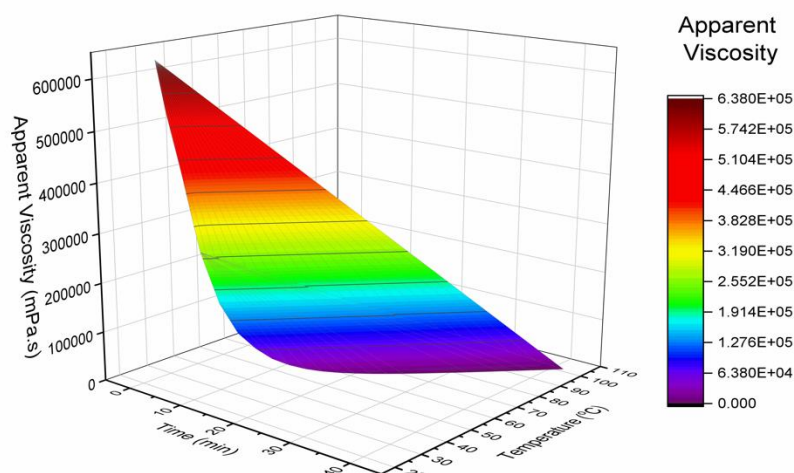


Figure 4.20:3D color surface showing the effect of temperature and time dimensions of the apparent viscosity on B-Al: MA NADES system

4.2.3 Oscillatory tests

4.2.3.1 Angular frequency sweep

Figure 4.21 shows the result of frequency sweep in a dynamic test through examining the G' against angular frequency (ω) of the ChCl:MA NADES system at different temperature values ranging from ambient temperature conditions, to a temperature of 85°C. At room temperature conditions, ChCl:MA showed the highest magnitude of G' with a value of 700 mPa over the low angular frequency range, as the angular frequency increased, the G' started to gradually increase. The trend in G' showed a significant

decrease with the increase of temperature, where at 105°C the value of G' was approximately 0.03 mPa and did not exceed 1 mPa.s at higher frequencies. This behavior of MA-based NADES suggests that at isothermal conditions, the general analogy of the NADES agrees with the findings under varied temperature conditions.

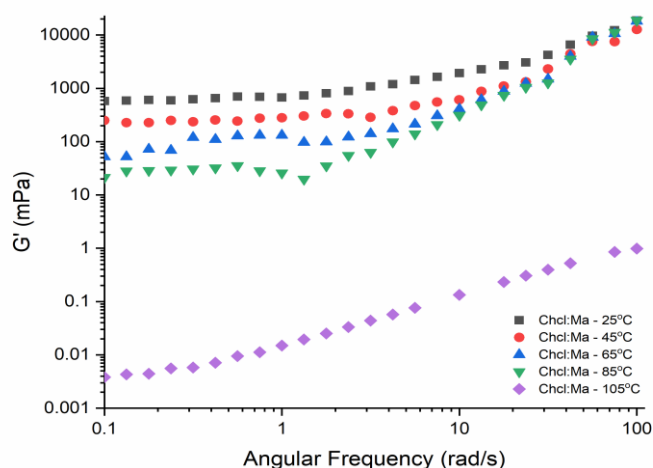


Figure 4.21: Effect of elevated temperatures on the storage modulus of ChCl:MA NADES system at room temperature conditions

Figure 4.22, demonstrates the complex viscosity variation for Be:MA, B-Al:MA and ChCl:MA NADES systems at high angular frequency of 100 rad.s^{-1} under heating from ambient temperature conditions to 105°C, which was maintained at a strain of 0.1% value just below the critical strain defined by the strain sweep, in order to ensure that the rheological characterization on the samples is independent of any strain levels or imposed stress. The complex viscosity trends show a clear effect of temperature stability on the MA-based NADES. All three samples represented an immediate effect with the increase of temperature. The complex viscosity of the ChCl:MA, Be:MA and

B-Al:MA showed a sharp decrease in viscosity over the temperature range. This drop is a result of the gel structure breakdown of the NADES systems.

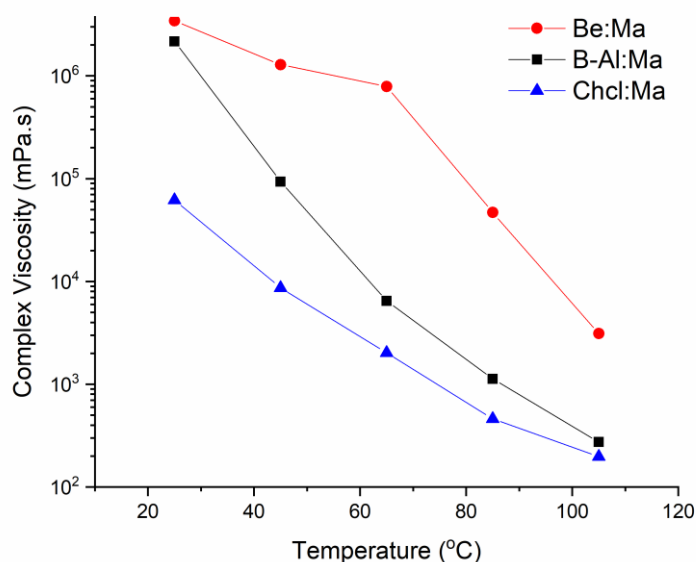


Figure 4.22: Complex viscosity variation for Be:MA, B-Al:MA and ChCl:MA NADES systems at high angular frequency of 100 rad.s^{-1} under heating from ambient temperature conditions to 105°C

4.2.3.2 Dynamic temperature ramp sweep

Figure 4.23, shows the elastic modulus (G') and viscous modulus (G'') at high angular frequency of 100 rad.s^{-1} for Be, B-Al, and ChCl:MA under the effect of heating from ambient conditions to 85°C . The results obtained from the dynamic temperature sweep confirm that all three MA-based NADES systems show relatively higher values of G'' than G' throughout the temperature domain. This clearly shows that all the MA-Based NADES systems are applicable for the use as sorbents, as their nature tends to show a

more viscous liquid and not a rigid solid material over the temperature interval. Minimal change in the structure of the NADES was observed for all the systems over the temperature range except for the G' for the B-Al:MA, which showed a steep breakdown after ambient temperature conditions. Moreover, no cross linking between the G' and G'' was achieved. The marginal difference between G' and G'' also revealed the effect of the HBA on the structural behavior under thermal effect, where the difference revealed the presence of components that exhibit a flow nature within the gel structure and as G' diminishes (i.e. $G' \rightarrow 0$), an ideal viscous flow behavior (i.e. less stiffness) is witnessed. This behavior of MA-based NADES revealed the potential of their usage for CO_2 capture under the current industrial conditions.

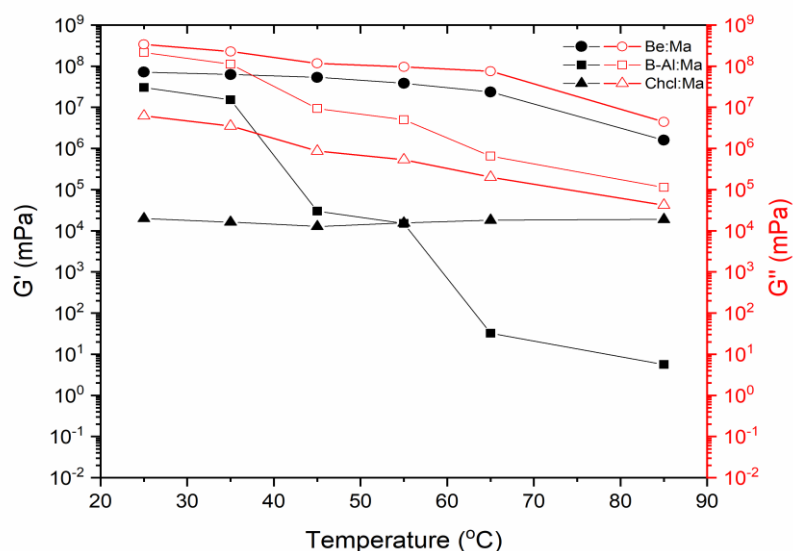


Figure 4.23: The storage modulus (G') and loss modulus (G'') at high angular frequency of $100 \text{ rad}\cdot\text{s}^{-1}$ for Be, B-Al, and ChCl:MA under the effect of heating from ambient conditions to 85°C

4.2.4 Thermal Stability

Figure 4.24 shows the thermal behavior of the NADES systems studied using TGA. The TGA was used to acquire the decomposition temperature (T_{dec}), which is an important property for solvents and mixtures that are currently under development. In order to optimize the working temperature conditions during their use in different applications. The T_{dec} for B-Al:MA, Be:MA and ChCl:MA are summarized in Table 6. It was also found that the T_{dec} for the Be:MA and ChCl:MA NADES herein had a single step degradation trends, while B-Al:MA showed two-step degradation temperatures mainly due to the relatively higher moisture content, and it is important to note that they were above 200°C. Hence, this shows the effect of the HBA in determining the thermal stability.

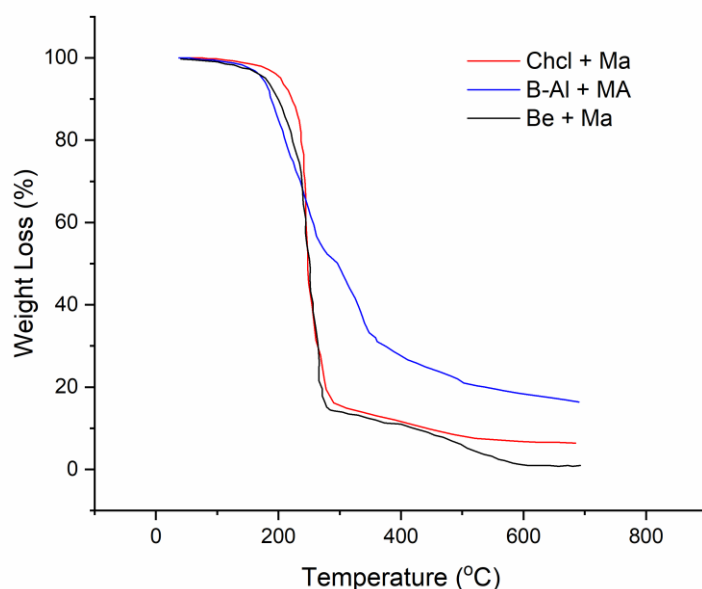


Figure 4.24: TGA thermographs of MA-based NADES systems

Table 4.2: Summary of the different NADES TGA analysis results obtained from the thermographs

NADES system	Single step T_{dec} (°C)	Two-step T_{dec} (°C)
Be:MA	220	-
B-Al:MA	220	320
ChCl:MA	207	-

4.2.5 Model regression

4.2.5.1 Bingham Model

In many industrial processes, some of these high viscous NADES required preheating before processing and need more pumping energy as well. As there are no available models to predict the viscosity of the NADESs, using rheological model such as Bingham model to fit the experimental measurements could be beneficial in assessing their applicability as well as building predictive models. Bingham plastic model can be used to describe the viscosity function and to estimate the Bingham yield stress (τ_B) values [104–106] The magnitude of τ_B is a useful parameter that can be used as indicative of the amount of minimum stress required disrupting the networked structure in order to initiate the flow which is normally correlated to the pumping energy required to initiate flow. Any stress below τ_B for the mixture means that the mixture behaves as a rigid solid. In this study, Bingham plastic model well described the flow behavior of the three NADES systems tested and the variation of yield stress as a function of the temperature for the studied NADES systems.

The results showed that the yield stresses of all MA-based NADESs decreased with increasing temperature as expected for the shear thinning materials. The differences in the yield stress values are mainly due to the changes in the interaction forces between the hydrogen bond donor and hydrogen acceptor of the NADES and the molecular weight [24][25]. The variations of the yield stress values as a function of temperature is similar to the viscosity data. It was found that the ChCl based NADES system had a lower yield stress values than B-Al and Be based NADES systems as shown in Table 4.3. In addition, at high temperature, the ChCl NADES yield stresses were less sensitive to the temperature as they remain almost constant. Lower yield stress values are of good advantage for industrial applications such as CO₂ capture.

Table 4.3: The results obtained from mathematical modelling of the rheogram data of ChCl: MA, Be: Ma, B-Al: MA at temperatures from 25-85 °C

	Temperature (°C)	τ_0 (mPa)	η (mPa.s)	R²
B-Al:Ma	25	6000000	150798	0.85
	45	536566	19542	0.97
	65	43104	3646.80	1.00
	85	6852.9	1884.60	1.00
Be:Ma	25	3000000	2000000	0.81
	45	829276	810.16	0.07
	65	356943	224.26	0.05
	85	34304	713.89	0.98
ChCl:Ma	25	958109	27492	0.95
	45	84657	9100.70	1.00
	65	4484.7	2509.00	1.00
	85	174.73	797.08	1.00

CHAPTER 5. CONCLUSIONS

The shear flow and viscoelasticity characterizations were thoroughly investigated for the use in several flow dependent applications, mainly focusing on CO₂ capture related conditions. NADES have been less elaborated from rheological perspective in comparison with ILs and it can be explained by their late development as sustainable and environmentally benign organic solvents. From the discussed results, literature clearly indicates that NADES rheological properties are tuned by changing the nature of the benefactor (i.e. HBD for NADES). NADES showed diverse behaviors under the effect of shear rate from Newtonian to non-Newtonian fluids. Moreover, the apparent viscosity of NADES has shown to be relatively high viscosities, where NADES's shear flow viscosity behaviors ranged from as low as 0.05 Pa.s to as high as 2000 Pa.s at ambient conditions over an incremented domain of applied shear.. On the other hand, the temperature dependency of both solvent families agrees with the direct proportionality analogy with viscosity as a function of shear rate. Although the viscoelastic properties are essential to determine the stability and destruction of formed networks upon characterization of the synthesized solvents, yet a lack of reported oscillatory measurements were found. Several rheological models were collected featuring a set of analyzed data from several research papers that validate the consistency of the measured apparent viscosity against shear and temperature.

A detailed stationary shear rheometry study was presented to explain the rheological behavior of six different La and Ma based NADES with a molar ratio of 1:1 under rotational and oscillatory shear, highlighting the influence of field operation temperature on different flow parameters and thixotropic descriptors for different NADESs. All the La-based NADES formulations presented an apparent non-Newtonian behavior characteristic with shear-thinning and time-dependent properties.

Rheological measurements showed a clear difference in the viscosity and strength of the viscoelastic properties between the three studied NADES systems. The apparent viscosity under the effect of temperature showed strong shear thinning effect similar to alternative IL sorbents. The dynamic frequency sweep tests (viscoelastic measurements) concluded that ChCl-based system was a more promising candidate for CO₂ capture than the B-Al: La and Be: La, since it had a more compact and resistive structural nature that exhibited a buildup behavior at elevated temperatures. The τ_0 parameter in the Bingham model confirmed that stress requirement for ChCl: La is extremely less in comparison with the magnitudes of B-Al and Be: LA.

CHAPTER 6. FUTURE PERSPECTIVES

For future work, improvements on the current thesis study can be presented in the following points:

- Rheological characterization on NADES systems loaded with CO₂
- DFT and molecular simulations investigation for the effect of the HBA on the viscosity of the mixture, through correlating the rheological results with the molecular simulation theoretical studies, the performance of the NADESs can be modulated, designing sorbents with optimal CO₂ uptake characteristics and an adequate consistency and stasis time at the administration site.
- Investigate the rheological behaviors under the effect of high pressure on the NADESs sample

REFERENCES

- [1] F. Del Monte, D. Carriazo, M.C. Serrano, M.C. Gutiérrez, M.L. Ferrer, Deep eutectic solvents in polymerizations: A greener alternative to conventional syntheses, *ChemSusChem*. 7 (2014) 999–1009. doi:10.1002/cssc.201300864.
- [2] K.A. Hoff, E.F. Da Silva, I. Kim, A. Grimstvedt, S. Ma'mun, Solvent development in post combustion CO₂capture -Selection criteria and optimization of solvent performance, cost and environmental impact, *Energy Procedia*. 37 (2013) 292–299. doi:10.1016/j.egypro.2013.05.114.
- [3] Y. Liu, J.B. Friesen, J.B. McAlpine, D.C. Lankin, S.N. Chen, G.F. Pauli, Natural Deep Eutectic Solvents: Properties, Applications, and Perspectives, *J. Nat. Prod.* 81 (2018) 679–690. doi:10.1021/acs.jnatprod.7b00945.
- [4] H. Vanda, Y. Dai, E.G. Wilson, R. Verpoorte, Y.H. Choi, Green solvents from ionic liquids and deep eutectic solvents to natural deep eutectic solvents, *Comptes Rendus Chim.* (2018) 1–11. doi:10.1016/j.crci.2018.04.002.
- [5] K. Zhang, Y. Hou, Y. Wang, K. Wang, S. Ren, W. Wu, Efficient and Reversible Absorption of CO₂ by Functional Deep Eutectic Solvents, *Energy & Fuels*. 32 (2018) 7727–7733. doi:10.1021/acs.energyfuels.8b01129.
- [6] X. Ge, C. Gu, X. Wang, J. Tu, Deep eutectic solvents (DESs)-derived advanced functional materials for energy and environmental applications: Challenges, opportunities, and future vision, *J. Mater. Chem. A*. 5 (2017) 8209–8229. doi:10.1039/c7ta01659j.
- [7] X. Li, K.H. Row, Development of deep eutectic solvents applied in extraction and separation, (n.d.) 1–46. doi:10.1002/jssc.201600633.This.
- [8] E.L. Smith*, Deep eutectic solvents (DESs) and the metal finishing industry: where are they now?, *Trans. IMF*. 91 (2013) 241–248.

doi:10.1179/0020296713Z.000000000120.

- [9] D.Z. Troter, Z.B. Todorović, D.R. Dokić-Stojanović, O.S. Stamenković, V.B. Veljković, Application of ionic liquids and deep eutectic solvents in biodiesel production: A review, *Renew. Sustain. Energy Rev.* 61 (2016) 473–500. doi:10.1016/j.rser.2016.04.011.
- [10] M. Bevilacqua, J. Filippi, A. Lavacchi, A. Marchionni, H.A. Miller, W. Oberhauser, F. Vizza, Dye-sensitized solar cells using an aqueous choline chloride- based deep eutectic solvent as an effective electrolyte solution, *Energy Technol.* 2 (2017).
- [11] M.H. Chakrabarti, F.S. Mjalli, I.M. Alnashef, M.A. Hashim, M.A. Hussain, L. Bahadori, C.T.J. Low, Prospects of applying ionic liquids and deep eutectic solvents for renewable energy storage by means of redox flow batteries, *Renew. Sustain. Energy Rev.* 30 (2014) 254–270. doi:10.1016/j.rser.2013.10.004.
- [12] T.J. Trivedi, J.H. Lee, H.J. Lee, Y.K. Jeong, J.W. Choi, Deep eutectic solvents as attractive media for CO₂ capture, *Green Chem.* 18 (2016) 2834–2842. doi:10.1039/c5gc02319j.
- [13] E. Ali, M.K. Hadj-Kali, S. Mulyono, I. Alnashef, A. Fakeeha, F. Mjalli, A. Hayyan, Solubility of CO₂ in deep eutectic solvents: Experiments and modelling using the Peng-Robinson equation of state, *Chem. Eng. Res. Des.* 92 (2014) 1898–1906. doi:10.1016/j.cherd.2014.02.004.
- [14] G. Li, D. Deng, Y. Chen, H. Shan, N. Ai, Solubilities and thermodynamic properties of CO₂ in choline-chloride based deep eutectic solvents, *J. Chem. Thermodyn.* 75 (2014) 58–62. doi:10.1016/j.jct.2014.04.012.
- [15] A. Kamgar, S. Mohsenpour, F. Esmailzadeh, Solubility prediction of CO₂, CH₄, H₂, CO and N₂ in Choline Chloride/Urea as a eutectic solvent using NRTL

- and COSMO-RS models, *J. Mol. Liq.* 247 (2017) 70–74. doi:10.1016/j.molliq.2017.09.101.
- [16] E. Ali, M.K. Hadj-Kali, S. Mulyono, I. Alnashef, Analysis of operating conditions for CO₂ capturing process using deep eutectic solvents, *Int. J. Greenh. Gas Control.* 47 (2016) 342–350. doi:10.1016/j.ijggc.2016.02.006.
- [17] D. Deng, Y. Jiang, X. Liu, Z. Zhang, N. Ai, Investigation of solubilities of carbon dioxide in five levulinic acid-based deep eutectic solvents and their thermodynamic properties, *J. Chem. Thermodyn.* 103 (2016) 212–217. doi:10.1016/j.jct.2016.08.015.
- [18] Y. Chen, N. Ai, G. Li, H. Shan, Y. Cui, D. Deng, Solubilities of carbon dioxide in eutectic mixtures of choline chloride and dihydric alcohols, *J. Chem. Eng. Data.* 59 (2014) 1247–1253. doi:10.1021/je400884v.
- [19] K. Mulia, S. Putri, E. Krisanti, Nasruddin, Natural deep eutectic solvents (NADES) as green solvents for carbon dioxide capture, *AIP Conf. Proc.* 1823 (2017). doi:10.1063/1.4978095.
- [20] A. Yadav, S. Pandey, Densities and viscosities of (choline chloride + urea) deep eutectic solvent and its aqueous mixtures in the temperature range 293.15 K to 363.15 K, *J. Chem. Eng. Data.* 59 (2014) 2221–2229. doi:10.1021/je5001796.
- [21] M. Lu, G. Han, Y. Jiang, X. Zhang, D. Deng, N. Ai, Solubilities of carbon dioxide in the eutectic mixture of levulinic acid (or furfuryl alcohol) and choline chloride, *J. Chem. Thermodyn.* 88 (2015) 72–77. doi:10.1016/j.jct.2015.04.021.
- [22] T. Altamash, M.S. Nasser, Y. Elhamarnah, M. Magzoub, R. Ullah, H. Qiblawey, S. Aparicio, M. Atilhan, Gas solubility and rheological behavior study of betaine and alanine based natural deep eutectic solvents (NADES), *J. Mol. Liq.* 256 (2018) 286–295. doi:10.1016/j.molliq.2018.02.049.

- [23] I. Adeyemi, M.R.M. Abu-Zahra, I. Alnashef, Experimental Study of the Solubility of CO₂ in Novel Amine Based Deep Eutectic Solvents, *Energy Procedia*. 105 (2017) 1394–1400. doi:10.1016/j.egypro.2017.03.519.
- [24] T. Altamash, M.S. Nasser, Y. Elhamarnah, M. Magzoub, R. Ullah, B. Anaya, S. Aparicio, M. Atilhan, Gas Solubility and Rheological Behavior of Natural Deep Eutectic Solvents (NADES) via Combined Experimental and Molecular Simulation Techniques, *ChemistrySelect*. 2 (2017) 7278–7295. doi:10.1002/slct.201701223.
- [25] T. Altamash, M. Atilhan, A. Aliyan, R. Ullah, M. Nasser, S. Aparicio, Rheological, Thermodynamic, and Gas Solubility Properties of Phenylacetic Acid-Based Deep Eutectic Solvents, *Chem. Eng. Technol.* 40 (2017) 778–790. doi:10.1002/ceat.201600475.
- [26] X. Li, M. Hou, B. Han, X. Wang, L. Zou, Solubility of CO₂ in a choline chloride + urea eutectic mixture, *J. Chem. Eng. Data*. 53 (2008) 548–550. doi:10.1021/je700638u.
- [27] R.B. Leron, M.H. Li, Solubility of carbon dioxide in a choline chloride-ethylene glycol based deep eutectic solvent, *Thermochim. Acta*. 551 (2013) 14–19. doi:10.1016/j.tca.2012.09.041.
- [28] A. Tatar, A. Barati-Harooni, A. Najafi-Marghmaleki, A. Bahadori, Accurate prediction of CO₂ solubility in eutectic mixture of levulinic acid (or furfuryl alcohol) and choline chloride, *Int. J. Greenh. Gas Control*. 58 (2017) 212–222. doi:10.1016/j.ijggc.2017.01.013.
- [29] T. Altamash, M. Atilhan, A. Aliyan, R. Ullah, G. García, S. Aparicio, Insights into choline chloride-phenylacetic acid deep eutectic solvent for CO₂ absorption, *RSC Adv.* 6 (2016) 109201–109210. doi:10.1039/c6ra22312e.

- [30] Y.A. Elhamarnah, M. Nasser, H. Qiblawey, A. Benamor, M. Atilhan, S. Aparicio, A comprehensive review on the rheological behavior of imidazolium based ionic liquids and natural deep eutectic solvents, *J. Mol. Liq.* 277 (2019) 932–958. doi:10.1016/j.molliq.2019.01.002.
- [31] A.P. Abbott, G. Capper, D.L. Davies, R.K. Rasheed, V. Tambyrajah, Novel Solvent Properties of Choline Chloride Urea Mixtures_Supplementaryinfo, (2003) 70–71.
- [32] L.I.N. Tomé, V. Baião, W. da Silva, C.M.A. Brett, Deep eutectic solvents for the production and application of new materials, *Appl. Mater. Today.* 10 (2018) 30–50. doi:10.1016/j.apmt.2017.11.005.
- [33] P.W. Stott, A.C. Williams, B.W. Barry, Transdermal delivery from eutectic systems: Enhanced permeation of a model drug, ibuprofen, *J. Control. Release.* 50 (1998) 297–308. doi:10.1016/S0168-3659(97)00153-3.
- [34] E.L. Smith, A.P. Abbott, K.S. Ryder, Deep Eutectic Solvents (DESs) and Their Applications, *Chem. Rev.* 114 (2014) 11060–11082. doi:10.1021/cr300162p.
- [35] Y.H. Choi, J. van Spronsen, Y. Dai, M. Verberne, F. Hollmann, I. W.C.E. Arends, G.-J. Witkamp, R. Verpoorte, Are Natural Deep Eutectic Solvents the Missing Link in Understanding Cellular Metabolism and Physiology?, *Plant Physiol.* 156 (2011) 1701–1705. doi:10.1104/pp.111.178426.
- [36] Y. Dai, G.J. Witkamp, R. Verpoorte, Y.H. Choi, Natural deep eutectic solvents as a new extraction media for phenolic metabolites in *carthamus tinctorius* L., *Anal. Chem.* 85 (2013) 6272–6278. doi:10.1021/ac400432p.
- [37] S. Roehrer, F. Bezold, E.M. Garcia, M. Minceva, Deep eutectic solvents in countercurrent and centrifugal partition chromatography, *J. Chromatogr. A.* 1434 (2016) 102–110. doi:10.1016/j.chroma.2016.01.024.

- [38] S.H. Wu, A.R. Caparanga, R.B. Leron, M.H. Li, Vapor pressure of aqueous choline chloride-based deep eutectic solvents (ethaline, glyceline, maline and reline) at 30-70 °c, *Thermochim. Acta.* 544 (2012) 1–5. doi:10.1016/j.tca.2012.05.031.
- [39] C. D’Agostino, R.C. Harris, A.P. Abbott, L.F. Gladden, M.D. Mantle, Molecular motion and ion diffusion in choline chloride based deep eutectic solvents studied by ¹H pulsed field gradient NMR spectroscopy, *Phys. Chem. Chem. Phys.* 13 (2011) 21383–21391. doi:10.1039/c1cp22554e.
- [40] A.P. Abbott, R.C. Harris, K.S. Ryder, Application of hole theory to define ionic liquids by their transport properties, *J. Phys. Chem. B.* 111 (2007) 4910–4913. doi:10.1021/jp0671998.
- [41] K. Shahbaz, S. Baroutian, F.S. Mjalli, M.A. Hashim, I.M. Alnashef, Densities of ammonium and phosphonium based deep eutectic solvents: Prediction using artificial intelligence and group contribution techniques, *Thermochim. Acta.* 527 (2012) 59–66. doi:10.1016/j.tca.2011.10.010.
- [42] A.P. Abbott, G. Capper, D.L. Davies, R.K. Rasheed, V. Tambyrajah, Novel solvent properties of choline chloride/urea mixtures, *Chem. Commun.* (2003) 70–71. doi:10.1039/b210714g.
- [43] A.P. Abbott, G. Capper, S. Gray, Design of improved deep eutectic solvents using hole theory, *ChemPhysChem.* 7 (2006) 803–806. doi:10.1002/cphc.200500489.
- [44] A.P. Abbott, D. Boothby, G. Capper, D.L. Davies, R. Rasheed, Deep Eutectic Solvents Formed Between Choline Chloride and Carboxylic Acids, *J. Am. Chem. Soc.* 126 (2004) 9142. doi:10.1021/ja048266j.
- [45] W. Guo, Y. Hou, S. Ren, S. Tian, W. Wu, Formation of deep eutectic solvents

- by phenols and choline chloride and their physical properties, *J. Chem. Eng. Data*. 58 (2013) 866–872. doi:10.1021/je300997v.
- [46] A.R.C. Duarte, A.S.D. Ferreira, S. Barreiros, E. Cabrita, R.L. Reis, A. Paiva, A comparison between pure active pharmaceutical ingredients and therapeutic deep eutectic solvents: Solubility and permeability studies, *Eur. J. Pharm. Biopharm.* 114 (2017) 296–304. doi:10.1016/j.ejpb.2017.02.003.
- [47] H. Wang, G. Gurau, J. Shamshina, O.A. Cojocaru, J. Janikowski, D.R. Macfarlane, J.H. Davis, R.D. Rogers, Simultaneous membrane transport of two active pharmaceutical ingredients by charge assisted hydrogen bond complex formation, *Chem. Sci.* 5 (2014) 3449–3456. doi:10.1039/c4sc01036a.
- [48] R. Paula, P. Craveiro, *Engineering Bio-based Polymers using Alternative Solvents and Processes*, (2015).
- [49] J.M. Silva, R.L. Reis, A. Paiva, A.R.C. Duarte, Design of Functional Therapeutic Deep Eutectic Solvents Based on Choline Chloride and Ascorbic Acid, *ACS Sustain. Chem. Eng.* 6 (2018) 10355–10363. doi:10.1021/acssuschemeng.8b01687.
- [50] A.Y. Malkin, A.I. Isayev, INTRODUCTION. RHEOLOGY: SUBJECT AND GOALS, in: A.Y. Malkin, A.I. Isayev (Eds.), *Rheol. Concepts, Methods, Appl.* (Second Ed., Second Edi, Elsevier, Oxford, 2012: pp. 1–8. doi:https://doi.org/10.1016/B978-1-895198-49-2.50005-0.
- [51] T. R??ther, K.R. Harris, M.D. Horne, M. Kanakubo, T. Rodopoulos, J.P. Veder, L.A. Woolf, Transport, electrochemical and thermophysical properties of two N-donor-functionalised ionic liquids, *Chem. - A Eur. J.* 19 (2013) 17733–17744. doi:10.1002/chem.201302258.
- [52] G.A. Hankins, E.F. Relf, *Fluid Mechanics*, Proc. Inst. Mech. Eng. (2007).

doi:10.1243/pime_proc_1947_157_039_02.

- [53] X. Cao, Z. Jiang, W. Cui, Y. Wang, P. Yang, Rheological Properties of Municipal Sewage Sludge: Dependency on Solid Concentration and Temperature, *Procedia Environ. Sci.* 31 (2016) 113–121. doi:10.1016/j.proenv.2016.02.016.
- [54] J. Singh, M. Rudman, H.M. Blackburn, A. Chryss, L. Pullum, L.J.W. Graham, The importance of rheology characterization in predicting turbulent pipe flow of generalized Newtonian fluids, *J. Nonnewton. Fluid Mech.* 232 (2016) 11–21. doi:10.1016/j.jnnfm.2016.03.013.
- [55] E. Lehtinen, *Papermaking Science and Technology: Pigment coating and surface sizing of paper.* Book 11, Fapet, 2000. <https://books.google.com.qa/books?id=IOmFPwAACAAJ>.
- [56] N. Eshtiaghi, F. Markis, S.D. Yap, J.C. Baudez, P. Slatter, Rheological characterisation of municipal sludge: A review, *Water Res.* 47 (2013) 5493–5510. doi:10.1016/j.watres.2013.07.001.
- [57] I.M. Aroso, A. Paiva, R.L. Reis, A.R.C. Duarte, Natural deep eutectic solvents from choline chloride and betaine – Physicochemical properties, *J. Mol. Liq.* 241 (2017) 654–661. doi:10.1016/j.molliq.2017.06.051.
- [58] T. Aissaoui, Y. Benguerba, M.K. AlOmar, I.M. AlNashef, Computational investigation of the microstructural characteristics and physical properties of glycerol-based deep eutectic solvents, *J. Mol. Model.* 23 (2017). doi:10.1007/s00894-017-3450-5.
- [59] R. Haghbakhsh, K. Parvaneh, S. Raeissi, A. Shariati, A general viscosity model for deep eutectic solvents: The free volume theory coupled with association equations of state, *Fluid Phase Equilib.* (2017). doi:10.1016/j.fluid.2017.08.024.

- [60] C. Florindo, L. Romero, I. Rintoul, L.C. Branco, I.M. Marrucho, From Phase Change Materials to Green Solvents: Hydrophobic Low Viscous Fatty Acid-Based Deep Eutectic Solvents, *ACS Sustain. Chem. Eng.* 6 (2018) 3888–3895. doi:10.1021/acssuschemeng.7b04235.
- [61] D. Troter, M. Zlatkovic, D. Djokic-Stojanovic, S. Konstantinovic, Z. Todorovic, Citric acid-based deep eutectic solvents: Physical properties and their use as cosolvents in sulphuric acid-catalysed ethanolysis of oleic acid, *Adv. Technol.* 5 (2016) 53–65. doi:10.5937/savteh1601053T.
- [62] A.K. Das, M. Sharma, D. Mondal, K. Prasad, Deep eutectic solvents as efficient solvent system for the extraction of κ -carrageenan from *Kappaphycus alvarezii*, *Carbohydr. Polym.* 136 (2016) 930–935. doi:10.1016/j.carbpol.2015.09.114.
- [63] I.M. Aroso, R. Craveiro, M. Dionisio, S. Barreiros, L. Rui, A. Paiva, A. Rita, Fundamental studies on natural deep eutectic solvents: physico-chemical, thermal and rheological properties Abstract / Introduction, (n.d.).
- [64] Y.C. Yan, W. Rashmi, M. Khalid, K. Shahbaz, T.C.S.M. Gupta, N. Mase, Potential application of deep eutectic solvents in heat transfer application, *J. Eng. Sci. Technol.* 12 (2017) 1–14.
- [65] A.K. Das, M. Sharma, D. Mondal, K. Prasad, Deep eutectic solvents as efficient solvent system for the extraction of κ -carrageenan from *Kappaphycus alvarezii*, *Carbohydr. Polym.* 136 (2016) 930–935. doi:10.1016/j.carbpol.2015.09.114.
- [66] H. Ghaedi, M. Ayoub, S. Sufian, A.M. Shariff, B. Lal, The study on temperature dependence of viscosity and surface tension of several Phosphonium-based deep eutectic solvents, *J. Mol. Liq.* 241 (2017) 500–510. doi:10.1016/j.molliq.2017.06.024.
- [67] M.K. Alomar, M. Hayyan, M.A. Alsaadi, S. Akib, A. Hayyan, M.A. Hashim,

- Glycerol-based deep eutectic solvents: Physical properties, *J. Mol. Liq.* 215 (2016) 98–103. doi:10.1016/j.molliq.2015.11.032.
- [68] F. Chemat, H. Anjum, A.M. Shariff, P. Kumar, T. Murugesan, Thermal and physical properties of (Choline chloride + urea + l-arginine) deep eutectic solvents, *J. Mol. Liq.* 218 (2016) 301–308. doi:10.1016/j.molliq.2016.02.062.
- [69] W.C. Su, D.S.H. Wong, M.H. Li, Effect of water on solubility of carbon dioxide in (aminomethanamide + 2-hydroxy-N,N,N-trimethylethanaminium chloride), *J. Chem. Eng. Data.* 54 (2009) 1951–1955. doi:10.1021/je900078k.
- [70] A.C. Dumetz, A.M. Chockla, E.W. Kaler, A.M. Lenhoff, Protein phase behavior in aqueous solutions: Crystallization, liquid-liquid phase separation, gels, and aggregates, *Biophys. J.* 94 (2008) 570–583. doi:10.1529/biophysj.107.116152.
- [71] G. García, M. Atilhan, S. Aparicio, Interfacial Properties of Deep Eutectic Solvents Regarding to CO₂ Capture, *J. Phys. Chem. C.* 119 (2015) 21413–21425. doi:10.1021/acs.jpcc.5b04585.
- [72] H.G. Liao, Y.X. Jiang, Z.Y. Zhou, S.P. Chen, S.G. Sun, Shape-controlled synthesis of gold nanoparticles in deep eutectic solvents for studies of structure-functionality relationships in electrocatalysis, *Angew. Chemie - Int. Ed.* 47 (2008) 9100–9103. doi:10.1002/anie.200803202.
- [73] T. Zhekenov, N. Toksanbayev, Z. Kazakbayeva, D. Shah, F.S. Mjalli, Formation of type III Deep Eutectic Solvents and effect of water on their intermolecular interactions, *Fluid Phase Equilib.* 441 (2017) 43–48. doi:10.1016/j.fluid.2017.01.022.
- [74] Y. Dai, G.J. Witkamp, R. Verpoorte, Y.H. Choi, Tailoring properties of natural deep eutectic solvents with water to facilitate their applications, *Food Chem.* 187 (2015) 14–19. doi:10.1016/j.foodchem.2015.03.123.

- [75] A.A. Barzinjy, M.M. Zankana, A Novel Application of the Quartz Crystal Microbalance for Determining the Rheological Properties of the Highly Viscous Liquids, *Acta Phys. Pol. A.* 130 (2016) 239–244. doi:10.12693/APhysPolA.130.239.
- [76] A. Basaiahgari, S. Panda, R.L. Gardas, Acoustic, volumetric, transport, optical and rheological properties of Benzyltripropylammonium based Deep Eutectic Solvents, *Fluid Phase Equilib.* 448 (2017) 41–49. doi:10.1016/j.fluid.2017.03.011.
- [77] A. Bund, E. Zschippang, Nickel Electrodeposition from a Room Temperature Eutectic Melt, *ECS Trans.* 3 (2007) 253–261. doi:10.1149/1.2798668.
- [78] M. Sharma, C. Mukesh, D. Mondal, K. Prasad, Dissolution of α -chitin in deep eutectic solvents, *RSC Adv.* 3 (2013) 18149. doi:10.1039/c3ra43404d.
- [79] F. Mano, I.M. Aroso, S. Barreiros, J.P. Borges, R.L. Reis, A.R.C. Duarte, A. Paiva, Production of poly(vinyl alcohol) (PVA) fibers with encapsulated natural deep eutectic solvent (NADES) using electrospinning, *ACS Sustain. Chem. Eng.* 3 (2015) 2504–2509. doi:10.1021/acssuschemeng.5b00613.
- [80] Y. Cui, C. Li, J. Yin, S. Li, Y. Jia, M. Bao, Design, synthesis and properties of acidic deep eutectic solvents based on choline chloride, Elsevier B.V, 2017. doi:10.1016/j.molliq.2017.04.052.
- [81] C. Mukesh, R. Gupta, D.N. Srivastava, S.K. Nataraj, K. Prasad, Preparation of a natural deep eutectic solvent mediated self polymerized highly flexible transparent gel having super capacitive behaviour, *RSC Adv.* 6 (2016) 28586–28592. doi:10.1039/C6RA03309A.
- [82] R. Pamies, C. Espejo, F.J. Carrión, A. Morina, A. Neville, M.D. Bermúdez, Rheological behavior of multiwalled carbon nanotube-imidazolium tosylate

- ionic liquid dispersions, *J. Rheol.* (N. Y. N. Y). 61 (2017) 279–289. doi:10.1122/1.4975108.
- [83] E. Altin, J. Gradl, W. Peukert, First studies on the rheological behavior of suspensions in ionic liquids, *Chem. Eng. Technol.* 29 (2006) 1347–1354. doi:10.1002/ceat.200600135.
- [84] D. Camargo, R.S. Andrade, G.A. Ferreira, H. Mazzer, L. Cardozo-Filho, M. Iglesias, Investigation of the rheological properties of protic ionic liquids, *J. Phys. Org. Chem.* 29 (2016) 604–612. doi:10.1002/poc.3553.
- [85] Hughes, *Practical Rheology - Kap.11*, (2005).
- [86] P. V. Liddell, D. V. Boger, Yield stress measurements with the vane, *J. Nonnewton. Fluid Mech.* 63 (1996) 235–261. doi:10.1016/0377-0257(95)01421-7.
- [87] T. Aissaoui, I.M. Alnashef, U.A. Qureshi, Y. Benguerba, Potential applications of deep eutectic solvents in natural gas sweetening for CO₂ capture, *Rev. Chem. Eng.* 33 (2017) 523–550. doi:10.1515/revce-2016-0013.
- [88] F.S. Mjalli, J. Naser, Viscosity model for choline chloride-based deep eutectic solvents, *Asia-Pacific J. Chem. Eng.* 10 (n.d.) 273–281. doi:10.1002/apj.1873.
- [89] L. Duan, L.-L. Dou, L. Guo, P. Li, E.-H. Liu, Comprehensive evaluation of deep eutectic solvents in extraction of bioactive natural products, *ACS Sustain. Chem. Eng.* 4 (2016) 2405–2411. doi:10.1021/acssuschemeng.6b00091.
- [90] M. Francisco, A. van den Bruinhorst, L.F. Zubeir, C.J. Peters, M.C. Kroon, A new low transition temperature mixture (LTTM) formed by choline chloride+lactic acid: Characterization as solvent for CO₂ capture, *Fluid Phase Equilib.* 340 (2013) 77–84. doi:10.1016/j.fluid.2012.12.001.
- [91] L. Bahadori, M.H. Chakrabarti, F.S. Mjalli, I.M. Alnashef, N.S.A. Manan, M.A.

- Hashim, Physicochemical properties of ammonium-based deep eutectic solvents and their electrochemical evaluation using organometallic reference redox systems, *Electrochim. Acta.* 113 (2013) 205–211. doi:10.1016/j.electacta.2013.09.102.
- [92] A. Hayyan, F.S. Mjalli, I.M. Alnashef, Y.M. Al-Wahaibi, T. Al-Wahaibi, M.A. Hashim, Glucose-based deep eutectic solvents: Physical properties, *J. Mol. Liq.* 178 (2013) 137–141. doi:10.1016/j.molliq.2012.11.025.
- [93] T. Tan, M. Zhang, Y. Wan, H. Qiu, Utilization of deep eutectic solvents as novel mobile phase additives for improving the separation of bioactive quaternary alkaloids, *Talanta.* 149 (2016) 85–90. doi:10.1016/j.talanta.2015.11.041.
- [94] C. Florindo, F.S. Oliveira, L.P.N. Rebelo, A.M. Fernandes, I.M. Marrucho, Insights into the synthesis and properties of deep eutectic solvents based on cholinium chloride and carboxylic acids, *ACS Sustain. Chem. Eng.* 2 (2014) 2416–2425. doi:10.1021/sc500439w.
- [95] B.D. Ribeiro, C. Florindo, L.C. Iff, M.A.Z. Coelho, I.M. Marrucho, Menthol-based eutectic mixtures: Hydrophobic low viscosity solvents, *ACS Sustain. Chem. Eng.* 3 (2015) 2469–2477. doi:10.1021/acssuschemeng.5b00532.
- [96] J. Of, N. Products, *Ionic Liquids and Deep Eutectic Solvents in Natural Products Research: Mixtures of Solids as Extraction Solvents*, (2013). doi:10.1021/np400051w.
- [97] M.C. Gutiérrez, M.L. Ferrer, C.R. Mateo, F. Del Monte, Freeze-drying of aqueous solutions of deep eutectic solvents: A suitable approach to deep eutectic suspensions of self-assembled structures, *Langmuir.* 25 (2009) 5509–5515. doi:10.1021/la900552b.
- [98] R. Craveiro, I. Aroso, V. Flammia, T. Carvalho, M.T. Viciosa, M. Dionísio, S.

- Barreiros, R.L. Reis, A.R.C. Duarte, A. Paiva, Properties and thermal behavior of natural deep eutectic solvents, *J. Mol. Liq.* 215 (2016) 534–540. doi:10.1016/j.molliq.2016.01.038.
- [99] N. Gonsior, M. Hetzer, W.M. Kulicke, H. Ritter, First studies on the influence of methylated β -cyclodextrin on the rheological behavior of 1-ethyl-3-methylimidazolium acetate, *J. Phys. Chem. B.* 114 (2010) 12468–12472. doi:10.1021/jp1036684.
- [100] W. Al-Sadat, M.S. Nasser, F. Chang, H.A. Nasr-El-Din, I.A. Hussein, Rheology of a viscoelastic zwitterionic surfactant used in acid stimulation: Effects of surfactant and electrolyte concentration, *J. Pet. Sci. Eng.* (2014). doi:10.1016/j.petrol.2014.09.014.
- [101] G. García, S. Aparicio, R. Ullah, M. Atilhan, Deep Eutectic Solvents: Physicochemical Properties and Gas Separation Applications, *Energy & Fuels.* 29 (2015) 2616–2644. doi:10.1021/ef5028873.
- [102] B. Jibril, F. Mjalli, J. Naser, Z. Gano, New tetrapropylammonium bromide-based deep eutectic solvents: Synthesis and characterizations, *J. Mol. Liq.* (2014). doi:10.1016/j.molliq.2014.08.004.
- [103] Q. Zhang, K. De Oliveira Vigier, S. Royer, F. Jérôme, Deep eutectic solvents: Syntheses, properties and applications, *Chem. Soc. Rev.* 41 (2012) 7108–7146. doi:10.1039/c2cs35178a.
- [104] M.S. Nasser, A.E. James, Effect of polyacrylamide polymers on floc size and rheological behaviour of kaolinite suspensions, *Colloids Surfaces A Physicochem. Eng. Asp.* (2007). doi:10.1016/j.colsurfa.2006.12.080.
- [105] M.S. Nasser, A.E. James, Compressive and shear properties of flocculated kaolinite-polyacrylamide suspensions, *Colloids Surfaces A Physicochem. Eng.*

Asp. (2008). doi:10.1016/j.colsurfa.2007.10.021.

[106] J.D. Ferry, *Viscoelastic Properties of Polymers*, 1980.